GRASSLAND/ATMOSPHERE RESPONSE
TO CHANGING CLIMATE:
COUPLING REGIONAL AND LOCAL SCALES

Final Report

M.B. Coughenour[1], T.G.F. Kittel[1] (PIs)
R.A. Pielke[2] and J. Eastman[2] (coPIs)

[1]Natural Resource Ecology Laboratory
[2]Department of Atmospheric Science

Colorado State University
Fort Collins, CO 80523

October 1993

Prepared for

NOTICE

MASTER

Table of Contents

Abstract

The objectives of the study were: (1) to evaluate the response of grassland ecosystems to atmospheric change at regional and site scales, and (2) to develop multiscaled modeling systems to relate ecological and atmospheric models with different spatial and temporal resolutions. A menu-driven shell was developed to facilitate use of models at different temporal scales and to facilitate exchange information between models at different temporal scales. A detailed ecosystem model predicted that C_3 temperate grasslands will respond more strongly to elevated CO_2 than temperate C_4 grasslands in the short-term while a large positive NPP response was predicted for a C_4 Kenyan grassland. Long-term climate change scenarios produced either decreases or increases in Colorado plant productivity (NPP) depending on rainfall, but uniform increases in NPP were predicted in Kenya. Elevated CO_2 is likely to have little effect on ecosystem carbon storage in Colorado while it will increase carbon storage in Kenya. A synoptic climate classification processor (SCP) was developed to evaluate results of GCM climate sensitivity experiments. Roughly 80% agreement was achieved with manual classifications. Comparison of 1x and 2xCO_2 GCM simulations revealed relatively small differences.

CHAPTER 1

Introduction

The potential ecological impacts of increasing levels of greenhouse gases were believed to be far-reaching and multifaceted when this research was originally proposed (1988). Both the climatic effects of rising concentrations of greenhouse gases and the direct physiological effects of elevated CO_2 were anticipated to have plant through ecosystem-level consequences. Such ecological changes were in turn expected to have feedbacks to climate thought their effects on biophysical properties of the land surface.

Prediction of ecological responses to CO_2 and climate change was proposed to require (1) simulation of the interaction of different ecological processes at multiple temporal scales and (2) translation of climatic and ecological responses to finer or coarser spatial scales. While existing models could be modified to address the problem of ecosystem CO_2 and climate changes individually, this fragmented approach would probably provide an inconsistent or confusing set of predictions because individual models were constructed for different purposes and at widely differing spatial and temporal scales. There was no modeling approach in 1988 that explicitly synthesized predictions at scales of leaves, plants, communities, ecosystems and regions, although paradigms had been proposed. Thus, a hierarchical modeling approach (Kittel and Coughenour 1988) was formulated. In this scheme, models within a hierarchical framework could be used to address questions of ecosystem and climate change at multiple spatial and temporal scales.

Ecological responses and ecological feedbacks to climate could, it was proposed, only be solved by linking ecological and climatic research. Climatic models also had problems of reconciling models at different spatial scales. A major problem with using general circulation model (GCM) results as inputs to ecological models was in translating the very coarse resolution results to a resolution closer to the scales of ecological spatial variation. Simple interpolation was inadequate due to sub-GCM scale heterogeneities in topography, vegetation and other factors. Therefore, a research priority of this project was to reconcile predictions of coarse- (GCM) with fine-scaled (mesoscale) climate models.

Literature Cited

Kittel, T.G.F. and M.B. Coughenour. 1988. Predictions of regional and local ecological change from global climate model results: A hierarchical modeling approach. In: Monitoring Climate for the Effects of Increasing Greenhouse Gas Concentrations. R.A. Pielke and T.G.F. Kittel, eds., Cooperative Institute for Research in the Atmosphere, Colorado State University, Fort Collins.

CHAPTER 2
GRASS 2.0 - A Mechanistic Model of Plant Growth

Introduction

The GRASS model of plant growth was originally published nearly a decade ago (Coughenour et al. 1984a,b; Coughenour 1984). Since that time, GRASS has undergone extensive revision, to incorporate more recent understanding, to improve model performance, to simplify model parameterization, and to make the model more robust. Efforts were made to minimize the number of parameters that vary among species and sites to facilitate cross-site parameterization and application.

Major submodels and information flows are diagrammed in Figure 1 while carbon and nitrogen flows are depicted in Figure 2. Plant growth submodels represent tillering, carbon and nitrogen budgets. Additional modules simulate light penetration and soil water and heat budgets (Coughenour 1984). The model uses a time step of two hours for diurnal processes such as leaf and soil energy balance and photosynthesis, and two days for other plant growth processes. The model is driven by daily weather data, although daily data can also be generated stochastically from monthly weather data.

In contrast to the first version of GRASS, the current version has been developed with much less attention to grazing responses, although most of the major mechanisms involved in plant grazing responses have been preserved. The current GRASS version was reformulated primarily to address questions of ecosystem responses to climatic change.

Abiotic Submodels Overview

GRASS is coupled to a daily time step soil water and heat flow submodel (Parton 1978), which has also been recoded since its original implementation. In contrast to Parton (1978) however, GRASS simulates transpiration explicitly, as it is coupled with photosynthetic processes through stomatal functioning. GRASS simulates bare soil evaporation explicitly as a part of the soil surface energy balance. Resultant soil surface temperature is the upper boundary condition for the soil heat flux submodel. Leaf and soil energy balance equations remain unchanged from the original version of GRASS. The canopy light interception submodel has changed slightly, in that sunlit and shaded leaf areas and incident radiation levels in each canopy layer are calculated. Photosynthetic rates and leaf energy balances are calculated for sunlit and all shaded leaves in each canopy layer.

Computing Daily Weather Data from Monthly Data, and Hourly Data from Daily Data

In contrast to the original GRASS model, simulation runs with the current version may run for 10 to >100 years. It is difficult to acquire and manage daily weather data over these time spans, especially for many different sites. Consequently, an algorithm was devised to stochastically generate daily data from monthly data.

Daily rainfall is generated from an empirical relationship between monthly rainfall and rainy days per month. The probability of a rainy day is then

$$Prain = \frac{Nstrm(mon)}{Nmdy(mon)}$$

where *Nstrm(mon)* is number of rainy days in month *mon* and *Nmdy* is number of days in the month. For each day in the month, a 0-1 random number is generated from a uniform distribution. If the number exceeds *Prain*, it is a rainy day. The fraction of monthly rainfall falling on a given day is generated as follows. A random number is generated for each rainy day *nd* in the month as

$$gama(nd) = \frac{1}{k} \ln \prod_{i=1}^{k} Rand$$

where *Rand* is a uniform random number and *k* is the shape parameter of the gama distribution. The fraction of monthly rain falling on each rainy day is then

$$prday(nd) = \frac{gama(nd)}{\sum_{nd}^{nstrm(mon)} gama(nd)}$$

and the quantity of rain falling on each rainy day is

$$pptmd(nd) = prday(nd) \times pptmn(mon)$$

where *pptmn(mon)* is monthly rainfall. This scheme preserves the monthly rainfall amount exactly.

Daily minimum and maximum temperatures (*Tmin, Tmax*) are generated by sampling from normal distributions with means *Tmin(mon)* and *Tmax(mon)*, which are the monthly mean daily temperatures. The standard deviation of both distributions is *Tmpstd* degrees C. Daily cloud cover, wind run and humidity are assumed fixed at the monthly values.

Hourly values for reference height temperature are computed from *Tmin* and *Tmax* using the model of Parton and Logan (1981). Diurnal variation in relative humidity is driven by diurnal temperature changes. The total water vapor content of air is assumed be constant, and is calculated from mean daily relative humidity mean daily temperature (T_{avg}), and computed saturation vapor pressure at mean temperature ($Esat(T_{avg})$).

Diurnal variations in radiation are computed from well known equations involving sun angle, time of day and site latitude (e.g., Spitters et al. 1986). Direct and diffuse components are separated as in Spitters et al. (1986).

Nutrient Cycling Submodel Overview

The CENTURY soil organic matter model (CSOM), comprised of the decomposition and nutrient cycling submodels of CENTURY (Parton et al. 1987), was isolated, implemented at a daily time step, and linked with GRASS. The daily and weekly SOM models use nearly identical parameters, but decomposition responds to actual daily soil

moisture content in the daily version and to the ratio of available water to PET in the weekly version.

Photosynthesis Submodel Overview

The photosynthesis submodel is described in Chen et al. (1993, preprint attached). The submodel for C_3 photosynthesis used in GRASS2 is based on the model of Farquhar et al. (1980), which considers the relative limitations of rates of ribulose 1,5-bisphosphate (RUBP) carboxylase fixation of internal leaf CO_2 and RUBP regeneration, and RUBP oxygenation. Reaction rates respond to temperature according to Arrhenius functions, which generally exhibit temperature optima. RUBP fixation is limited by mesophyll CO_2 concentration in C_3 species and by bundle heath CO_2 concentration in C_4 species. The maximum rate of RUBP regeneration is asymptotically light limited. The C_4 cycle, present only in C_4 species, is limited by phosphoenylpyruvate (PEP) carboxylase fixation, which responds to mesophyll CO_2 concentration (Chen and Coughenour 1993). Assimilation rate is reduced by low soil water content and leaf nitrogen. Dark respiration responds to temperature with a Q10 function.

The empirical stomatal conductance submodel of Ball et al. (1980) is used to simulate diffusion of CO_2 from the atmosphere into the mesophyll. In this model stomatal conductance is linearly related to the quantity

$$g_s = b + \frac{e_m A_n R_h}{C_a}$$

so that stomatal conductance (g_s) responds to leaf surface CO_2 concentration (C_a), relative humidity (R_h) and net assimilation rate (A_n). Thus, a simultaneous solution for photosynthesis rate and stomatal conductance is required. The model calculates a simultaneous solution for mesophyll and bundle sheath CO_2, due to A_n and diffusion through stomates. The value of g_s influences latent heat loss in the leaf energy balance equation.

Plant growth and photosynthesis in the original GRASS model was strongly influenced by plant or leaf water potentials, according to the prevailing views of plant physiology at that time. Since then, evidence has accumulated that stomatal conductance, photosynthesis and growth respond to root zone water potential, through hormonal signals that are passed from root to shoot (Chapin 1991, Davies et al 1990, Tardieu et al 1991, Golan et al. 1986). Experiments have shown maintenance of photosynthesis while leaf water potential declines. In other experiments, portions of the root system have been stressed, leading to changes in photosynthesis with no alteration of leaf water potential. This proves to be fortuitous for modeling as it is much easier to model plant responses to soil water potential. It is now unnecessary to predict leaf water potential from the complex balance of transpiration and root water uptake, and there are many fewer parameters.

Net assimilation rate is affected by water, leaf nitrogen concentration and leaf age as

$$A_n = A_{n0} \times \text{Ewps}(W_s) \times \text{Enps}(N_l) \times \text{Psage}(Age_l)$$

where Ewps is a function of soil water potential (W_s), Enps is a function of leaf percent nitrogen concentration (N_l) and Ageps is a function of leaf age (Age_l). Stomates respond to water and nitrogen through resultant changes in A_n.

An initial objective of the GRASS model was to integrate effects of light, biomass, nitrogen and leaf age distributions within the canopy on canopy photosynthesis. The model simulates younger leaf ages and higher N contents towards the top of the canopy. An alternative hypothesis is that plants allocate nitrogen towards the top of the canopy to make optimum use of intercepted light (Field 1983, Hirose and Werger 1987, Schimel et al. 1991). Accordingly, an option to distribute nitrogen among canopy layers in proportion to light intensity was added to the model.

The scaling of stomatal conductance and photosynthesis from leaf to canopy scales was changed. In the previous model version the scaling was achieved by calculating leaf responses for leaves in five classes of incident light intensity, irrespective of canopy layer. As a result, the relationship between canopy layer and leaf nitrogen content was obscured in some cases. Now, leaf responses are determined for sunlit and shaded leaves in each canopy layer. The canopy response is the leaf area weighted response.

Tillering

The tillering submodel simulates the numbers and types of apical meristems in relationship to the density of root crowns, temperature, nitrogen, labile carbon and apical dominance. Simulated plants regulate shoot meristem numbers per unit of crown mass as

$$Eff = \min[\text{Ewgr}(Wp), \text{Engr}(Pnc), \text{Eftc}(Tnc), \text{Apdcl}(Pculm)] \times \text{Etgr}(T_{lf})$$

$$Snum = Crwn \times (Sn_{min} + (Sn_{max} - Sn_{min})) \times Eff$$

where Sn_{min} and Sn_{max} are minimum and maximum numbers of shoots per gram of crown carbon, $Crwn$ is crown mass (g C/m^2). Ewgr(Wp) is a function of water potential, Engr(Pnc) is a function of plant N:C ratio, Eftnc(Tnc) is a function of labile C concentration, Apdcl($Pculm$) is a function of the proportion of shoots that are culms, and Etgr(T_{lf}) is a function of leaf temperature. Eftnc equals 0.0 when Tnc equals $Tncmn$ and 1.0 when Tnc equals $Tncmx$ (i.e., the minimum and maximum labile C concentrations).

The rate of new tiller formation is

$$Trt_{max} = Shpr \times Crwn \times \text{Elaitl}(Lait) \times \text{Etgr}(T_{lf})$$

$$Snew = \min[Trt_{max}, (Snum - Totsh)]$$

as long as $Snum > Totsh$, where $Totsh$ is total number of shoots per g crown C. $Shpr$ is a maximum rate (number per day per gC of crown) and Elaitl($Lait$) is a function of total leaf area index.

5

Three types of shoot meristems are recognized: tillers (culmless shoots), vegetative culms and reproductive culms. Meristems are allocated among types as

$$Culms = Totsh \times (Vgcl_{min} + (Vgcl_{max} - Vgcl_{min}) \times \text{Eftnc}(Tnc))$$

$$Culms_{rep} = Culms \times (Flcl_{min} + (Flcl_{max} - Flcl_{min}) \times \text{Eftnc}(Tnc))$$

where $Culms$ is total number of culms and $Culms_{rep}$ is number of reproductive culms per gC crown mass, $Vgcl_{min}$ and $Vgcl_{max}$ are minimum and maximum densities of culms per gC crown, and $Flcl_{min}$ and $Flcl_{max}$ are minimum and maximum densities of flowering culms per gC crown mass.

Shoot meristem mortality occurs if there is an excess number relative to crown mass, when crown mass dies, when temperatures are low, and when flowering culms have completed reproduction. The excess meristem density is

$$Shdrex = \text{Max}[0., Snum - \frac{Totsh}{Crwn}]$$

while meristem death rate is

$$Shndr = \text{Max}[Crdr, Tldth, \text{Eftsd}(T_{min}), \frac{Shdrex}{Totsh}, Fshdr]$$

where $Crdr$ is crown tissue death rate, $Tldth$ is a nominal meristem death rate, $\text{Eftsd}(T_{min})$ is a function of minimum daily air temperature, and $Fshdr$ is flowering culm death rate, which applies only to flowering culms when phenophase is 0 (quiescent) or 4 (post flowering).

Growth, Allocation and Carbon Reserves

The original GRASS model implemented a scheme, similar to models of Thornley (1972), in which root and shoot growth rates depended on labile carbon and nitrogen contents. While this scheme is physiologically realistic, it is difficult to parameterize to achieve proper root:shoot ratios at daily time steps. The translocation equation of Bachelet et al. (1989), also used in Hunt et al. (1991), was implemented in the new version of GRASS. In this formula the <u>fraction</u> of photosynthate used by shoots declines with increasing water or nitrogen stress. An increase in photosynthate due to elevated CO_2 increases both shoots and roots, even though the fractional allocation is unaffected. Observations of increased root:shoot allocation under high CO_2 (e.g., Larigauderie et al. 1988, Curtis et al. 1989) may result from depressed N/C ratios that occur when there is relatively greater C input to the plant.

The total fraction of current photosynthate that is allocated to shoots is

$$Sfrac = Shfr_{min} + (Shfr_{max} - Shfr_{min}) \times \text{Engr}(Pnc) \times \text{Ewgr}(Wp) \times \text{Ephshf}(Phen)$$

where $Shfr_{min}$ and $Shfr_{max}$ are minimum and maximum fractions allocated to shoots and where $\text{Ephshf}(Phen)$ is a function of phenology, $\text{Engr}(Pnc)$ and $\text{Ewgr}(Wp)$ are functions of

6

plant nitrogen and water potential. The function Engr and Ewgr can also be thought of as stressor effects on shoot growth rate, but the end result is the same: as stress increases allocation to shoots decreases.

The treatment of labile or non-structural carbon in the GRASS model has been revised. The prevailing pattern of carbohydrate concentration observed in grasses is a draw-down in early to mid-season, followed by an increase before quiescence (Trlica 1977). In the original GRASS model, this pattern could be simulated by careful adjustment of a number of growth and translocation parameters. A more parsimonious explanation is that plants regulate their carbon reserves in relation to phenology. This regulation is achieved by limiting growth rates when reserves are low, and also through mortality of structural plant tissues which causes a concentration of non-structural carbon in the surviving portion of the plant. It is critical that an adequate level of reserves exists within the plant to initiate regrowth in the following growing season, as well as to support continued maintenance respiration.

Shoot growth can also be supported by translocation from roots and crowns. Simulated plants are assumed to regulate their carbon reserves in relation to phenology. During initial shoot growth reserves may be depleted, eventually to a mid-season minimum, followed by a late-season period of replenishment that ensures dormancy is entered with an adequate supply to support the next year of regrowth. The quantity of labile carbon that is available to support shoot growth is

$$Avrsv = (Tnc - Rsv_{min}) \times Rpool$$

$$Rsv_{min} = \text{Trphen}(Phen) + 3.31 \times Pnc$$

where Tnc is concentration of non-structural carbon (gC/gC), $Rsvmn$ is minimum non-structural carbon concentration. Trphen($Phen$) is non-structural carbohydrate concentration as a function of phenology. Trphen equals $0.85 Tncmn$ at $Phen=0$, $Tncmn$ when $1.0 < Phen \leq 2.5$, and $Tncmx$ at $Phen=4$. Protein carbon is calculated from plant nitrogen concentration (Pnc) and the C:N ratio of plant protein (3.31). The maximum use of available reserves is then

$$Trmx = Utrmx \times Avrsv \times \text{Min}[\text{Engr}(Pnc), \text{Ewgr}(Wp)] \times \text{Etgr}(T_{ip})$$

where $Utrmx$ is maximum fraction of available reserve used per day.

When $Rtnx < Rsvmn$ it is assumed that carbon reserves are must be replenished. $Avrsv$ and $Trmx$ are set to zero and a fraction ($Trlabc$) of available carbon ($Availc$) is replenishes reserves each time step.

$$Availc = (Ps \times Sfrac) + Trmx$$

$$Replen = Trlabc \times Availc$$

The final amount of carbon that is available to support shoot growth is then

Shoot growth demands may also be restricted by maximum potential growth rate, which occurs when photosynthesis is unlimiting and there is no water or nitrogen stress.

7

$$Availc_{sg} = Availc - Replen$$

The potential growth rate of shoot type j is

$$Sgr_{pot}(j) = Sgr_{max}(nph,j) \times Shn(j) \times Etgr(T_{lf}) \times Szgr(Shsz) * 2500.$$

where $Sgr_{max}(npj,j)$ is maximal growth rate of shoot type j in growth phase nph (mg biomass/shoot/d), $Shn(j)$ is shoot number per m^2, $Etgr(T_{lf})$ is a function of leaf temperature, $Szgr(Shsz)$ is a function of physiological shoot size and 2500. Converts from mg biomass to gC. Maximum growth rates may vary among growth phases. Growth phase 1 occurs in early phenology ($Phen \leq 1$), phase 2 is during pre-reproductive culm growth ($1 < Phen < 2$) and phase 3 occurs during and after reproduction ($Phen > 2$). Culmless shoots grow indeterminately in the sense that they grow to attain a maximal green leaf mass per shoot. Vegetative culm growth can be indeterminate if plants tiller aerially (i.e., from elevated axillary meristems on vegetative culms). Reproductive culm growth is assumed to be determinate in that shoot size ($Shsz$) is derived from the total quantity of biomass produced per shoot.

When the supply of available carbon ($Avail_{sgr}$) is less that the total potential growth demand, including growth respiration costs, then actual shoot growth is

$$Sgr_{act}(j) = \frac{Availc_{sg}}{\sum_j Sgr_{pot}(j) \times (1 + Grsr)} \times Sgr_{pot}(j)$$

where $Grsr$ is growth respiration costs (gC/gC). This simply scales back growth of each shoot type so that total growth does not exceed available carbon. When shoot growth demands exceed supplies, then this equation effectively partitions available carbon among shoot types. Note that if $Shr_{max}(j)$ are set to high values, then shoot growth is controlled entirely by root:shoot allocation ($Sfrac$).

Shoot growth is partitioned among leaf blades, sheaths and stems as

$$Blg(j) = Sgr_{act}(j) \times Bla(nph,j)$$

$$Shg(j) = Sgr_{act}(j) \times Sha(nph,j)$$

$$Stg(j) = Sgr_{act}(j) \times Sta(nph,j)$$

where $Bla(nph,j)$, $Sha(nph,j)$ and $Sta(nph,j)$ are fractions allocated to blades sheath and stem by shoot type j in growth phase nph.

Shoot growth is partitioned among canopy layers in relationship to mean shoot height. The function $Htwt(Shsz)$ relates shoot height (Ht) to shoot weight. Growth is partitioned among five height classes defined by $Ht(1-2Hstd(j))$, $Ht(1-Hstd(j))$, Ht, $Ht(1+Hstd(j))$ and $Ht(1+2Hstd(j))$. The fractions of growth partitioned into each class are $Frly(l)$, $l=1,5$. Shoot tissue age is simulated by tracking the amounts of tissues in each of fifteen age classes.

8

Since shoot tissues are cross-classified by age, shoot type, tissue type and canopy layer, many shoot state variables are simulated. The state variables are $Blade(j,n,l)$, $Sheath(j,n,l)$ and $Stem(j,n,l)$ for $j=1,3$ shoot types, $n=1,15$ age classes and $l=1,3$ canopy layers. Although there are 405 of these underlying state variables, this level of detail obviously has little significance for a model user. However, total shoot mass, proportions of blade, sheath and stem, and proportions of biomass in each canopy layer are derived from these states, and do have significance. The underlying cross-classification is required to generate tissue type and age class distributions among canopy layers, which impact light penetration and photosynthesis.

Belowground growth rate can be constrained by a temperature limited maximal growth rate or by available carbon. Maximum root plus crown growth rate is

$$Bgrt_{max} = (Roots + Crwn) \times Rgrt \times Etgr(T_{soil}) \times Rgni(Pnc)$$

where $Roots$ and $Crwn$ are root and crown mass (gC/m^2), $Rgrt$ is a maximum relative growth rate, $Etgr(T_{soil})$ is a function of soil temperature, and $Rgni(Pnc)$ is a function of plant nitrogen. $Rgni$ take the value of 0.0 when Pnc equals $Pncmn$, and the value of 1.0 when

$$Pnc = Pncmn + (Pncmx - Pncmn) \times 0.5$$

The amount of carbon that is available to support belowground growth and respiration is

$$Availc_{bg} = Ps - \sum_j Sgr_{act}(j) - Gresl - Rms - Rstr - Rsup - Replen$$

where Ps is net photosynthate, and $Gresr$, Rms, $Rstr$, $Rsup$ are respiratory costs of shoot growth and maintenance, translocation and nitrogen uptake. The total demand for carbon belowground is

$$Demc_{bg} = Bgrt + Gresr + Rmrt$$

which includes growth and maintenance respiration. Belowground growth is partitioned among roots and crowns as a function of root:crown ratio ($Rtcr$).

$$Rtgr = Bgrt \times Rtcrr(Rtcr)$$

$$Crgr = Bgrt \times (1 - Rtcrr(Rtcr))$$

The function Rtcrr take a value of 1.0 when $Rtcr$ equals $Rtcrmx$ and 0.0 when $Rtcr$ equals $Rtcrmn$. When carbon demands exceed $Availc_{bg}$, all of the demands are reduced proportionately, by multiplying each by the ratio of $Availc_{bg}:Dem_{bg}$. Significantly then, root maintenance respiration is limited by available carbon, which corresponds with observed correlations of photosynthetic rate and root respiration.

The total amount of carbon left after growth and respiration is added to non-structural carbon reserves. Total carbon available for reserve replenishment is

9

$$C_{repl}=Ps-(\sum_{j} Sgr(j)+Gresl+Rms+Crgr+Rtgr+Gresr+Rmrt+Rstr+Rsup)$$

Respiration

Respiratory costs are incurred for growth, maintenance, carbon translocation, nitrogen uptake and nitrogen translocation. The respiration equations used in GRASS have been improved to reflect a growing body of evidence that maintenance respiration is proportional to tissue protein content (Ryan 1991). This allows a single base respiration rate to be used for all tissue types, which vary mainly in their nitrogen contents. Estimates of growth respiration costs have also become more refined (Ryan 1991). If maintenance respiration is proportional to nitrogen content, then observations of decreased respiration rate per unit biomass under elevated CO_2 (e.g., Bunce and Caulfield 1991) could be a result of reduced tissue nitrogen concentration.

Shoot and belowground growth respiration costs are

$$Gresl=\sum_{j} Sgr_{act}(j)\times Grsr$$

$$Gresr=(Rtgr+Crgr)\times Grsr$$

where $Grsr$ is the growth respiration coefficient. Maintenance respiration is thought to be dependent on protein concentration (Ryan 1991). Shoot maintenance respiration is

$$Rms=Rmrl\times(24-Dln)\times Shootn\times e^{\frac{Log(Q10Rs)\times(T_{br}-20)}{10}}$$

where $Rmrl$ is the hourly respiration rate per gram of shoot nitrogen (gC/gN/hr) at 20°C, $Shootn$ is shoot N, Dln is day-length, and $Q10Rs$ is the Q10 of the temperature response. Daytime respiration of shoots is treated in the photosynthesis submodel. Root maintenance respiration is similarly modeled, with a 20°C respiration rate of $Rmrs$.

$$Rms=Rmrt\times24\times Rootn\times e^{\frac{Log(Q10Rs)\times(T_{soil}-20)}{10}}$$

Translocation costs are

$$Tran=Ps-\sum_{j} Sgr(j)-Gresl$$

$$Rstr=.05\times Abs(Tran)$$

where 0.05 is the gC respired per gram C translocated.
Costs of nitrogen uptake and translocation are

10

$$Rsup = 0.874 Nup + 0.1 Trann$$

where 0.874 corresponds to 1.01 mole C per mole N uptake. Respiratory coefficients and Q10s are taken from Ryan (1991).

Senescence, Mortality and Dead-Fall

Shoot tissues die due to ageing, water stress, death of supporting crowns, shading and carbon stress.

$$Shdr = \text{Max}[\text{Agedth}(Age), \text{Ewsd}(Wp), \text{Tshd}(Lait), Crdr, Dthlc)]$$

where Agedth(Age) is death rate as a function of tissue age, Ewsd(Wp) is death rate as a function of water potential, Tshd($Lait$) is death rate as a function of total leaf area index, $Crdr$ is crown tissue death rate. $Dthlc$ is plant death rate due to carbon stress, calculated as

$$Dthlc = Dlcred \times \frac{Rsvmn - Tnc}{Rsvmn}$$

where $Rsvmn$ is minimum and Tnc is current non-structural carbon concentration, and $Dlcred$ is a rate constant. Stem death rate is a fraction $Stmdr$ of $Shdr$.

Root mortality rate (gC/gC/d) is

$$Rtdr = \text{Max}[\text{Ewrd}(Wp), \text{Eftrd}(T_{soil}), Dthlc]$$

where Ewrd(Wp) is death rate as a function of water potential, Eftrd(T_{soil}) is a death rate as a function of soil temperature. Crown death rate is a fraction $Crdth$ of $Rtdr$.

When shoot tissues die they are transferred to standing dead. The subsequent rate of transfer of standing dead shoots to litter is

$$Dfrt = Dflr \times \text{Efpdf}(Ppt_{avg}) \times \text{Eftdf}(T_{avg})$$

where $Dflr$ is a maximum rate, Efpdf(Ppt_{avg}) is a function of mean daily precipitation rate (cm/d) and Eftdf(T_{avg}) is a function of mean daily temperature.

Plant Nitrogen Uptake and Allocation

Nitrogen uptake follows a two site Michaelis-Menten function.

11

$$Effup(l) = Uptr(l) \times Etgr(T_{soil}) \times Rnup(Pnc) \times Ewnup(Wp)$$

$$nup(l) = Roots \times Proot(l) \times Effup(l) \times \frac{Vamx \times [N]}{Uka \times [N] + [N]} \times \frac{Vbmx \times [N]}{Ukb \times [N] + [N]}$$

where *Proot(l)* is fraction of roots in soil layer *l*, $Etgr(T_{soil})$ is a function of soil temperature, Rnup(*Pnc*) is a function of plant N:C ratio, and Ewnup(*Wp*) is a function of water potential. *Vka* and *Vkb* are maximal uptake rates (gN/g root C/d), *Uka* and *Ukb* are half-saturation constants, and *[N]* is soil nitrogen concentration (gN/g soil). *Rnup* equals 1.0 when

$$Pnc = Pncmn + (Pncmx - Pncmn) \times 0.66$$

where *Pncmx* and *Pncmn* are the maximum and minimum plant N:C ratios. *Rnup* equals 0.0 when *Pnc = Pncmx*.

Nitrogen is allocated in the plant among different aged shoot tissues using the sink strength concept. Total sink strength of shoot tissues in age class *n* is

$$Sslv_n = \frac{Rlnss(Age_n) \times Leaf_n}{\sum_n (Rlnss(Age_n) \times Leaf_n) + (Roots + Crwn)}$$

where $Rlnss_n$ is relative sink strength of age class *n*, which is a function of age and where $Leaf_n$ is gC of blade and sheath tissues in age class *n*. The relative sink strength of roots and crowns is 1.0. Leaf N:C ratio in age class *n* is then

$$Lfnc_n = Sslv_n \times Plantn$$

where *Plantn* is total plant nitrogen.

When tissues die, nitrogen can be retranslocated to the remaining living portions of the plant. Total shoot nitrogen death is

$$Dshtn = (Bldth \times Dlfnc(Pnc)) + (Stdth \times Dstnc(Pnc))$$

where *Lfdth* and *Stdth* are total amounts of leaf and stem carbon deaths, Dlfnc(*Pnc*) and Dstnc(*Pnc*) are dead leaf and stem N:C ratios as functions of plant N:C ratio.

Nitrogen is distributed among canopy layers in one of two ways.
In the first option, it is simply a result of the distribution of leaf ages among canopy layers. Thus the total grams of nitrogen in canopy layer *l* is

$$Vrni(l) = \sum_k Blnc(k) \times Leaf(k,l)$$

$$Vrni(l) = \sum_k Blnc(k) \times Leaf(k,l)$$

where $Blnc(l)$ is N:C ratio of leaves in age class k, $Leaf(k,l)$ is blade plus leaf tissue in age class k in layer l. In the second option, nitrogen is distributed in relationship to the distribution of light. It has been hypothesized that plants do might do this to optimize nitrogen use efficiency (Field 1983, Hirose and Werner 1987). Thus

$$Vrni(l) = Leafn \times \frac{Avpar(l) \times Leaf(l))}{\sum_l Avpar(l) \times Leaf(l)}$$

where $Leafn$ is total leaf nitrogen and $Avpar(l)$ is daily average light intensity on leaves in layer l.

Phenology

Five phenophases are recognized: 0-quiescent, $Phen \geq 1$ - early vegetative growth, $2 \leq Phen < 3$ - late vegetative growth, $3 \leq Phen < 4$ - flowering and fruiting and 4- post-fruiting. Early and late vegetative growth correspond to pre-culm and culmed phases of shoot growth. Phenological advancement is related to total degree-days since breaking dormancy, or since the start of the last phenological cycle. Total degree-days is

$$Degdy = \sum_{t_0}^{t} Max[0., T_{avg} - Phtmn)] \times dt$$

where t_0 time of growth initiation, T_{avg} is average daily temperature, and $Phtmn$ is a threshold temperature. Similarly, the degree-days since onset of flowering is calculated as

$$Fdegdy = \sum_{t_{flw}}^{t} (T_{avg} - Phtmn) \times dt$$

where t_{flw} is time at the onset of flowering ($Phen = 3$).

Plants break dormancy when several conditions are met:

$$(Phen = 0 \lor Phen = 4) \land$$
$$(Phavsw < Phwmn) \land$$
$$(T_{soil} < Phtmn) \land$$
$$(Dln > Grwdl)$$

where the "or" operator points down, the "and" operator points up. Soil temperature (T_{soil}), daylength and average soil water potential must all exceed the specified thresholds. The moving average water potential is calculated based on Wp in the last $Nmav$ time

13

steps. *Wp* at each time step is the depth-weighted average *Wp* in the top *Nslph* soil water layers.

Phenophases are

$$Phen = 1.0 + \frac{Degdy}{Pheat(1)} \quad Degdy < Pheat(1)$$

$$Phen = 2.0 + \frac{Degdy - Pheat(1)}{Pheat(2) - Pheat(1)} \quad Pheat(1) \leq Degdy < Pheat(2)$$

$$Phen = 3 + \frac{Fdegdy}{Fheat} \quad (Pheat(2) \leq Degdy < Pheat(3))$$

Where *Pheat*(1-3) are degree-days at phenophases 2,3 and 4. In addition, for flowering to occur (*Phen*≥), daylength be in the range *Flwdl*(1)≥*Dln*≥*Flwdl*(2).

Plants may be induced into dormancy if

$$(Degdy > Pheat(3)) \wedge$$
$$(Dln < Drmdl \vee Phavsw > Swpdrm)$$

where *Drmdl* is a daylength threshold and *Swpdrm* is a soil water potential threshold.

Of course, not all of these requirements for dormancy-breaking and induction, and flowering are operative in all species. For example, daylength may not affect flowering and soil temperature may not affect dormancy in some tropical plant species. In such cases parameters are set so that the non-operative condition always tests true.

Model Tests

The photosynthesis submodel was tested against measurements of photosynthetic responses to leaf internal (mesophyll) CO_2 concentration (A/C_i curves), incident photosynthetically active radiation (PAR), and leaf temperature (Monson et al. 1982a,b, Knapp et al. 1992, Polly et al. 1992). The measurements provided data for a tall C_4 grass (*Andropogon gerardii*), a short C_4 grass (*Bouteloua gracilis*) and mid height C_3 grass (*Agropyron smithii*), all from North America. To support predictions of ecosystem responses to climatic change, it is important to demonstrate that simulated plants respond realistically to temperature and CO_2. Since C_i depends upon stomatal conductance, A/C_i curves are also affected by the stomatal submodel (Ball et. al. 1987, Chen and Coughenour 1993).

Simulated A/C_i curves compared favorably with data (Fig. 3a-c). Ambient CO_2 concentrations of 350 ppm produced C_i's of 200-250 ppm. Assimilation rates of the C_4 plants were close to being saturated at 350 ppm CO_2 ambient, due to concentration of CO_2 by PEP carboxylase into bundle sheath cells. The ratio of An at 700 ppm to that at 350 ppm CO_2 was 1.02 in *A. gerardii*, 1.03 in *B. gracilis*, and 1.28 in *A. smithii*. The CO_2 compensation points (X-intercepts) were near 0 ppm for C_4 species, and 50 ppm for the C_3 species due to their differences in photorespiration.

Light responses were accurately simulated (Fig. 4a-c). The quantum efficiencies (initial slopes of the light response curves) were correct, as were light compensation points (X-intercepts). The C_3 species was nearly saturated at 1500 μmol/m²/sec while the C_4 plants were not. The light response curve of the C_3 plant at 800 ppm CO_2 and 2% O_2 was also correctly simulated.

Simulated and measured temperature response curves compared favorably, despite a wide range of shapes (Fig. 5a-c). The C_4 plants exhibited higher temperature optima than the C_3 plants (36-38°C vs. 27°C) as expected. While An in the C_3 grass was still active at 5°C, in the C_4 grass *A. gerardii* it was insignificant. However, the *B. gracilis* C_4 assimilation was active even at 5°C. *B. gracilis* also performed best at high temperatures, while the C_3 plant was inactive at 50°. Temperature optima for photosynthesis may be shifted higher under elevated CO_2 concentrations due to differential temperature sensitivities of solubilities and RuBp affinities for CO_2 and O_2 (Long 1991). The shift was greatest in the C_3 grass, as expected due to lack of CO_2 saturation of RuBp by PEP. There was no shift in the optimum for *A. gerardii* as expected for C_4 plants where RuBP competitive O_2 affinity becomes insignificant. However, the model predicted a shift in optimum for the C_4 grass *B. gracilis*, which was due to the shape of the temperature response function. When the *A. gerardii* temperature functions were used, there was no CO_2 induced shift in the temperature optimum of *B. gracilis*.

Photosynthetic light responses of the Kenyan C_4 grass *Themeda triandra* (Kinyamario and Imbamba 1992) at different canopy heights were compared with model simulations at different leaf nitrogen concentrations (Fig. 6). Leaves higher in the canopy tend to have higher nitrogen concentrations. Top canopy leaves were assumed to have maximal nitrogen concentrations (e.g., Schimel et al. 1991). The favorable comparisons supported model predictions of maximal photosynthetic rates of this species, as well as responses to light and nitrogen.

The GRASS model has been parameterized for the Colorado site (CPER). Irrigation and nitrogen fertilization experiments that were conducted at CPER during the IBP Grassland Biome studies (Lauenroth and Dodd 1978, Dodd and Lauenroth 1979) provided an opportunity to test the model over a wide range of conditions and over several weather years. The model was also parameterized for an intensively studied grassland site near Nairobi, Kenya (Kinyamario and Imbamba 1992). This site has been studied since 1984 to improve understanding of productivity of tropical grasslands (see Long et al. 1989,1992). Above and belowground biomass, photosynthesis, leaf area, transpiration, light interception were frequently sampled over a several year period, providing an opportunity to thoroughly parameterize and test the GRASS model.

The GRASS-CSOM model was tested against biomass dynamics and primary productivity data from the CPER and the Nairobi sites (Fig. 7a,b). Both live and dead aboveground biomass dynamics were well simulated, with a few exceptions. Highly unusual data patterns such as at CPER in 1973 could not and possible should not have been simulated by the model. Correlations between observed and predicted values for green shoots (Fig. 8a,b) were highly significant, although the r^2 value was low for the CPER data, due to several outliers. For CPER, 46% of the model predictions fell within ±25% of the observed data value, while for Nairobi 46% fell within the ±25% interval. However for Nairobi, many predicted values were only just outside the ±25% limits. Predictions of aboveground net primary production (ANPP) and peak live shoot mass were more precise (Fig. 9a,b). Over 90% of the variance in ANPP and 56% of the variance in

peak biomass was explained by the model. There was a slight tendency to overpredict ANPP at low values, as reflected by the positive Y-intercept.

Conclusions

The GRASS model revision has been successful on two main counts. Firstly, the model works. GRASS successfully predicted inter-annual biomass dynamics for a temperate as well as a tropical grassland. The model responded well to a demanding test: simulating responses to the irrigation and nitrogen fertilization treatments at CPER. Photosynthetic responses to light, temperature, and CO_2 were accurate.

Secondly, model robustness and utility have increased. This is significant, because experience with detailed, daily-time step models during the 1970's and 80's led to beliefs that detailed, mechanistic models were too cumbersome and required too much information to apply at the ecosystem level, and that they could not be run successfully for more than 1-5 years due to computational demands and dynamic instability. However, these problems were not due to model complexity per se, but to limitations on our ability to construct robust complex models, limitations in programming tools, and limitations in computing hardware. Improved programming techniques have improved ability to manage complexity. Code is written in structured Fortran-77 rather than unstructured (spaghetti) Fortran-66 and code is well-documented. Hardware limitations are rapidly lifting. Long-term model runs are possible on current microprocessors (e.g., 100 years in 30 minutes). There are now markedly fewer parameters and the remaining parameters are easier to estimate.

It is encouraging that many parameter values have been found to apply generally, for different grass species and sites. This will facilitate model parameterization for a wider range of sites over larger spatial scales. We expect that patterns of parameter relationships with climate and site factors will emerge as the model is applied across a wider range of sites. A potential outcome of parameter generalization, is a theoretical tie to theories of plant growth strategies. Fundamental trade-offs between different parameter values arise due to physiological and morphological constraints (Orians and Solbrig 1977, Grime 1977, Chapin 1980, Mooney and Gulman 1982, Tilman 1988). Knowledge of these trade-offs should be useful for developing generalized parameter sets. Ultimately, it should be possible to derive most biological and physical parameters from minimal information on soil type and climatic conditions at a site.

This progress suggests that one viable way forward for ecosystem modeling is to increase the robustness and generality of detailed models. Certainly, simplified models are also needed. For the time being, higher levels of modeling productivity can be achieved by using simplified models. However, models that appear complex and are demanding of time and information now may eventually evolve into applications that are friendly, fast, and powerful. For this reason, complex modeling efforts must proceed.

Literature Cited

Ball, J.T., Woodrow, I.E. and Berry, J.A., 1987. A model predicting stomatal conductance and its contribution to the control of photosynthesis under different environmental conditions. In Progress in Photosynthesis Research, vol. IV (Ed. I. Biggins), pp.221-224. Martinees Nijhoff, Dordrecht.

Chapin, F.S. III. 1980. The mineral nutrition of wild plants. Ann. Rev. Ecol. Syst. 11:233-60.

Chapin, F.S. III. 1991. Integrated responses of plants to stress.: A centralized system of physiological responses. Bioscience 41:29-36.

Chen, D.-X., Coughenour, M.B., Knapp, A.K, and Owensby, C.E. 1993. Mathematical simulation of C_4 grass photosynthesis in ambient and elevated CO_2. Ecol. Model. (in press).

Coughenour, M.B. 1984. A mechanistic simulation of water use, leaf angles and grazing in east African graminoids. Ecol. Model. 26:127-1284.

Coughenour, M.B., S.J. McNaughton, L.L. Wallace. 1984a. Modeling primary production of perennial graminoids: Uniting physiological processes and morphometric traits. Ecol. Model. 23:101-134.

Coughenour, M. B., S. J. McNaughton, and L. L. Wallace. 1984b. Simulation study of Serengeti perennial graminoid responses to defoliation. Ecological Modelling 26:177-201.

Collatz, G. J., Ribas-Carbo, M. and Berry, J. A., 1992. Coupled photosynthesis-stomatal conductance model for leaves of C_4 plants. Aust. J. Plant Physiol.,19, in press.

Curtis, P.S., B.G. Drake, P.W. Leadly, W.J. Arp, and D.F. Whigham. 1989. Growth and senescence in plant communities exposed to elevated CO_2 concentrations on an estuarine marsh. Oecologia 78:20-26.

Davies, W.J., J. Metcalfe, T.A. Lodge, and A.R. de Costa. 1986. Plant growth substances and the regulation of growth under drought. Aust. J. Pl. Physiol. 13:105-125.

Dodd, J.L., and W.K. Lauenroth. 1979. Analysis of the responses of a grassland ecosystem to stress. Ch. 3 in: Perspectives in grassland ecology, N.R. French (ed.). Springer Verlag.

Farquhar, G.D., Caemmerer, S. von and Berry, J.A., 1980. A biochemical model of photosynthetic CO_2 assimilation in leaves of C_3 species. Planta, 149:78-90

Field, C. 1983. Allocating leaf nitrogen for the maximization of carbon gain: leaf age as a control on the allocation program. Oecologia 56:341-347.

17

Gollan, T., J.B. Passioura and R. Munns. 1986. Soil water status affects the stomatal conductance of fully turgid wheat and sunflower leaves. Aust. J. Pl. Physiol. 13:469-464.

Grime, J.P. 1977. Evidence for the existence of three primary strategies in plants and its relevance to ecological and evolutionary theory. Am. Nat. 111:1169-1194.

Harley, P.C., Thomas, R.B., Reynolds, J.F. and Strain, B.R., 1992. Modelling photosynthesis of cotton grown in elevated CO_2. Plant, Cell & Environment, 15:271-282

Hirose, T. and M.J. Werger. 1987. Maximizing daily canopy photosynthesis with respect to the leaf nitrogen allocation pattern in the canopy. Oecologia 72:520-526.

Kinyamario, J.I. and S.K. Imbamba. 1992. Savanna at Nairobi National Park, Nairobi. Chap. 2 in: S.P. Long, M.B. Jones and M.J. Roberts (eds.), Primary Productivity of Grass Ecosystems. Chapman and Hall. London.

Larigauderie, A., D.W. Hilbert and W. C. Oechel. 1988. Effect of CO_2 enrichment and nitrogen availability on resource acquisition and resource allocation in a grass, Bromus mollis. Oecologia 77:544-549.

Lauenroth, W.K. and J.L. Dodd. 1978. The effects of water- and nitrogen-induced stress on plant community structure in a semiarid grassland. Oecologia 36:211-222.

Long, S.P., 1991. Modification of the response of photosynthetic productivity to rising temperature by atmospheric CO_2 concentrations: Has its importance been underestimated? Plant, Cell and Environ., 14:729-739

Long, S.P., E. Garcia-Moya, S.K. Imbamba, A. Kamnalrut, M.T.F. Piedade, J.M.O. Scurlock, Y.K. Shen and D. O. Hall. 1989. Primary productivity of natural grass ecosystems of the tropics: a reappraisal. Plant and Soil 115:9-20.

Long, S.P., M.B. Jones and M.J. Roberts, eds. 1992. Primary Productivity of Grass Ecosystems. Chapman and Hall. London.

Milchunas, D.G., and W.K. Lauenroth. 1992. Carbon dynamics and estimates of primary production by harvest, ^{14}C dilution and ^{14}C turnover. Ecology 73:593-607.

Mooney, H.A. and S.L. Gulmon. 1982. Constraints on leaf structure and function in reference to herbivory. Bioscience 32:198-206.

Monson, R.K., M.A. Stidham, G.J. Williams III, and G.E. Edwards. 1982. Temperature dependence of photosynthesis in *Agropyron smithii* Rydb. Plant Physiol. 69:921-928.

Monson, R.K., R.O. Littlejohn Jr. and G.J. Williams III. 1983. Photosynthetic adaptation to temperature in four species from the Colorado shortgrass steppe: a physiological model for coexistence. Oecologia 58:43-51.

Orians, O. and O.T. Solbrig. 1977. A cost income model of leaves and roots with special reeference to arid and semiarid areas. Am. Nat. 111:677-690.

Owensby, C.E., Coyne, P.I., Ham, J.M., Aven, C.A. and Knapp, A.K., 1993. Biomass production in a tallgrass prairie ecosystem exposed to ambient and elevated levels of CO_2. Ecological Applications, submitted.

Parton, W.J. 1978. Abiotic submodel of ELM grassland simulation model. in: G. Innis, ed., Grassland Simulation Model. Springer-Verlag.

Parton, W.J. and J.A. Logan. 1981. A model for diurnal variation in soil and air temperature. Agric. Meteorol. 23: 205-216.

Parton, W.J., D.S. Schimel, C.V. Cole, and D.S. Ojima. 1987. Analysis of factors controlling soil organic matter levels in Great Plains Grasslands. Soil Sci. Soc. Am. J. 51:1173-1179.

Polley, H.W., J.M. Norman, T.J. Arkebauer, E.A. Walter-Shae, D.H. Greegor Jr. and B. Bramer. 1992. Leaf gas exchange of *Andropogon gerardii* Vitman, *Panicum virgatum* L., and *Sorgastrum nutans* (L.) Nash in a tallgrass prairie. J. Geoph. Res. 97:18,837-18,444.

Ryan, M. 1991. The effects of climate change on plant respiration. Ecol. Appl. 1:157-167.

Schimel, D.S., Kittel, T.G., Knapp, A.K., Seastedt, T.R., Parton, W. and Brown, V.B., 1991. Physiological interactions along resource gradients in a tallgrass prairie. Ecology, 72:672-684

Sims, P.L. and J.S. Singh. 1978. The structure and function of ten western North American grasslands. II. Intra-seasonal dynamics in primary producer compartments. J. Ecol. 66:547-572.

Spitters, C.J.T., H.A.J.M. Toussaint and J. Goudriaan. 1986. Separating the diffuse and direct component of global radiation and its implications for modeling canopy photosynthesis. Part I. Components of incoming radiation. Agric. For. Meteorol. 38:217-229.

Thornley, J.H.M. 1972. A balanced qualitative model for root:shoot ratios in vegetative plants. Ann. Bot. 36:431-441.

Tilman, D. 1988. Plant strategies and the Dynamics and structure of plant communities. Princeton Univ. Press, Princeton.

Trlica, M.J. 1977. Distribution and utilization of carbohydrate reserves in range plants. Ch. 3. in: Rangeland Plant Physiology. R.E. Sosebee (ed.). Range Sci. Ser. 4, Society for Range Management, Denver.

Figure Legends

Figure 1. Major submodules in the GRASS-CSOM model and flows of information among submodules. LAI-leaf area index, Nl-leaf nitrogen, Al-leaf age, Cl-labile carbon, Ns-soil N, Bl-litter biomass, Ws-soil water, Ts- soil temperature, PAR-photosynthetically active radiation, gs-stomatal conductance, Ev-soil evaporation, Ws-soil water, Tc- canopy temperature, Uc-windspeed, RHc-humidity, Tr-transpiration, Rg-global radiation.

Figure 2. Flows of carbon and nitrogen in the GRASS-CSOM model. Ws-Soil water potential, Np-plant N:C ratio, Cl- labile carbon concentration, Tl- leaf temperature, Ta- air temperature, Al-leaf age, I-irradiance, RH-relative humidity, Ph-phenology, Ns- soil nitrogen concentration, Nr- root N:C ratio, Nl-leaf N:C ratio, Nd- dead N:C, No- soil organic matter N:C ratio.

Figure 3. Comparison of observed (points) and simulated (lines) responses of net assimilation (An) to leaf internal CO_2. Observed data for *B. gracilis* (C_4) are from Monson et al. (1983) (warm-grown plants). Data for *A. gerardii* (C_4) are from Polley et al. (1992). Data for *A. smithii* (C_3) are from Monson et al. (1983). *B. gracilis* measured at 2000 µmol/m²/s, 30°C, 80% RH, and no water or nitrogen stress. *A. smithii* measured at 25°C, 2000 µmol/m²/s, and no water or nitrogen stress. *A. gerardii* data were determined at 60% RH, 1.2 MPa, 1.17% N, 39°C, 1400 µmol/m²/s.

Figure 4. Comparison of observed (points) and simulated (lines) responses of net assimilation (An) to PAR. Observed data for *B. gracilis* (C_4) are from Monson et al. (1983) (mean of cool- and warm-grown plants). Data for *A. gerardii* (C_4) are from Polley et al. (1992). Data for *A. gerardii* (C_4) are from A. Knapp (T_1 curve, pers. comm., see Chen and Coughenour 1993). Data for *A. smithii* (C_3) are from Monson et al. (1983) (340 ppm CO_2), and Monson et al. 1982 (800 ppm CO_2). Conditions as in Fig. 2 except *A. gerardii* temperature was 37°C.

Figure 5. Comparison of observed (points) and simulated (lines) responses of net assimilation (An) to leaf internal CO_2 (Ci). Observed data for *B. gracilis* (C_4) are from Monson et al. (1983) (mean of cool- and warm-grown plants). Data for *A. smithii* (C_3) are from Monson et al. (1982). Conditions as in Fig. 2 except in *A. gerardii* curve is for 40% RH, 1000 µmol/m²/s, 1.2 MPa, 1.05% N.

Figure 6. Light response curves of the African grass *T. triandra* at different leaf nitrogen levels, meant to represent leaves at different canopy positions. Observed data (points) from Kinyamario and Imbamba (1992). Conditions are 50% RH, 27°C, .47 MPa.

Figure 7. Comparison of observed and GRASS-simulated aboveground biomass dynamics at two sites. Large points, solid line - observed and simulated green shoots. Small points, dashed line - standing dead shoots. Observed CPER data from IBP/CPER-LTER data bank. Observed Nairobi data from D. Hall et al. and J. Kinyamario (pers. comm.), and Kinyamario and Imbamba (1992).

21

Figure 8. Correlations between observed and GRASS-simulated green biomass observations. Lines represent equality of simulated and observed data. Dashed lines indicate ±25% of observed data. Data sources as in Fig. 5.

Figure 9. Correlations between observed and GRASS-simulated aboveground production (a) and peak live aboveground biomass (b). ●-CPER nitrogen+irrigated, X-CPER irrigated, ●-CPER nitrogen, ■-CPER control, ▲-Nairobi. CPER data from 1970-75, Nairobi from 1988-89. Data sources as in Fig. 5.
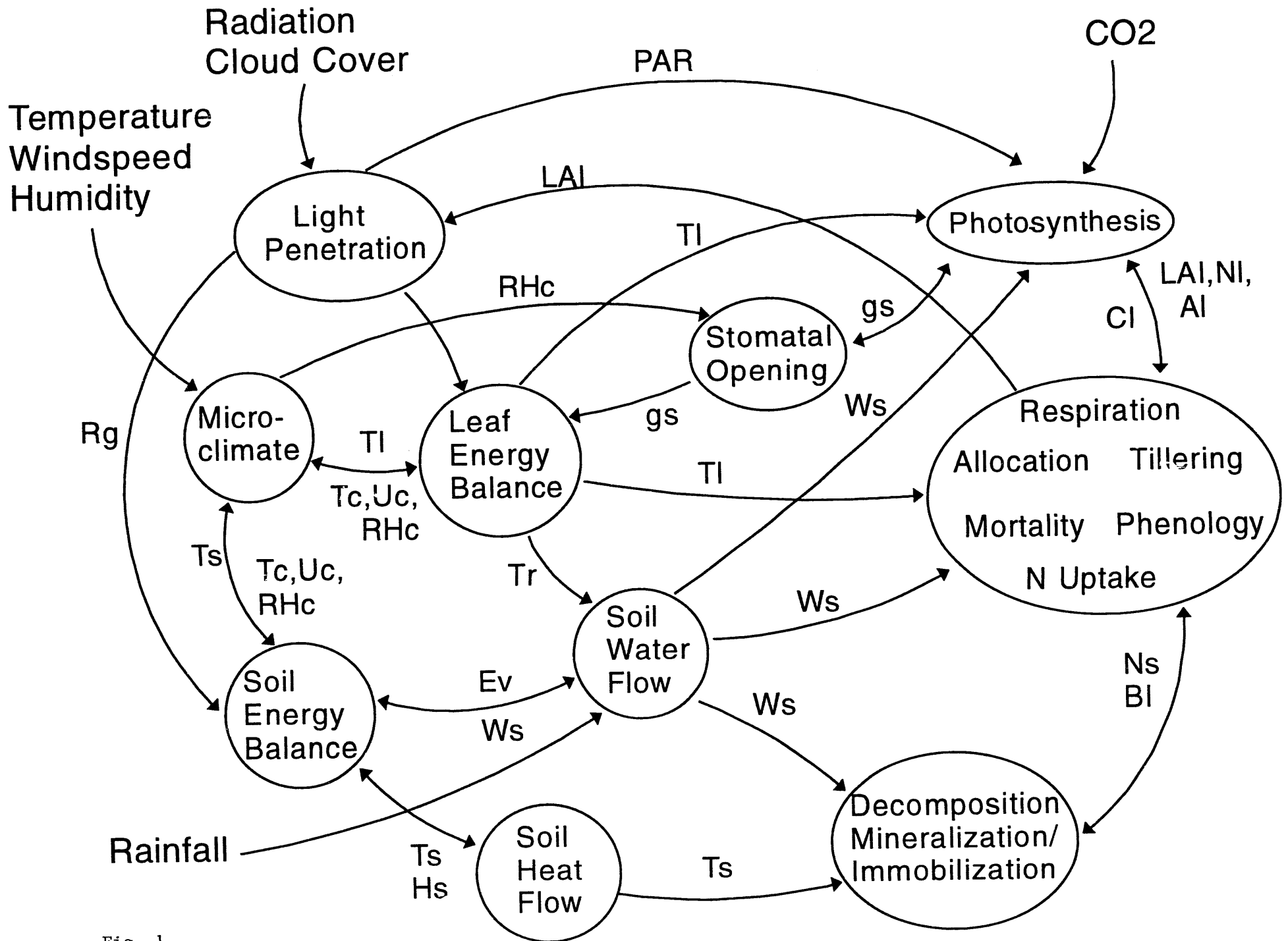
Fig. 1
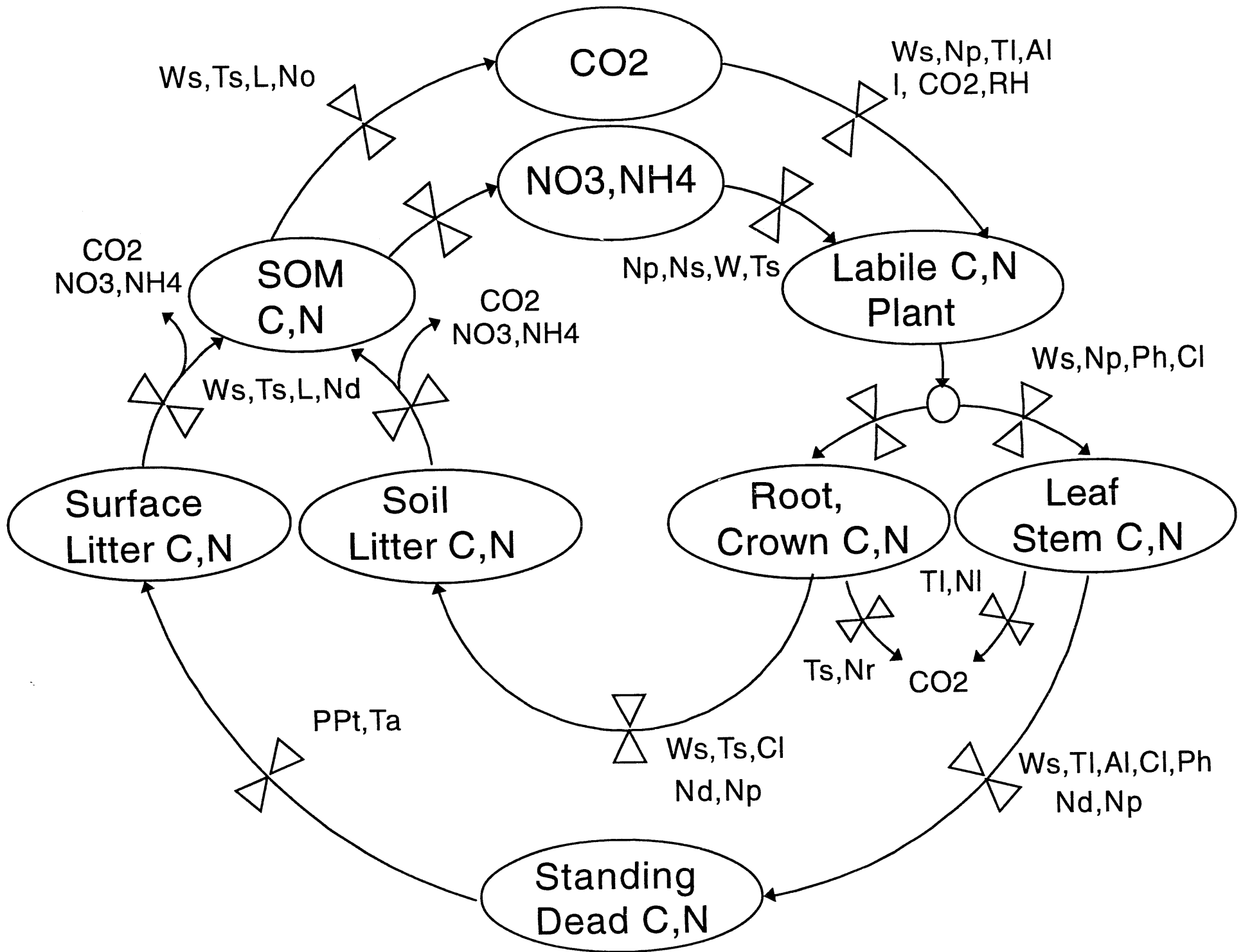
Fig. 2

Bouteloua gracilis
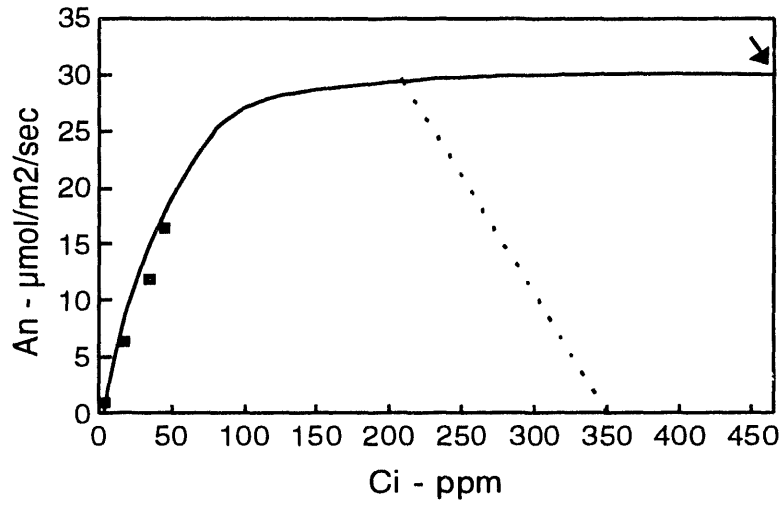
Andropogon gerardii
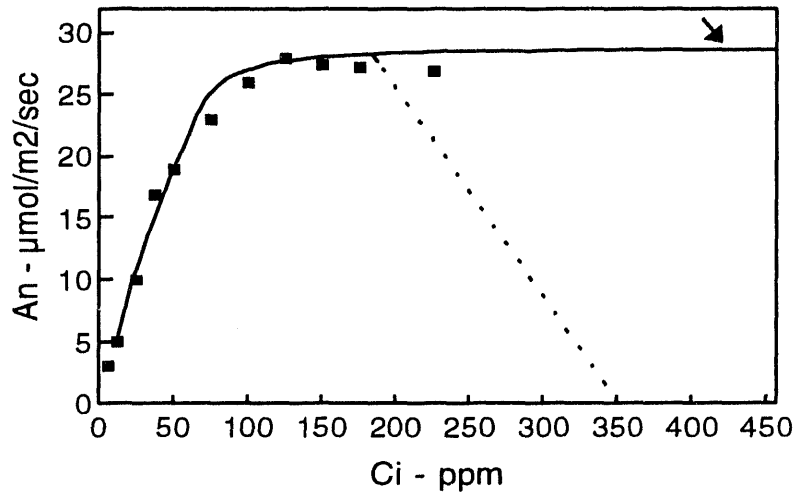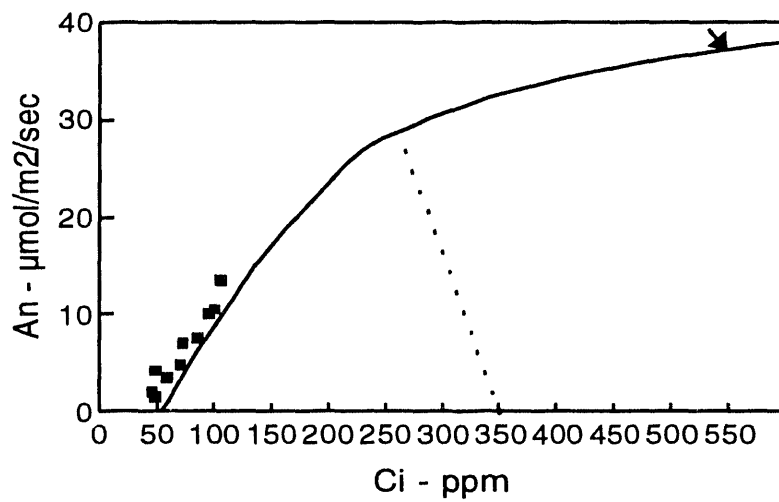
Agropyron smithii

Fig. 3

Bouteloua gracilis
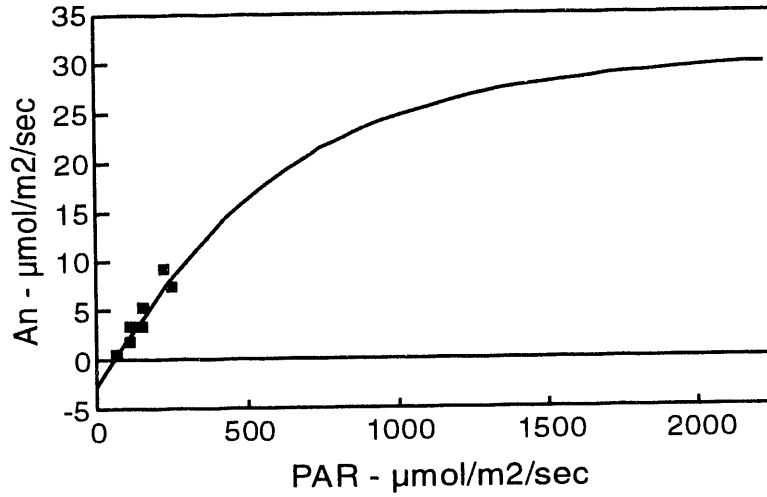
Andropogon gerardii
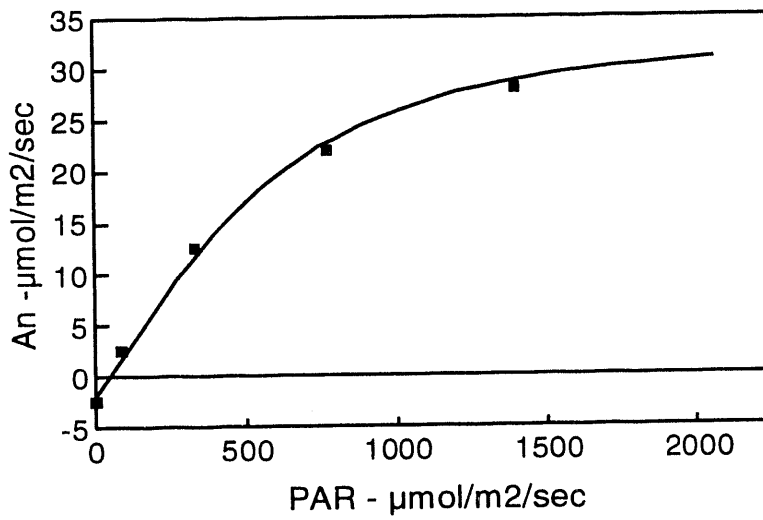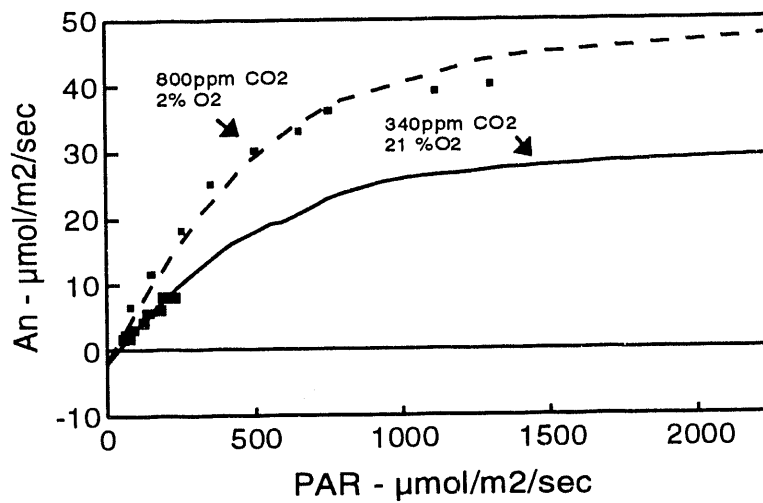
Agropyron smithii

Fig. 4

Bouteloua gracilis
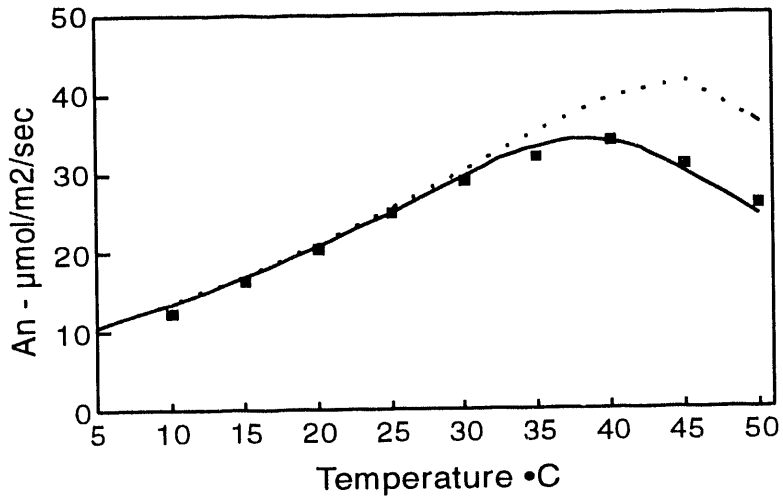
Andropogon gerardii
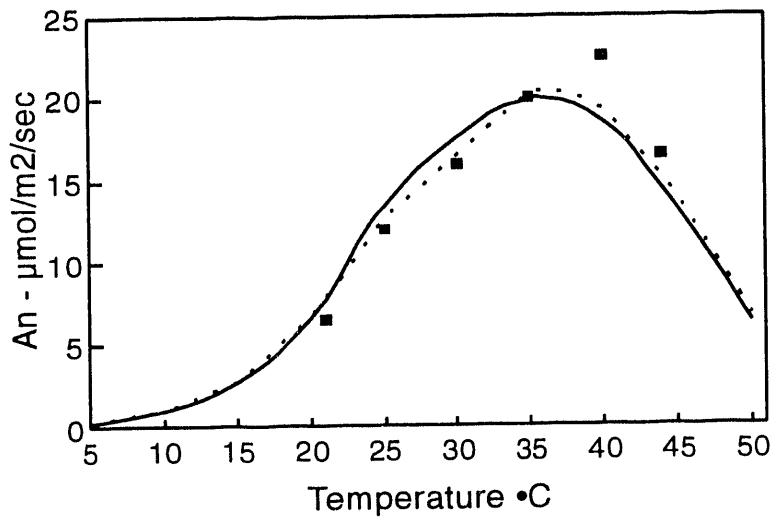
Agropyron smithii

Fig. 5

Themeda triandra

Fig. 6

a) Central Plains Experimental Range
GRASS Model 1973-1975
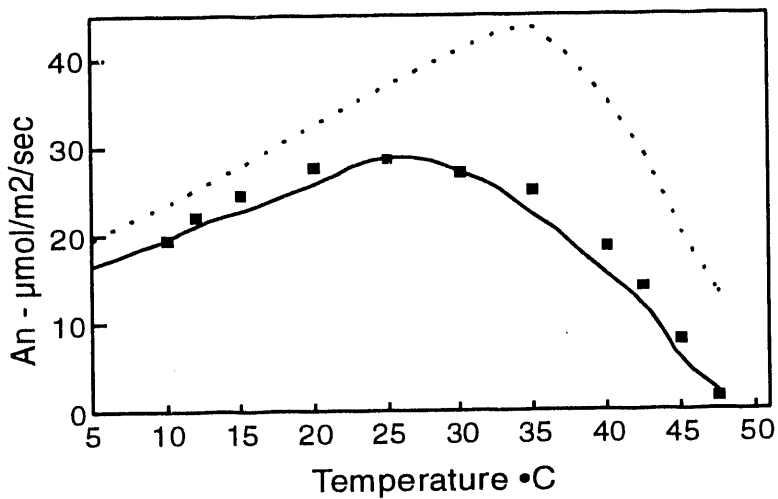
b) Nairobi National Park
GRASS Model 1984-1990
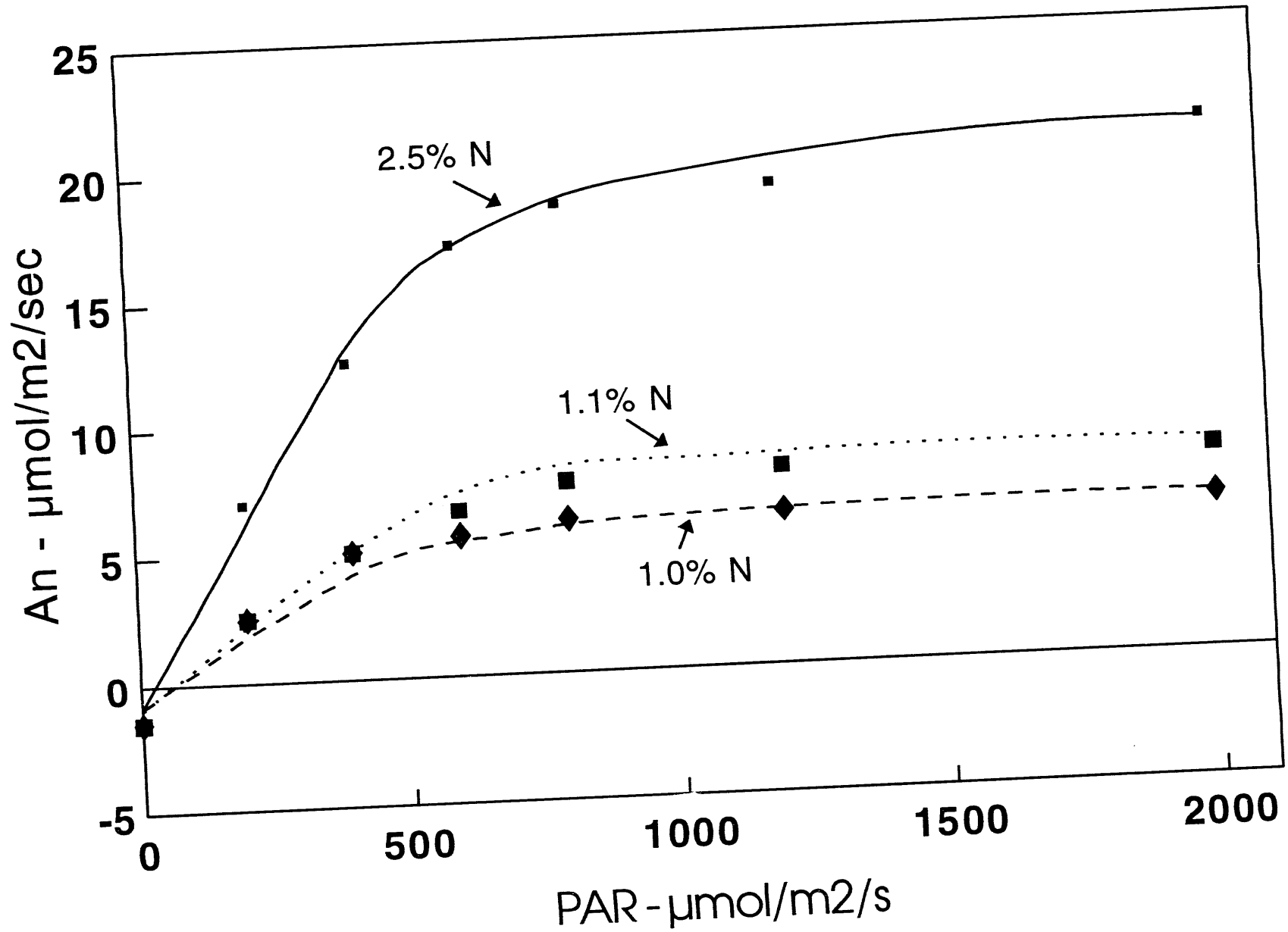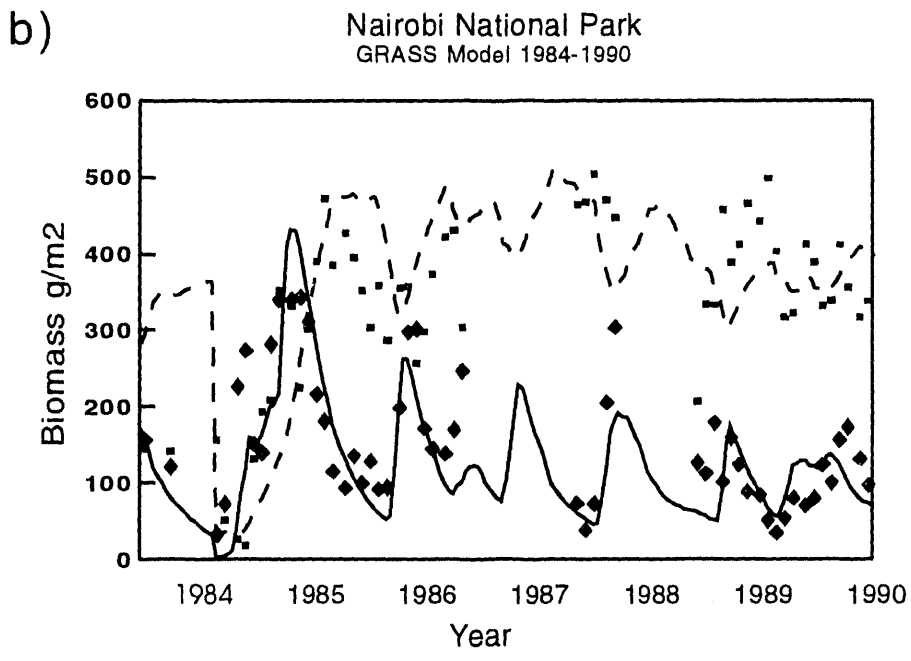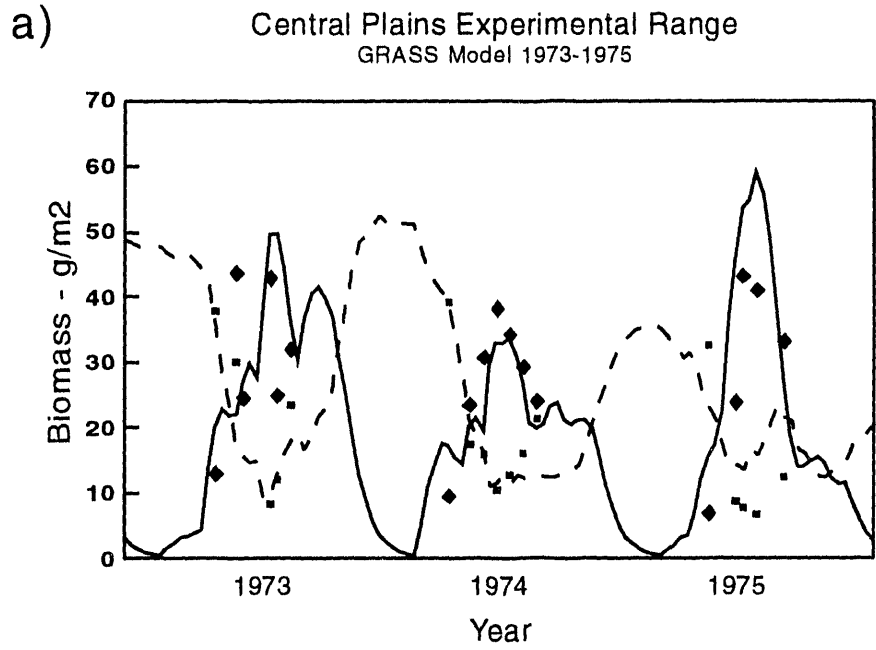
Fig. 7

a)

Green Biomass - Central Plains Experimental Range
1973-1975

$y=10.8+0.73x$ $r2=.35$
$p=0.01$
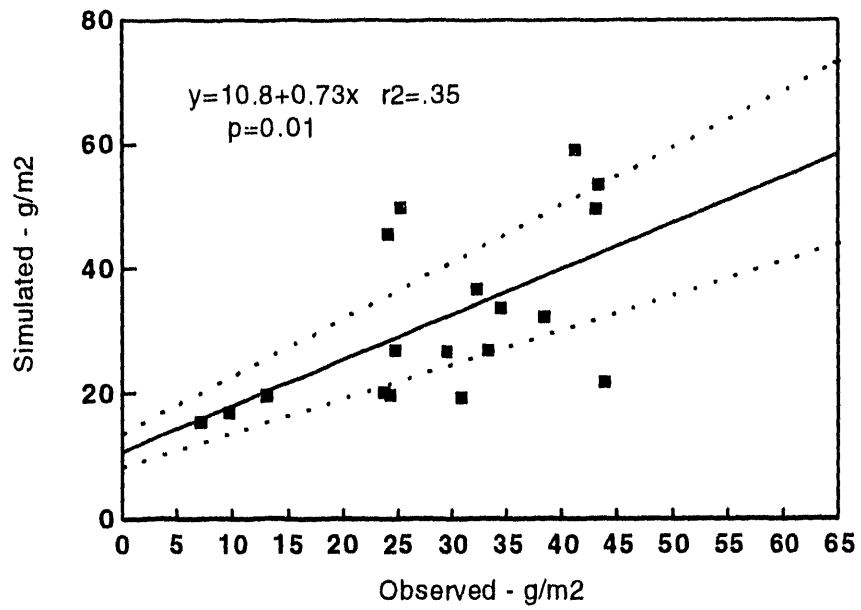
b)

Green Biomass - Nairobi National Park
1984-1990

$y=57+0.72x$ $r2=.56$
$p<0.001$

Fig. 8

a)

Aboveground Net Primary Production

y=54+0.91x   r2=.91

Simulated -g/m2

Observed -g/m2

b)

Peak Live Biomass

y=15+0.90x   r2=0.78

Simulated - g/m2

Observed - g/m2
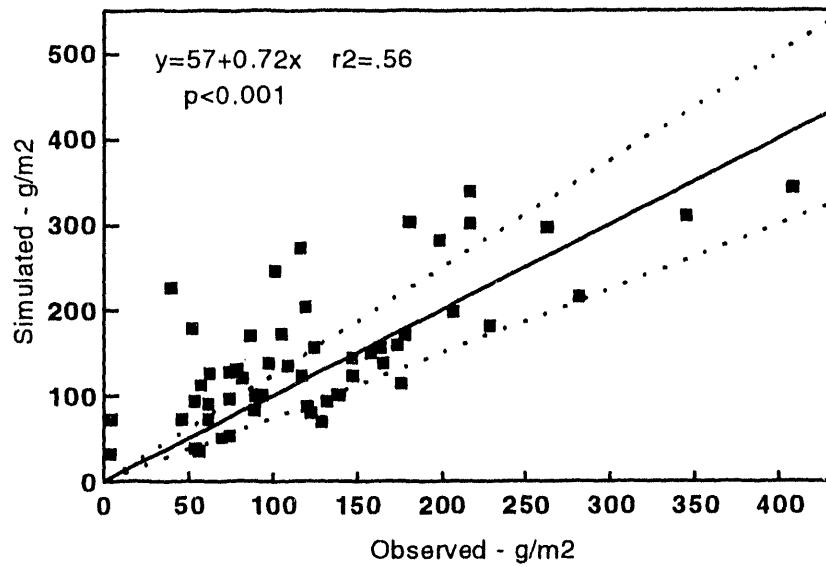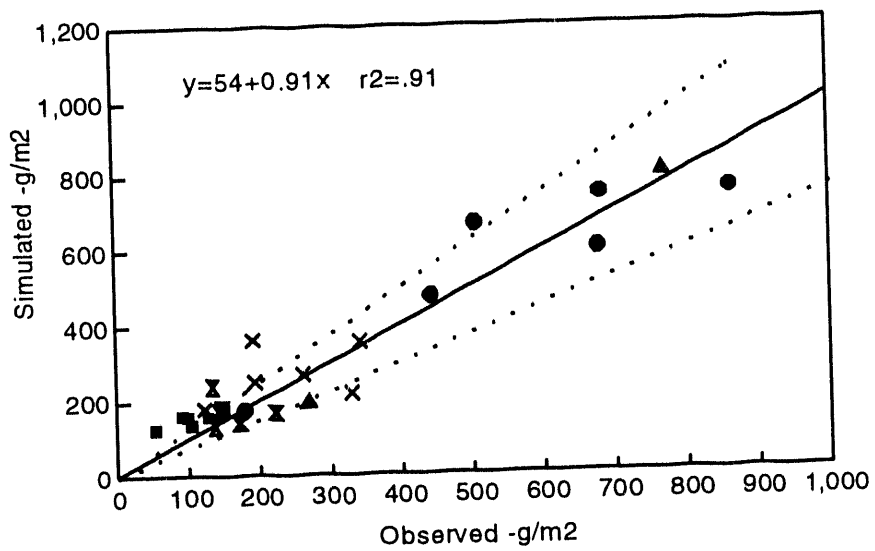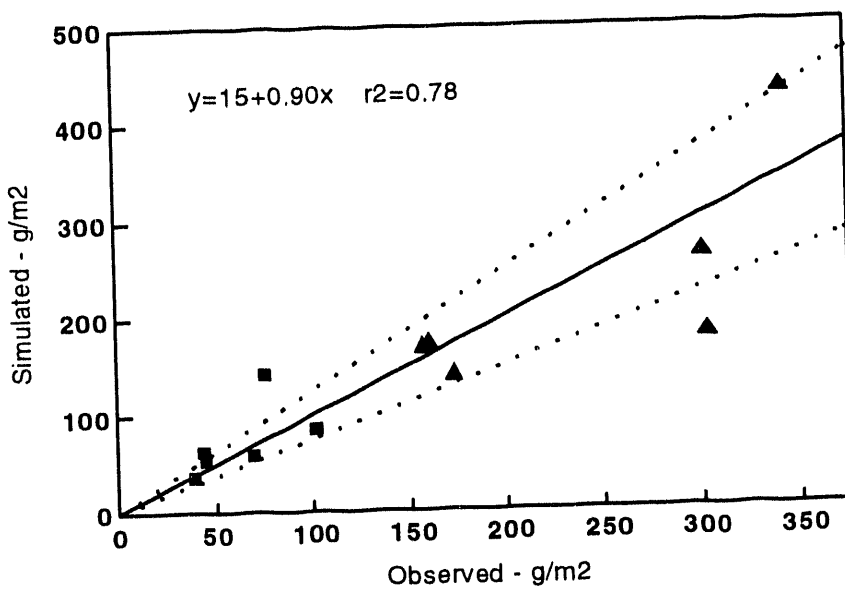
Fig. 9

CHAPTER 3
Potential Effects of Climate Change and Elevated CO_2
in Grasslands - Predictions of a High Resolution Ecosystem Model

Introduction

The effects of rising atmospheric CO_2 and climatic change on ecosystems are far from being well understood. There have been many short-term empirical studies of plant growth responses to CO_2 (reviewed by Kimball 1983, Cure and Acock 1985, Bazazz 1990). However, there is widespread concern that conclusions based on short-term studies, particularly of potted plants, do not account for processes such a acclimation, nutrient limitations and interactions with realistic climatic regimes (Dahlman 1985, Mooney et al. 1990, Drake 1992). The few field studies that have been conducted in grasslands have provided conflicting results. While a tussock tundra study showed no CO_2 effect on growth rate or photosynthesis (Tissue and Oechel 1987), C_3 plants in a salt marsh responded strongly and C_4 plants did not respond to elevated CO_2 (Curtis et al. 1989a,b). In a tallgrass prairie, however, C_4 grass production was substantially increased by elevated CO_2 (Owensby et al. 1993). A reasonable hypothesis is that these conflicting results are due to differences in nutrient, temperature and water limitations on productivity in these widely differing environments.

While simulation models have long been available to predict ecosystem responses to changed climate, few if any ecosystem level models have been capable of predicting plant responses to CO_2 with the level of mechanism required to capture all facets of the response (Reynolds and Acock 1985, Dahlman 1985). Highly simplified CO_2 effects on plant growth rate have been parameterized into some ecosystem models (e.g., Hanson et al. 1993, Leadly and Reynolds 1992). Detailed photosynthetic models respond realistically to CO_2 (Farquhar et al. 1980, Collatz et al. 1992, Chen et al. 1993), however there have been few attempts to incorporate detailed models at the ecosystem level. There is widespread fear that this is not appropriate, but this fear seems unjustified. Indeed, a detailed photosynthesis and plant growth model has been assembled and linked with an robust nutrient cycling model to conduct long-term simulations of 10->100 years (Coughenour, ms.). This model was used here to predict both short and long-term responses to changes in climate and atmospheric CO_2 concentrations.

The GRASS Model

The GRASS model simulates physiological and morphological details of plant growth. Plant growth is simulated with a two-day time step while photosynthesis and transpiration are simulated with two-hour time steps on alternate days. The GRASS model (Coughenour et al., 1984, Coughenour 1984) has evolved over the last several years. Its photosynthesis submodel is derived from the C_3 model of Farquhar et al. (1980), with extensions to simulate C_4 photosynthesis (Chen and Coughenour, in press), and linkages with the stomatal conductance submodel of Ball et al. (1987). Transpiration is predicted as part of leaf energy balance. Labile carbon reserves and phenology, and growth and maintenance respiration are simulated. Maintenance respiration is related to tissue nitrogen content (Ryan 1991). Plants take up mineral nitrogen is affected by soil N concentration and plant N:C ratio. GRASS plant growth submodels are linked with a daily time step implementation of the decomposition and nutrient cycling submodel of

CENTURY (daily CSOM). Decomposition responds to daily soil water content rather than monthly available water:PET ratio. Soil moisture budgets are simulated by coupling energy balance, transpiration and bare soil evaporation submodels with a daily soil water flux submodel (Parton 1978).

Photosynthesis and respiration interact to determine simulated growth responses to temperature. Photosynthesis is maximal at intermediate temperatures, with C_4 species exhibiting higher temperature optima that C_3 species (Pearcy and Ehleringer 1984, Kemp and Williams 1980). Respiration increases with temperature according to a Q10 function. Temperature affects growth initiation, phenology, senescence and mortality rates in the model. Temperature indirectly affects plant growth through its impact on rates of bare soil evaporation, decomposition and nitrogen mineralization. Water stress decreases photosynthesis, increases relative allocation of photosynthate belowground, and increases tissue mortality.

Simulated photosynthetic responses to atmospheric CO_2 involve biochemical and stomatal processes. Rubisco, the main carboxylating enzyme, responds to CO_2 concentration inside the leaf. The optimum temperature for photosynthesis is shifted upwards by elevated CO_2 in C_3 species due to reduced photorespiration (Long 1991). In C_4 species, CO_2-concentrating processes prevent Rubisco from being CO_2-limited at low CO_2, thus weakening the response of photosynthesis to CO_2. However, stomata close in response to elevated CO_2 (Ball et al. 1987, Collatz et al. 1992). Stomatal closure decreases water loss through transpiration while elevated CO_2 increases gaseous CO_2 flux through stomates. The overall result of stomatal closure responses to elevated CO_2 in both C_3 and C_4 species is an increase in water-use-efficiency (WUE).

Increased WUE of C_3 and C_4 plants enhances photosynthesis. Since less water is lost through transpiration, more photosynthate is produced from each mm of precipitation. Therefore, increased WUE will increase net primary production in water-limited environments. However, increased WUE will have little or no effect when water is not limiting. The increase in WUE leads to increased soil moisture levels, which ameliorates negative effects of water stress on other processes. Increased soil moisture content increases carbon allocation to shoots, reduces photosynthesis rate, reduces leaf senescence rate, and increases decomposition and N mineralization rates.

In some CO_2 response studies (Owensby et al. 1992b,) elevated CO_2 reduced plant nitrogen concentrations, while in others no effects were observed (Havelka et al. 1984, Loomis and Lafitte 1987). Curtis et al. (1989) found decreases in a C_3 species but not a C_4 species. Explanations for the decreases are still lacking. It has been hypothesized that increased carbon fixation dilutes nitrogen, but reduced N concentrations have been observed even when there is excess nitrogen in the environment (e.g., Larigauderie et al. 1988, Hocking and Meyer 1991, Conroy 1992). To dilute N concentrations to observed levels also requires unrealistically large increases in labile carbon in plant tissues. There is increasing evidence that CO_2 may regulate biochemical-level processes directly (Stitt 1991). Since the mechanisms are not understood, a 20% decrease in plant N:C is imposed as CO_2 increases from 350 to 700 ppm. This reduces dead tissue N:C correspondingly. Secondary effects of lower N concentration include: decreased maintenance respiration rate (which is directly proportional to tissue N concentration in the model, after Ryan [1991]), decreased photosynthetic light compensation point, reduced litter quality, and slower decomposition and N mineralization rates.

GRASS Model Responses to CO_2, Temperature and Precipitation

To better understand simulated plant responses to changed climate scenarios, the model was subjected to a factorial experiment with three levels of temperature and five levels of CO_2 and two precipitation levels (Fig. 1). Simulations were for ten year periods, with 0°, 3°, and 5°C temperature increases at 200, 350, 500, 750, and 900 ppm ambient CO_2, and precipitation amounts of +0% and +50% those observed over a 10 year period. A C_4 and a C_3 grass (*Bouteloua gracilis* and *Pascopyrum smithii* respectively) were simulated using 1970-79 Colorado shortgrass plains climate data, while a C_4 tropical grass (*Themeda triandra*) was simulated using 1980-89 Nairobi, Kenya climate data.

Total net primary production (NPP) of the Colorado C_4 grass responded in a weak asymptotic manner to increased CO_2, in parallel with an increase in WUE (grams C NPP per kg water transpired). Between 350 ppm and 750 ppm NPP increased by 9% at current temperatures. At +3°C and +5°C the increases were 11% and 12%. Increasing temperatures decreased NPP at current rainfall, but increased NPP under +50% rainfall. At +50% precipitation, responses to CO_2 were less pronounced: NPP increased 2-3% between 350 and 750 ppm at all temperatures.

The NPP responses of the Colorado C_3 grass to increasing CO_2 were larger than the C_4 responses. The increase in NPP between 350 and 750 ppm CO_2 was 15% under current climate conditions, but NPP increased by 41% and 66% at +3°C and +5°C. The larger relative increases at higher temperatures were mainly results of reduced NPP under elevated temperatures at 350 ppm CO_2. Elevated CO_2 reversed expected negative responses to increased temperature in the C_3 species, as predicted by Long (1991). At +50% precipitation, the NPP increases were reduced to 8-9%. While a 5°C temperature increment decreased NPP by 25% and 18% at 200 and 350 ppm CO_2, it increased NPP slightly (5-7%) at higher CO_2 concentrations, reflecting a shift in the photosynthetic temperature optima at high CO_2. Under +50% rainfall, however, 5°C temperature increases increased plant growth by 20%.

The tropical C_4 grass response to CO_2 was stronger than that of the temperate species. Between 350 ppm and 750 ppm CO_2, NPP increased 47%, 59% and 37% at +0°, +3° and +5°C. At +50% rainfall, the increases were less marked: 17%, 19% and 25%. Unlike the temperate species, a +5°C temperature increase caused a dramatic decrease in NPP. Although WUE remained relatively high at the high temperature total transpiration declined, indicating that stomates were more tightly closed.

The C_3 temperate grassland responded more strongly to elevated CO_2 than the C_4 grassland, as expected due to the near-saturation of C_4 photosynthesis with CO_2 above 350 ppm. CO_2 affected stomates and WUE in C_4 as well as C_3 species. However, water-limited C_4 grasses responded positively to elevated CO_2 through increased WUE. The positive NPP response of the C_4 tropical grass was equivalent to that of the temperate C_3 grass. The large response of the tropical grassland involved ecosystem level processes, such as increases in nitrogen mineralization rate due to moister soils. The strong water limitation of NPP at the Kenya site greatly increased positive responses to CO_2. When rainfall was increased by 50%, NPP enhancements due to elevated CO_2 were modest. Positive responses to CO_2 were weaker when water was less limiting, in both C_3 and C_4 plants.

The fact that 50% higher rainfall diminished positive responses to CO_2 at all three simulated grasslands is potentially important in that most climate change scenarios predict higher rainfall. Elevated rainfall actually reversed the negative effects of higher

temperature on NPP at the Colorado C_3 and C_4 sites, and diminished the negative effect of high temperature at the Kenya site.

Responses to elevated CO_2 in short-term experiments are partly due to transient ecosystem responses. Over longer time periods, transient responses may be diminished as system variables like soil nutrient pools adjust to the altered scenario. Although a ten year simulation experiment is long relative to the length of many empirical studies, it is important to also look at changes over multiple decades.

GRASS Model Responses to Climate Change Scenarios

The GRASS-daily CSOM model was subjected to $2xCO_2$ climate change scenarios generated from the Canadian Climate Centre (CCC) and Geophysical Fluid Dynamics Laboratory, High Scenario (GFHI) models of global climate change. Both scenarios were model generated from simulations of a projected doubling of atmospheric CO_2. According to the IPCC Scenario A (Houghton et al. 1990), these conditions should be reached over a 50 year period. While the two GSMs simulate similar changes in mean annual air temperature (2-5°C increases), predicted changes in precipitation were different. The GFHI model showed increases in precipitation for all regions, while the CCC model showed decreased in precipitation in the temperate steppe and humid savannas, and increases in other grassland regions.

The GRASS model was used to simulate C_4 (B. gracilis) and C_3 (P. smithii) ecosystems in Colorado and a C_4 grass (T. triandra) ecosystem in Kenya, with the same repeating patterns of base weather data that were used in the CENTURY experiments, with and without CO_2 doubling. Day and night temperatures were increased equally. Relative humidity and cloud cover were not changed. The model was run for an initial 50 years with no climatic changes. Then, the climate was gradually ramped-up to the CCC and GFHI $2xCO_2$ scenarios over a 50-year period, followed by a 25-year period over which the model was allowed to adjust to the scenarios. The mean results of the 25-year period after the end of the ramp change are shown in Figs. 2-5. Dynamics in Fig. 6 begin 25 years prior to the start of the ramp.

The GRASS model responded quite differently to the CCC and GFHI climate-change-only scenarios at the Colorado site (Fig. 2). The CCC scenario without a CO_2 doubling decreased NPP 52% in the C_3 grass and 48% in the C_4 grass. In contrast, the GFHI scenario increased C_3 NPP by 13% and decreased C_4 NPP by 12%. At the Kenya site, the differences between scenarios were much less pronounced. NPP decreased 3% under the CCC scenario and 6% under the GFHI scenario, without CO_2 doubling.

The large discrepancies in model responses to the two climate change scenarios in Colorado can be attributed mainly to precipitation. While the CCC model predicted a 5.2 mm increase in annual precipitation, the GFHI model predicted a 38.0 mm increase (Table 2). During the March-August growing season, CCC predicted a 9.2 mm decrease while GFHI predicted a 27.5 mm increase. At the Kenya site, CCC predicted a 2.9 mm annual decrease while GFHI predicted a 72.0 mm annual increase. However, during the November-May wet season, both models predicted increased rainfall: CCC added +18.6 mm while GFHI added +36.0 mm.

Doubling CO_2 without climatic change increased NPP 6%, 5% and 40% in the Colorado C_4 and C_3, and the Kenya C_4 grasslands, respectively. Doubling CO_2 ameliorated negative NPP responses to climate change scenarios in Colorado and accentuated positive NPP responses in Kenya. The CCC scenario with CO_2 doubling decreased NPP by 20% in

the C_3 grass and 37% in the C_4 grass, relative to the control. NPP increased 46% in Kenya under both scenarios of CO_2 doubling and climatic change.

Elevated CO_2 concentrations might favor C_3 over C_4 species (e.g., Carter and Peterson 1983, Bazazz et al. 1989). This hypothesis was only supported by the Colorado short-term simulations (Fig. 1). It was not supported by the long-term simulations (Fig. 2). In the long-term simulations, total NPP of C_3 and C_4 grasses responded similarly to CO_2 alone: $2xCO_2$ increased NPP 5% in the C_3 grass and 7% in the C_4 grass. The CCC scenario with $2xCO_2$ decreased NPP by 25% and 37% in C_3 and C_4 grasses respectively, which would suggest a competitive advantage for C_4 species under this warm, dry scenario. The GFHI scenario with $2xCO_2$ increased NPP 13% in the C_3 and 21% in the C_4 grass, which also indicated that C_4 grasses might be favored. Indeed, the large stimulation of NPP in the tropical C_4 grassland suggested that C_4 species would fare quite well in warm, water-limited ecosystems.

Transpiration rate responses to climate and CO_2 varied among sites (Fig. 3). Minor reductions in transpiration rate in response to $2xCO_2$ were simulated at the Colorado C_4 site. In contrast, transpiration rates were much reduced by elevated CO_2 at the C_3 site, but less so with the increased moisture of the GFHI scenario. Differences in transpiration responses likely contributed to different C_3 and C_4 NPP responses to CO_2. The greater reduction in transpiration rate of the C_3 species was due to greater stomatal and carbon assimilation (An) response of C_3 species to elevated CO_2. The magnitude of stomatal opening in response to elevated An and closing in response to elevated CO_2 is greater in C_3 species (see Ball et al. 1987) than C_4 species (see Collatz et al. 1992).

Transpiration rates at the Kenya site were lower than at Colorado sites, due to much higher (e.g., 5x) leaf area indices. In contrast to the Colorado C_4 site, elevated CO_2 reduced transpiration rate significantly in Kenya. The reduction in transpiration rate was much larger than the Colorado C_4 response. Stomatal closure due to elevated CO_2 decreased moisture stress on plants and decomposers in Kenya. Responses were not reduced by low temperatures as they were in Colorado. This generated a positive feedback as plant growth was accelerated by lower water stress and by increased nitrogen availability.

Climate change and CO_2 doubling affected net nitrogen mineralization (Nmin) rates (Fig. 4). Nmin responses contributed to differences in NPP responses among sites. Doubling CO_2 alone decreased Nmin at both Colorado sites, but more so at the C_3 site. This response was caused by the negative effect of reduced litter nitrogen concentration. Significantly, despite this reduced N availability, NPP was not diminished but was increased by elevated CO_2 (Fig. 1) due to increased plant nitrogen use efficiency (NUE). It is likely that nitrogen mineralization would have been stimulated, or that it would not have declined if litter N concentrations were not reduced, since NPP and soil moisture were enhanced by CO_2. Thus, while nutrient limitation did reverse positive responses to CO_2, the reversal could be weakened by increased NUE.

The CCC climate scenario alone reduced N mineralization (Nmin) on both the C_3 and C_4 sites, due to drier soil conditions and smaller litter inputs. The GFHI climate scenario alone increased Nmin at the C_3 and C_4 sites, due to reduced moisture limitations on decomposition rate. Adding $2xCO_2$ to the CCC scenario decreased Nmin very slightly at the C_4 site, and increased Nmin at the C_4 site. This was probably due to the greater NPP response of the C_3 grassland, with consequently higher litter inputs. Adding $2xCO_2$ to the GFHI scenario decreased Nmin slightly at the C_4 site, but greatly decreased Nmin

at the C_3 site. The reduction in Nmin with GFHI suggesting increased importance of litter quality when litter inputs are large.

Both climate change scenarios alone elevated Nmin greatly at the Kenya site, due to moisture soil. Surprisingly, doubling CO_2 increased Nmin by 24% despite decreases in litter quality. Nmin at the Kenyan site was primarily limited by soil moisture, in contrast to the Colorado site where temperature played a large role. The increased WUE of the C_4 grass under $2xCO_2$ increased soil moisture, which then increased decomposition rate. Similarly, Rice et al. (1992) observed elevated microbial biomass and respiration under elevated CO_2 in a dry year, but not in a wet year. Increased Nmin likely contributed to increased plant growth, which was then recycled through decomposition, thus further elevating Nmin. This positive feedback loop was undoubtedly enhanced by the high rate of N recycling in this tropical system relative to more temperature-limited systems.

The effect of $2xCO_2$ alone at the Kenya site was to increase NPP by 40%, despite only a 24% increase in Nmin and a 19% increase in plant N uptake. This can be explained by the 15% lower nitrogen concentrations in dying roots and shoots, and the associated increase in nitrogen use efficiency. The total amount of N in the system was actually slightly lower (5%) in the elevated CO_2 simulation due to greater fire losses. Thus, $2xCO_2$ enhanced nitrogen recycling rate. Greater total quantities of nitrogen uptake (kgN/ha) have also been observed in a tallgrass prairie, despite reduced %N concentrations in plant biomass (C. Owensby et al. 1992b).

Soil organic matter (SOM) was reduced by 25-27% by the CCC scenario without $2xCO_2$ in Colorado (Fig. 5), due to lower carbon inputs from NPP. With $2xCO_2$, SOM was reduced only 5% under C_3 grass, but still declined by 22% under C_4 grass. In Kenya, the CCC scenario without $2xCO_2$ decreased SOM 5%, but with $2xCO_2$, it increased SOM by 10%. SOM declined by 1-2% under the GFHI scenario in Colorado. With $2xCO_2$, however, GFHI decreased SOM 1% under C_4 and increased SOM 3% under C_3 grasses. In Kenya, the GFHI scenario decreased SOM by 8% without $2xCO_2$, and increased SOM by 8% with $2xCO_2$. Increased soil carbon under elevated CO_2 was not accompanied by elevated soil N. Instead, the C:N ratio of the soil organic matter increased by 6%. To summarize, elevated CO_2 is likely to have little effect on ecosystem carbon storage in Colorado while it will increase carbon storage 8-10% in Kenya.

Modeled responses to changed climate and CO_2 demonstrated considerable interannual variability (Fig. 6). For example, under the GFHI climate scenario, Colorado C_3 NPP increased by 50-80% in some years, while in other years there were little, no, or even negative responses. Simulations indicated that CO_2 increases may ameliorate the negative effects of dry years. For example, periodic dry years in the Kenyan climate data reduced NPP, even under the climate change scenarios (Fig. 6c). However, CO_2 doubling often prevented these decreases. Indeed, most of the positive response to CO_2 could be attributed to greater increases in the drier years, as would be expected from the relatively greater importance of an increase in WUE in drier years. Similarly, Owensby et al. (1993a) found that NPP of a C_4 grass was stimulated by CO_2 in a dry rainfall year, while it was not stimulated in a wet year.

GRASS-daily CSOM modeling experiments indicated that GCM predictions of precipitation have considerable influence on predicted ecosystem responses. Unfortunately, there appears to be large uncertainty in GCM precipitation predictions. Since much of the predicted ecosystem responses to changed climate are due to altered precipitation, this uncertainty undermines confidence in ecological model predictions. For

example, the CCC scenario with $2xCO_2$ decreased simulated NPP 20-37% in Colorado the GFHI scenario with $2xCO_2$ increased NPP by 20%.

Elevated CO_2 may cause relatively small increases in NPP at some sites and large increases at others. Plant responses to CO_2 are modified in complex ways by moisture and nutrient availabilities. In general, the model suggested that CO_2 has less of an effect under reduced moisture stress. However, nutrient limitations reduced CO_2 responses. Similarly, response predictions that are based solely C_3 vs C_4 photosynthetic characteristics are likely to be oversimplifications. C_4 and C_3 responses are each modified by moisture stress and temperature.

Elevated CO_2 counteracts negative effects of increased temperatures and decreased precipitation. The reversed negative impact of elevated temperatures on C_3 species is particularly notable (e.g., Fig. 1b), and is probably caused by a shift in photosynthetic temperature optima (Long 1991). The increased importance of CO_2 in dry years is important, in that negative effects of periodic droughts could be smoothed ameliorated, thus reducing inter-annual variability in NPP.

Ecosystem modeling clearly showed that indirect effects and interactions among many processes are important. Responses to single variables were modified by responses to other variables. Positive effects of predicted increases in rainfall are diminished by increased temperature, for example. At the Kenyan site, the GRASS model predicted a 6% decrease in NPP due to the GFHI climate change alone, despite a +72.0 mm/yr increase in rainfall. Interactions among plant and soil processes elicited system-level responses. Thus, while $2xCO_2$ increased Nmin in Kenya it decreased Nmin in Colorado due to differences in the indirect effects of plants on soil moisture and decomposition rate at the two sites.

Literature Cited

Ball, J.T., Woodrow, I.E. and J.A. Berry. 1987. A model predicting stomatal conductance its contribution to the control of photosynthesis under different environmental conditions. in: I. Biggins, (ed.), Progress in Photosynthesis Research. Vol. IV. Martinees Nijhof, Dordrecht. pp. 221-224.

Bazazz, F.A. 1990. The responses of natural ecosystems to the rising global CO_2 levels. Annu. Rev. Ecol. Syst. 21:167-196.

Bazazz, F.A., K. Garbutt, E.G. Reekie and W.E. Williams. 1989. Using growth analysis to interpret competition between a C_3 and a C_4 annual under ambient and elevated CO_2. Oecologia 79:223-235.

Carter, D.R. and K.M. Peterson. 1983. Effects of a CO_2-enriched atmosphere on the growth and competitive interaction of a C_3 and C_4 grass. Oecologia 58:188-193.

Chen, D.-X., Coughenour, M.B., Knapp, A.K, and Owensby, C.E. 1993. Mathematical simulation of C_4 grass photosynthesis in ambient and elevated CO_2. Ecol. Model. (in press).

Collatz, G.J., M. Ribas-Carbo and J.A. Berry. 1992. Coupled photosynthesis-stomatal conductance model for leaves of C_4 plants. Aust. J. Plant Physiol. 19: - .

Conroy, J. 1992. Influence of elevated atmospheric CO_2 concentrations on plant nutrition. Aust. J. Biol. Sci. xx:xx-xx.

Coughenour, M.B. 1984. A mechanistic simulation of water use, leaf angles and grazing in east African graminoids. Ecol. Model. 26:127-1284.

Coughenour, M.B., S.J. McNaughton, L.L. Wallace. 1984. Modeling primary production of perennial graminoids: Uniting physiological processes and morphometric traits. Ecol. Model. 23:101-134.

Cure, J.D. and B. Acock. 1986. Crop response to carbon dioxide doubling: a literature survey. Agric. For. Meteorol. 38:127-145.

Curtis, P.S., B.G. Drake, P.W. Leadly, W.J. Arp, and D.F. Whigham. 1989. Growth and senescence in plant communities exposed to elevated CO_2 concentrations on an estuarine marsh. Oecologia 78:20-26.

Curtis, P.S., G.G. Drake and D.F. Whigham. 1989b. Nitrogen and carbon dynamics in C_3 and C_4 estuarine marsh plants under elevated CO_2 in situ. Oecologia 78:297-301.

Drake, B.G. 1992. The impact of rising CO_2 on ecosystem production. Water, Air and Soil Pollution 64:25-44.

Dahlman, R.C. 1985. Modeling needs for predicting responses to CO_2 enrichment: Plants communities and ecosystems. Ecol. Model. 29:77-106.

Farquhar, G.D., S. Von Caemmerer and J.A. Berry. 1980. A biochemical model of photosynthetic CO_2 assimilation in leaves of C_3 species. Planta 149:78-90.

Hanson, J.D., B.B. Baker and R.M. Bourdon. 1993. Comparison of the effects of different climate change scenarios on rangeland livestock production. Agric. Syst. 41, in press.

Havelka, U.D., V.A. Wittenbach and M.G. Boyle. 1984. CO_2 enrichment effects on wheat yield and physiology. Crop Sci. 24:1146-1150.

Hocking, P.J. and C.P. Meyer. 1991. Carbon dioxide enrichment decreases critical nitrate and nitrogen concentrations in wheat. J. Plant Nutr. 14:571-584.

Houghton, J.T. G.J. Jenkins and J.J. Ephraums, Eds. 1990. Climate Change: The IPCC Scientific Assessment. Cambridge University Press.

Hunt, H.W., M.J. Trlica, E.F. Redente, J.C. Moore, J.K. Detling, T.G.F. Kittel, D.E. Walter, M.C. Fowler, D.A. Klein, and E.T. Elliott. 1991. Simulation model for the ecosystem level effects of climate change in temperate grasslands. Ecological Modelling, 53:205-246.

Kemp, P.R. and G.J. Williams III. 1980. A physiological basis for niche separation between *Agropyron smithii* (C_3) and *Bouteloua gracilis* (C_4). Ecol. 61:846-858.

Kimball, B.A. 1983. Carbon dioxide and agricultural yield: an assemblage and analysis of 430 prior observations. Agron. J. 75:779-788.

Larigauderie, A., D.W. Hilbert and W.C. Owchel. 1988. Effect of CO_2 enrichment and nitrogen availability on resource acquisition and resource allocation in a grass, *Bromis mollis*. Oecologia 77:544-549.

Leadley, P.W. and J.F. Reynolds. 1992. Long-term response of an arctic sedge to climate change: a simulation study. Ecol. Appl. 2:323-340.

Loomis, R.S. and H.R. Lafitte. 1987. The carbon economy of a maize crop exposed to elevated CO_2 concentrations and water stress, as determined by elemental analysis. Field Crops Res. 17:63-74.

Long, S.P. 1991. Modification of the response of photosynthetic productivity to rising temperature by atmospheric CO_2 concentrations: Has its importance been underestimated? Plant, Cell and Environ. 14:729-739.

Mooney, H.A., B.G. Drake, R.J. Luxmore, W.C. Oechel and L.F. Pitelka. 1990. Predicting ecosystem responses to elevated CO_2 concentrations. Bioscience 41:96-104.

Owensby, C.E., P.I. Coyne, J.M. Ham, L.M. Auen and A.K. Knapp. 1993a. Biomass production in a tallgrass prairie ecosystem exposed to ambient and elevated levels of CO_2. Ecol. Appl. in press.

Owensby, C.E., P.I. Coyne and L.M. Auen. 1993b. Nitrogen and phosphorous dynamics of a tallgrass prairie ecosystem exposed to elevated carbon dioxide. manuscript.

Parton, W.J. 1978. Abiotic submodel of ELM grassland simulation model. in: G. Innis, ed., Grassland Simulation Model. Springer-Verlag.

Pearcy, R.W. and J. Ehleringer. 1984. Comparative ecophysiology of C_3 and C_4 plants. Plant Cell Environ. 7:1-13.

Reynolds, J.F. and B. Acock 1985. Predicting the responses of plants to increasing carbon dioxide: a critique of plant growth models. Ecol. Model. 29:107-129.

Rice, C.W., F.O. Garcia, C.O. Hampton and C.E. Owensby. 1992. Soil microbial biomass and respiration under increased levels of atmospheric CO_2. Agron. Abstr. p. 258.

Ryan, M. 1991. The effects of climate change on plant respiration. Ecol. Appl. 1:157-167.

Stitt, M. 1991. Rising CO_2 levels and their potential significance for carbon flow in photosynthetic cells. Plant, Cell and Environ. 14:741-762.

Tissue, D.L., and W.C. Oechel. 1987. Physiological response of *Eriophorum vaginatum* to field elevated CO_2 and temperature in the Alaskan tussock tundra. Ecol. 68:401-410.

Figure Legends

Figure 1. GRASS-daily CSOM model responses to CO_2 and temperature with ten years of observed climate data. (a) Colorado C_4 species (*B. grama*), (b) Colorado C_3 species (*A. pascopyrum*), (c), Kenyan C_4 species (*T. triandra*), (d) Colorado C_4 species with +50% precipitation, (e) Colorado C_3 species with +50% precipitation, (f) Kenya with +50% rainfall.

Figure 2. GRASS-daily CSOM model mean annual net primary production (NPP) responses in the final 25 years of simulations in which the first 50 years were subject to an observed repeated 25-year weather data set, the next 50 years were subject to a gradual ramp-up to doubled CO_2 or doubled CO_2 and changed climate scenarios, and the final 25 years were held constant at the final scenario. CCC-Canadian Climate Center model, GFHI-Geophysical Fluid Dynamics Lab High scenarios. The control run has no climate or CO_2 change. The +CO_2 run is a 2xCO_2 ramp change only.

Figure 3. GRASS-daily CSOM responses of transpiration rate per unit leaf area index (LAI) in the final 25 years of the climate change scenarios in Fig. 2. Transpiration rate was calculated by dividing season-long transpiration by peak leaf area index.

Figure 4. GRASS-daily CSOM responses of annual net nitrogen mineralization in the final 25 years of the climate change scenarios in Fig. 2.

Figure 5. GRASS-daily CSOM responses of total soil carbon in the final 25 years of the climate change scenarios in Fig. 2.

Figure 6. Temporal dynamics of total annual NPP responses to the GFHI ramp scenarios of Figs. 2-5. (a) Colorado C_4 grassland,(b) Colorado C_3 grassland,(c) Kenyan C_4 grassland.

Figure 7. Temporal dynamics of total annual NPP responses to the CCC ramp scenarios of Figs. 2-5. (a) Colorado C_4 grassland, (b) Colorado C_3 grassland, (c) Kenyan C_4 grassland.
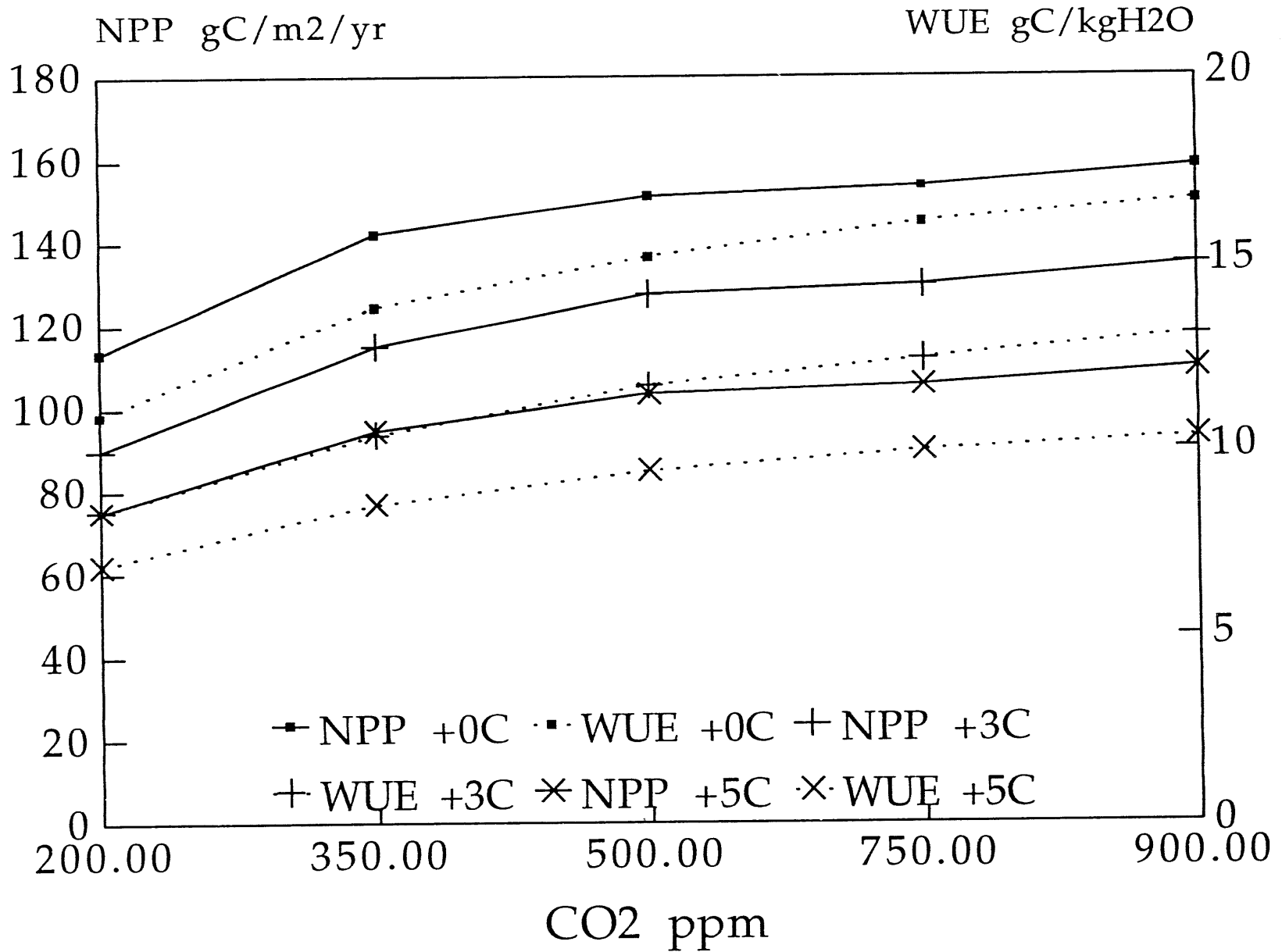
Fig. 1a
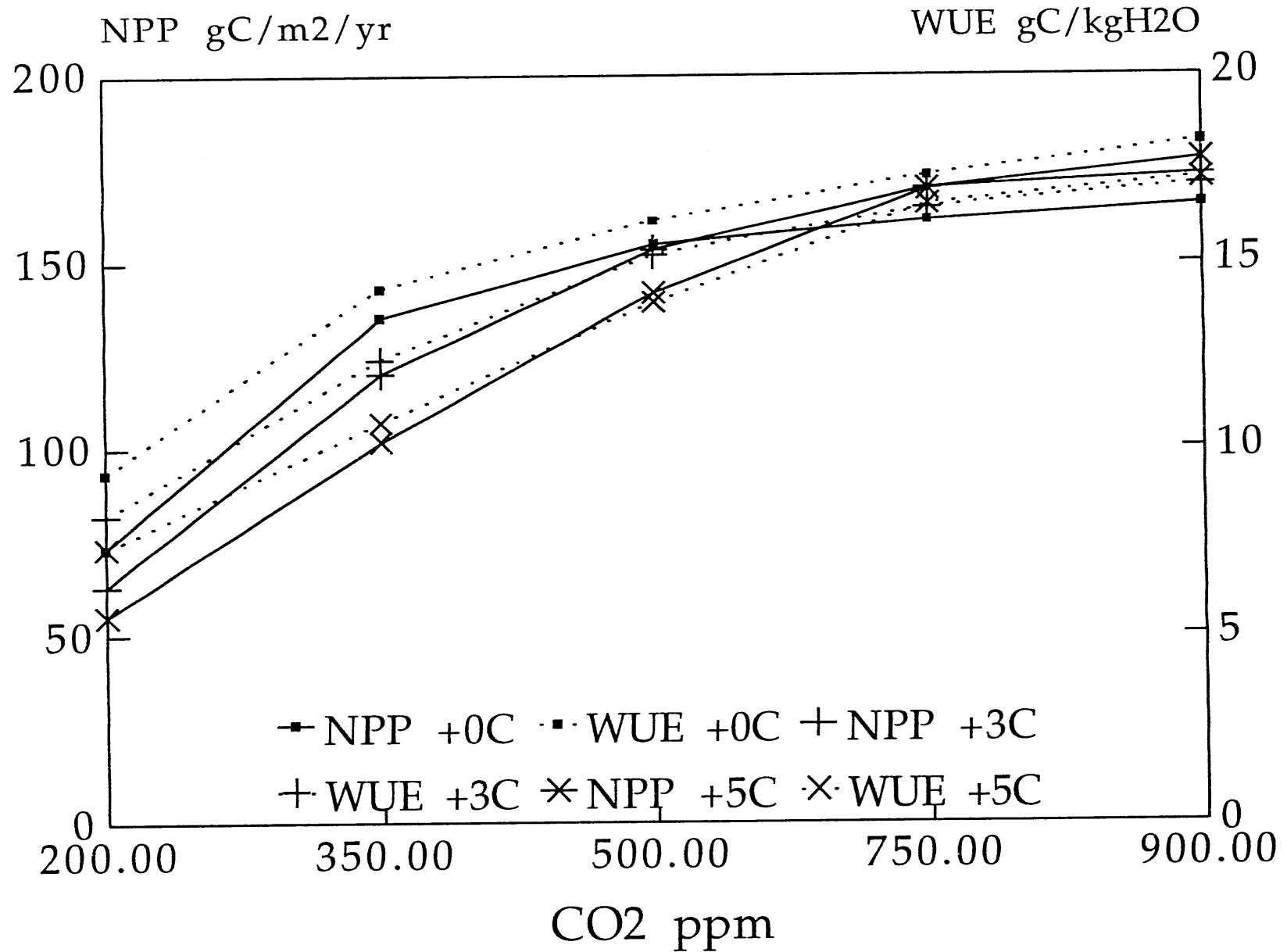
Colorado - C3

Fig. 1b

Kenya - C4
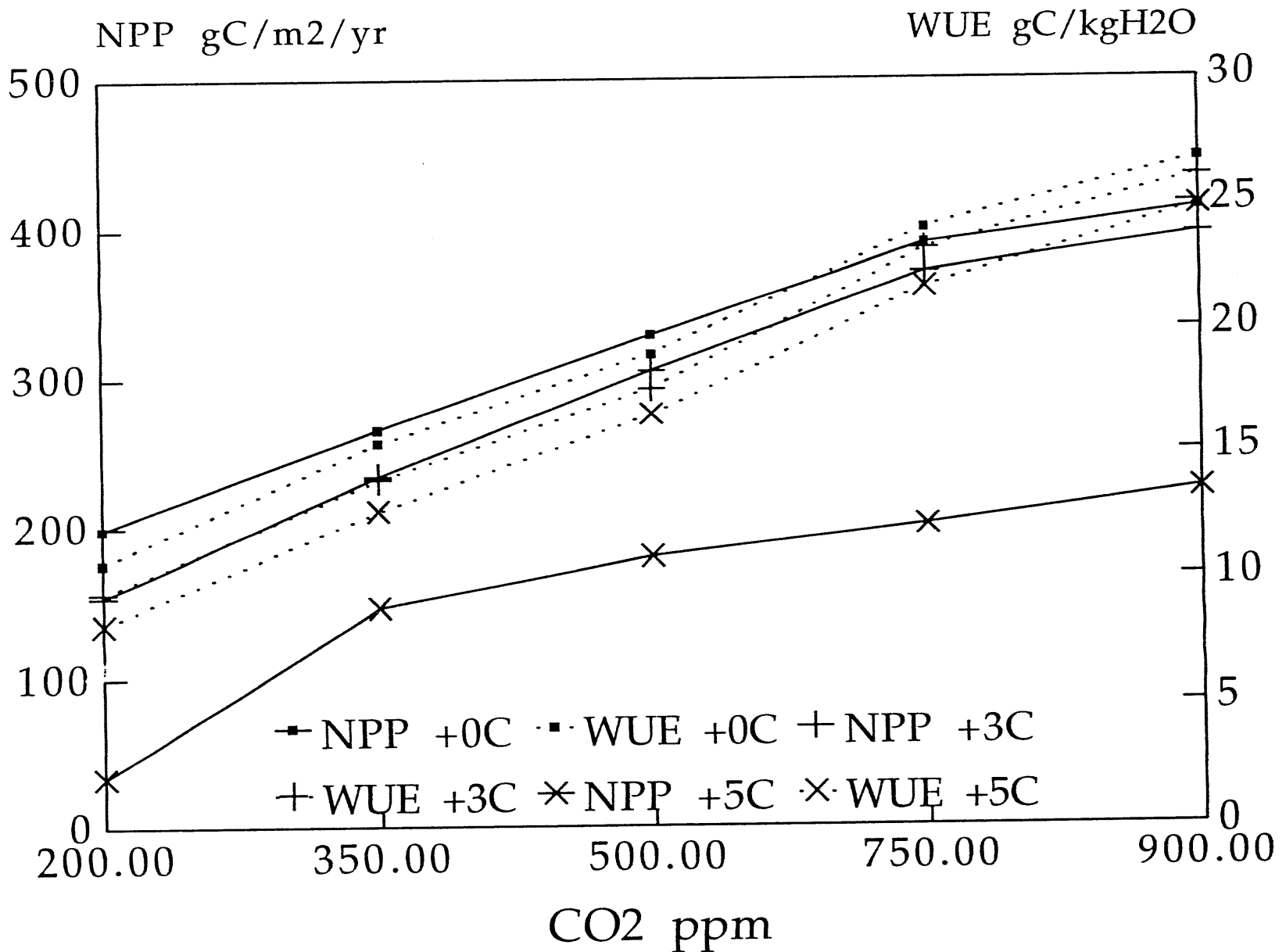
Fig. 1c

Colorado - C4
+50% Rainfall

NPP gC/m2/yr

WUE gC/kgH2O

CO2 ppm

Legend:
- NPP +0C
- WUE +0C
- NPP +3C
- WUE +3C
- NPP +5C
- WUE +5C
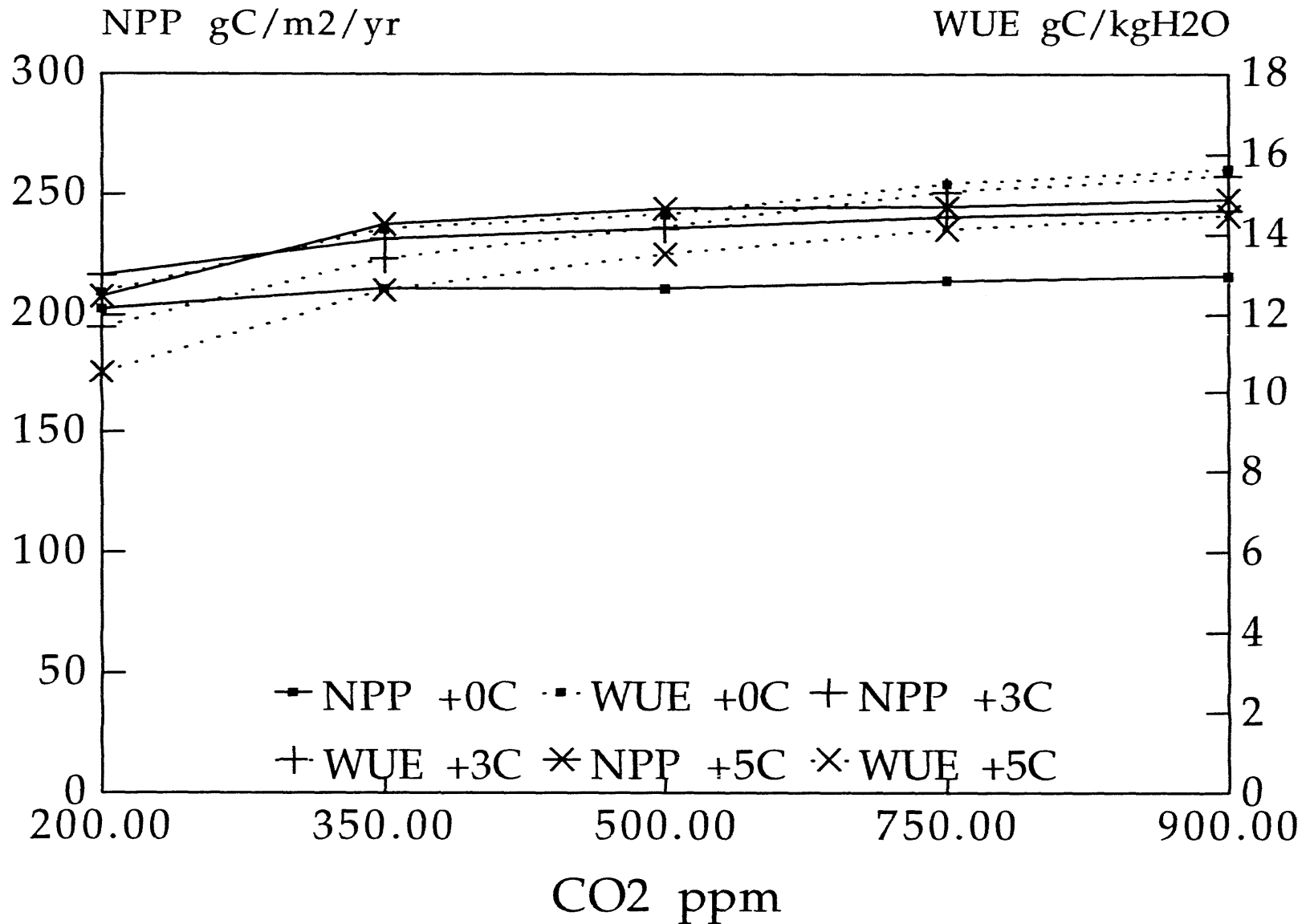
Fig. 1d

Colorado - C3

+50% Rainfall

NPP gC/m2/yr

WUE gC/kgH2O

Legend: ■ NPP +0C ···■ WUE +0C ┼ NPP +3C ╪ WUE +3C ✳ NPP +5C ✕ WUE +5C

CO2 ppm
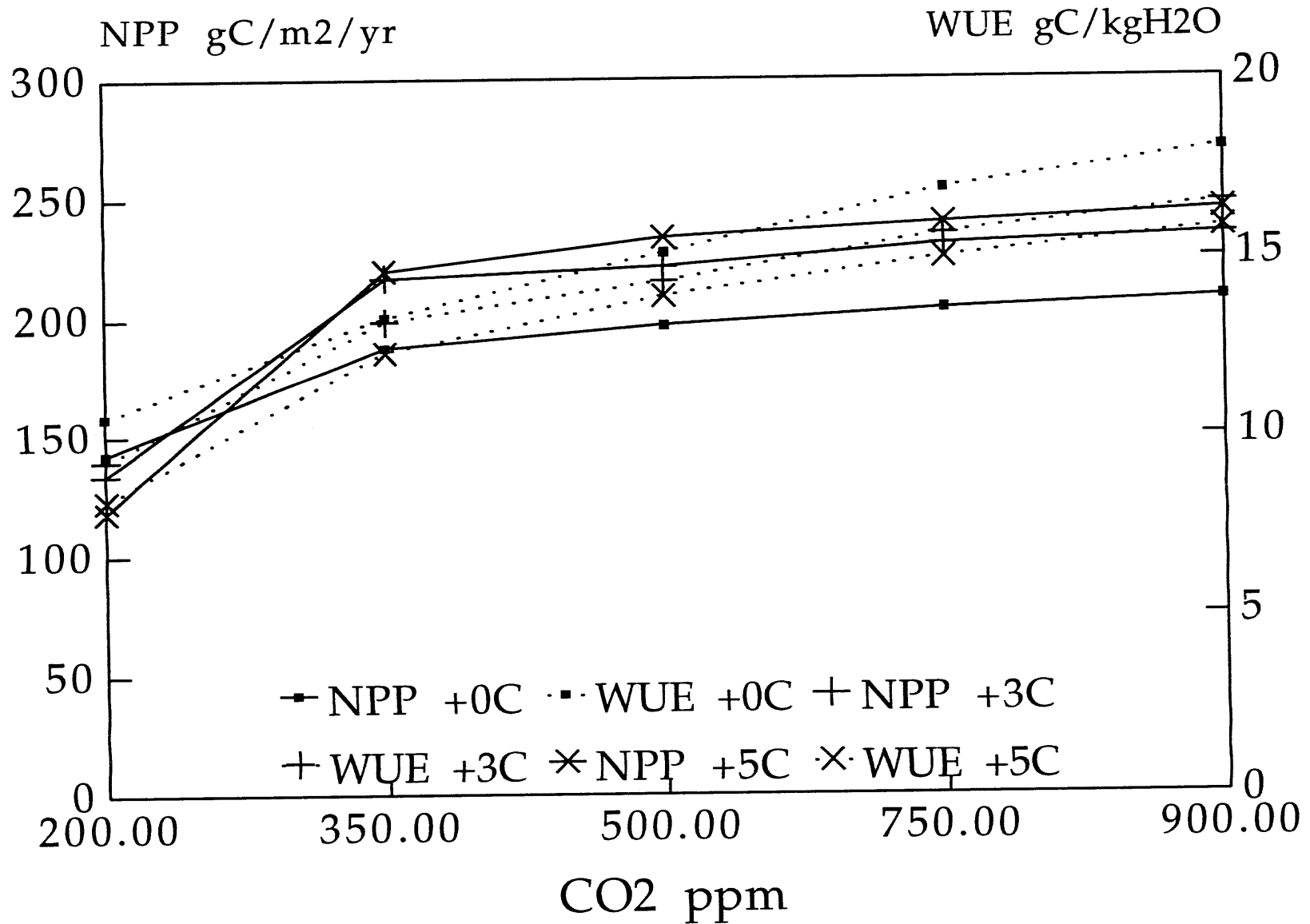
Fig. 1e

Kenya - C4
+50% Rainfall

NPP gC/m2/yr

WUE gC/kgH2O

CO2 ppm

Fig. 1f

Annual Net Primary Production

NPP gC/m2/yr

Legend:
- Control
- +CO2
- CCC Climate
- CCC Climate + CO2
- GSHI Climate
- GSHI Climate + CO2
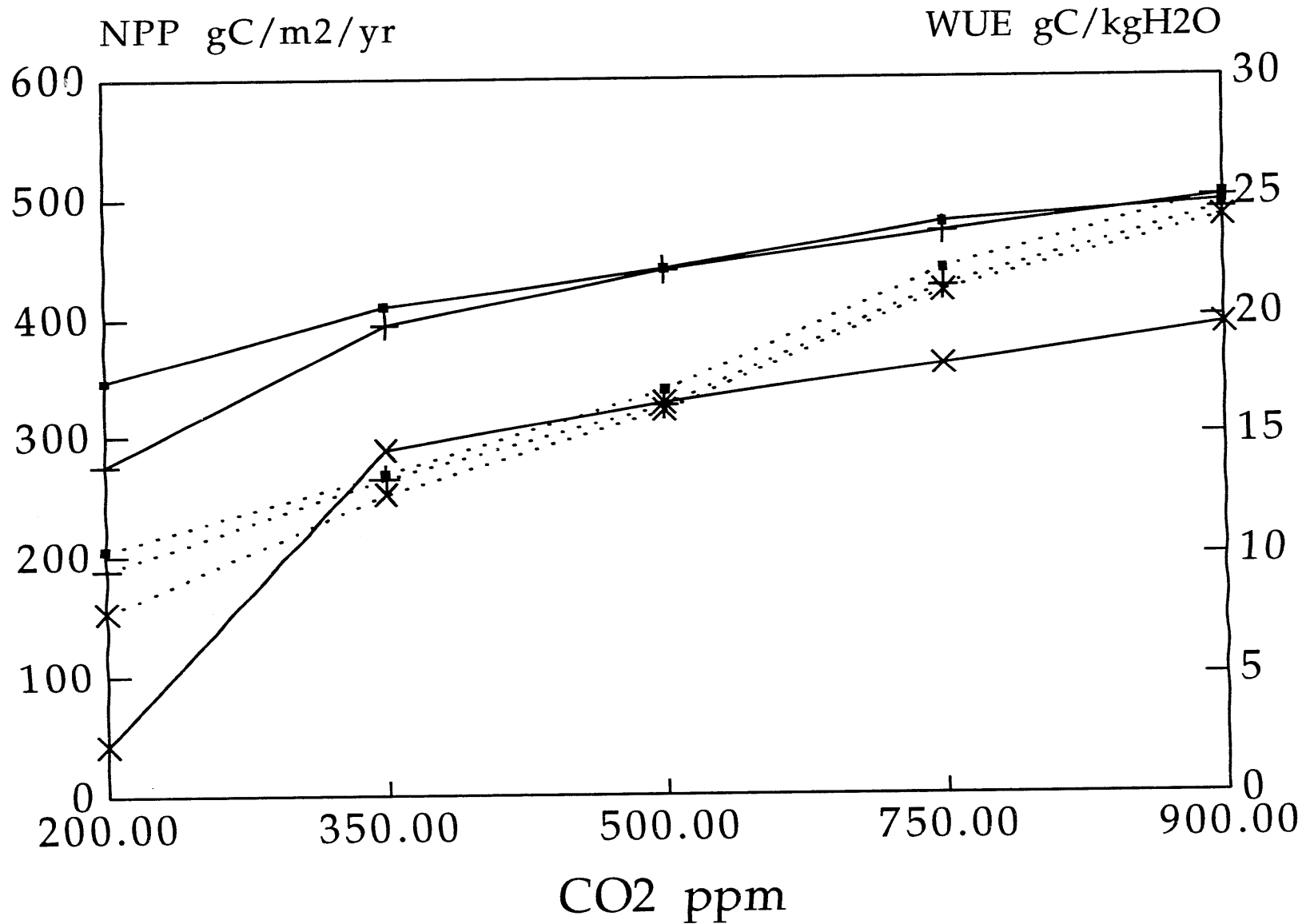
Colorado - C4   Colorado - C3   Kenya - C4
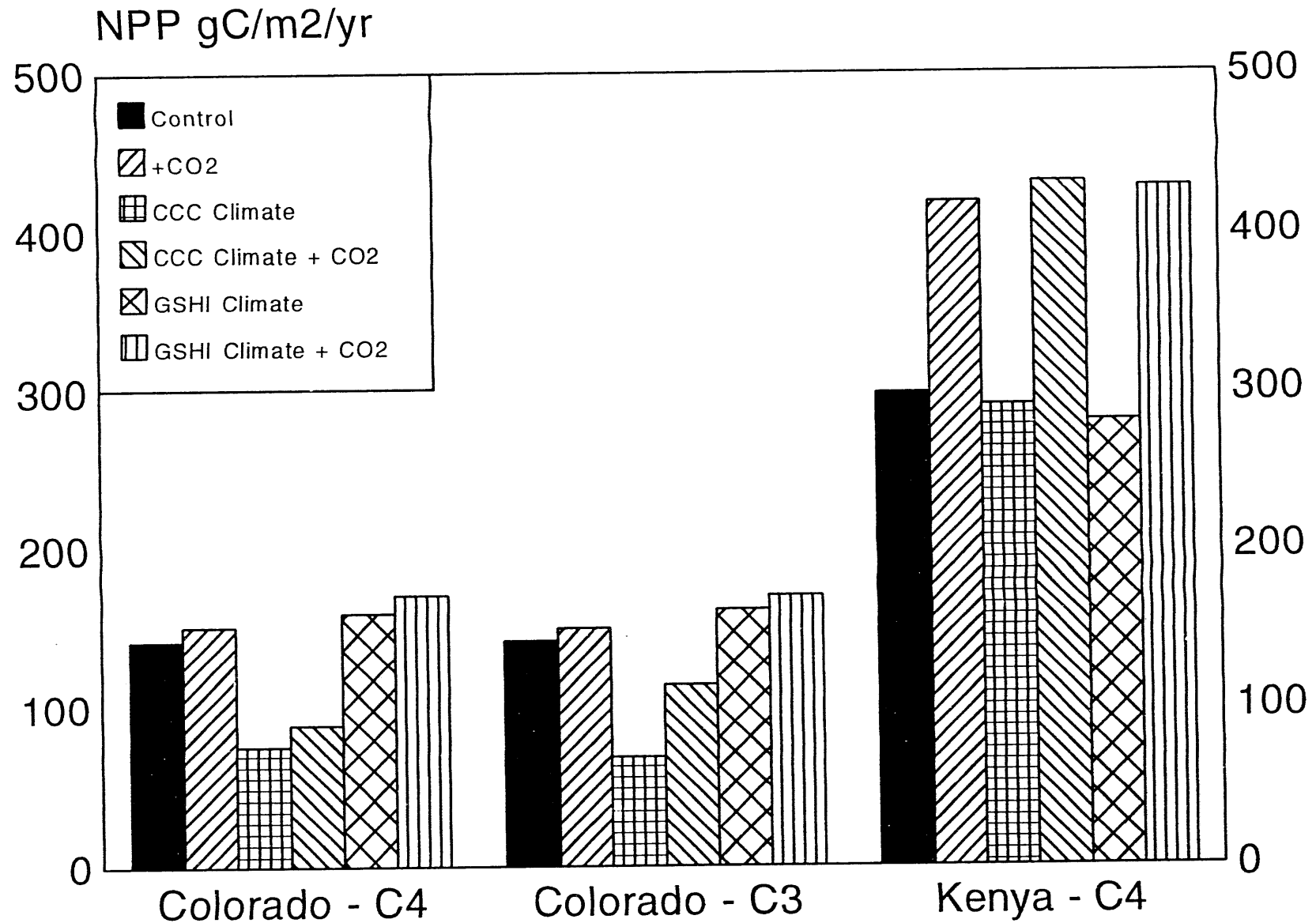
Fig. 2

Transpiration:Peak LAI Ratio

kg H2O/m2 Leaf Area/yr

Legend:
- Control
- +CO2
- CCC Climate
- CCC Climate + CO2
- GFHI Climate
- GFHI Climate + CO2

X-axis: Colorado - C4, Colorado - C3, Kenya - C4
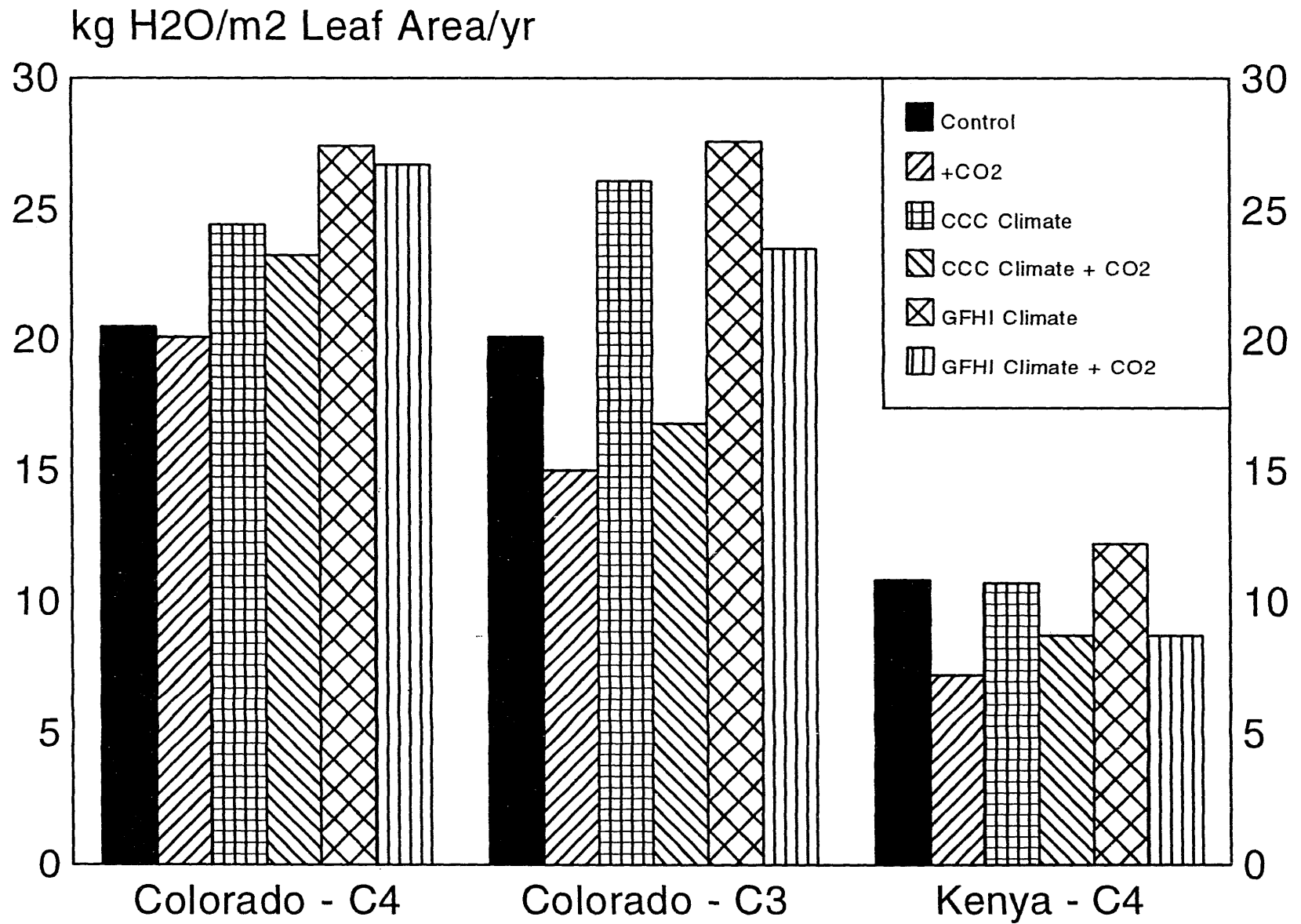
Fig. 3

Annual Net N Mineralization

Fig. 4

Total Soil Carbon

gC/m2 (Thousands)

Legend:
- ■ Control
- ▨ +CO2
- ▦ CCC Climate
- ◩ CCC Climate + CO2
- ⊠ GFHI Climate
- ⊞ GFHI Climate + CO2
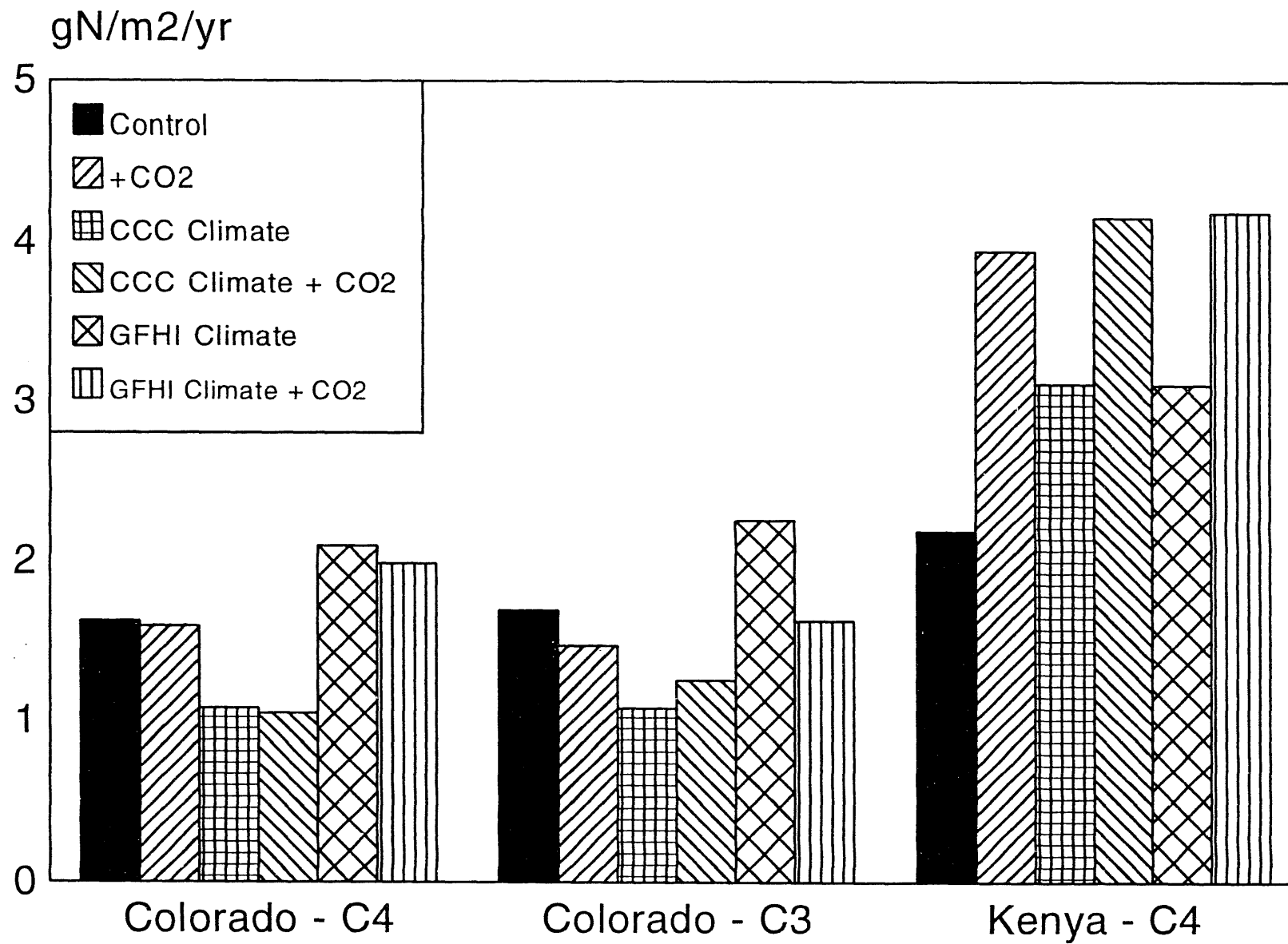
Colorado - C4   Colorado - C3   Kenya - C4
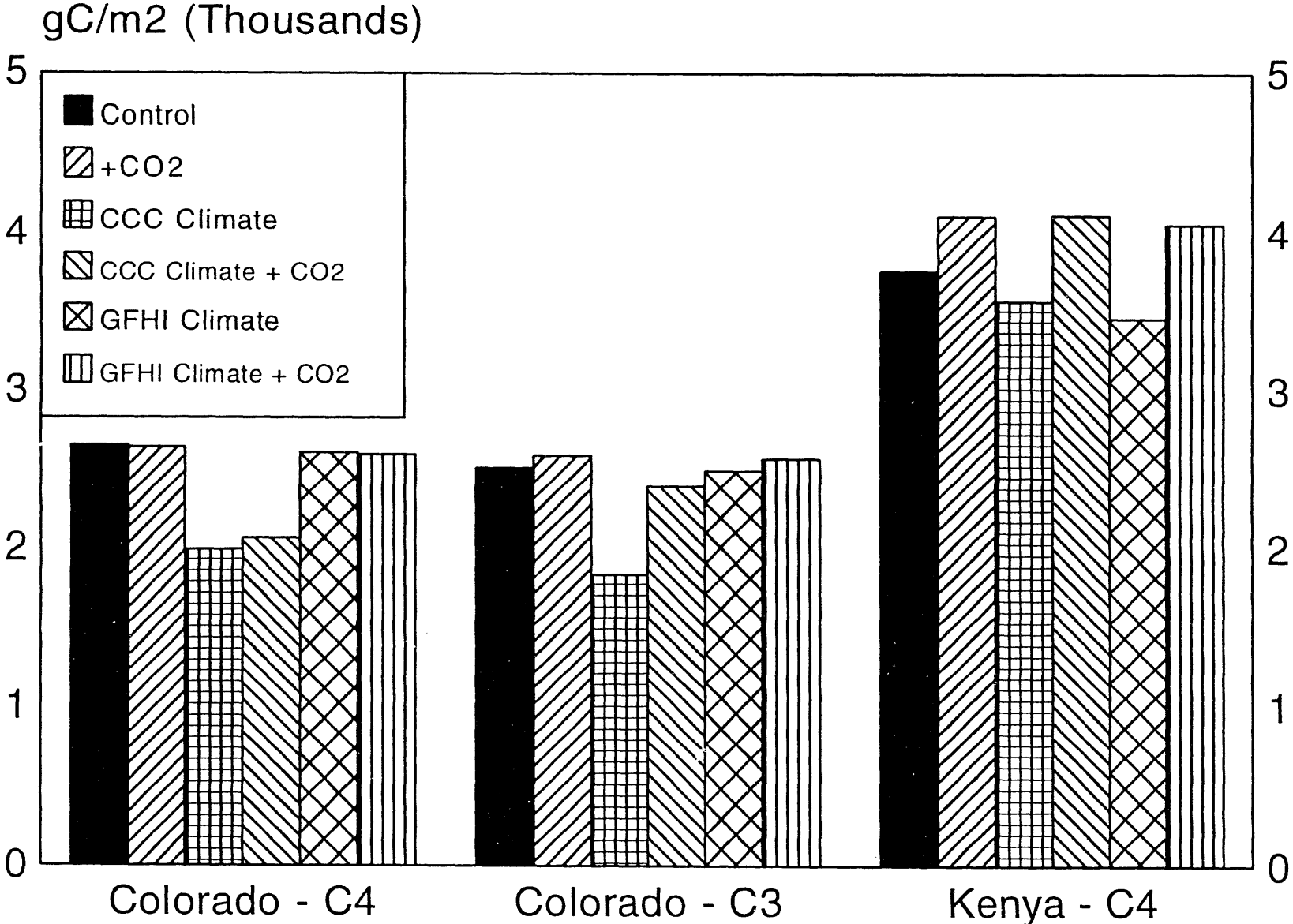
Fig. 5

Colorado C4 - NPP
GFHI Model

Annual Net Primary Production g/m2/yr

— Control ···1xCO2 --2xCO2

Year

350 300 250 200 150 100 50 0
1991 2016 2041 2066
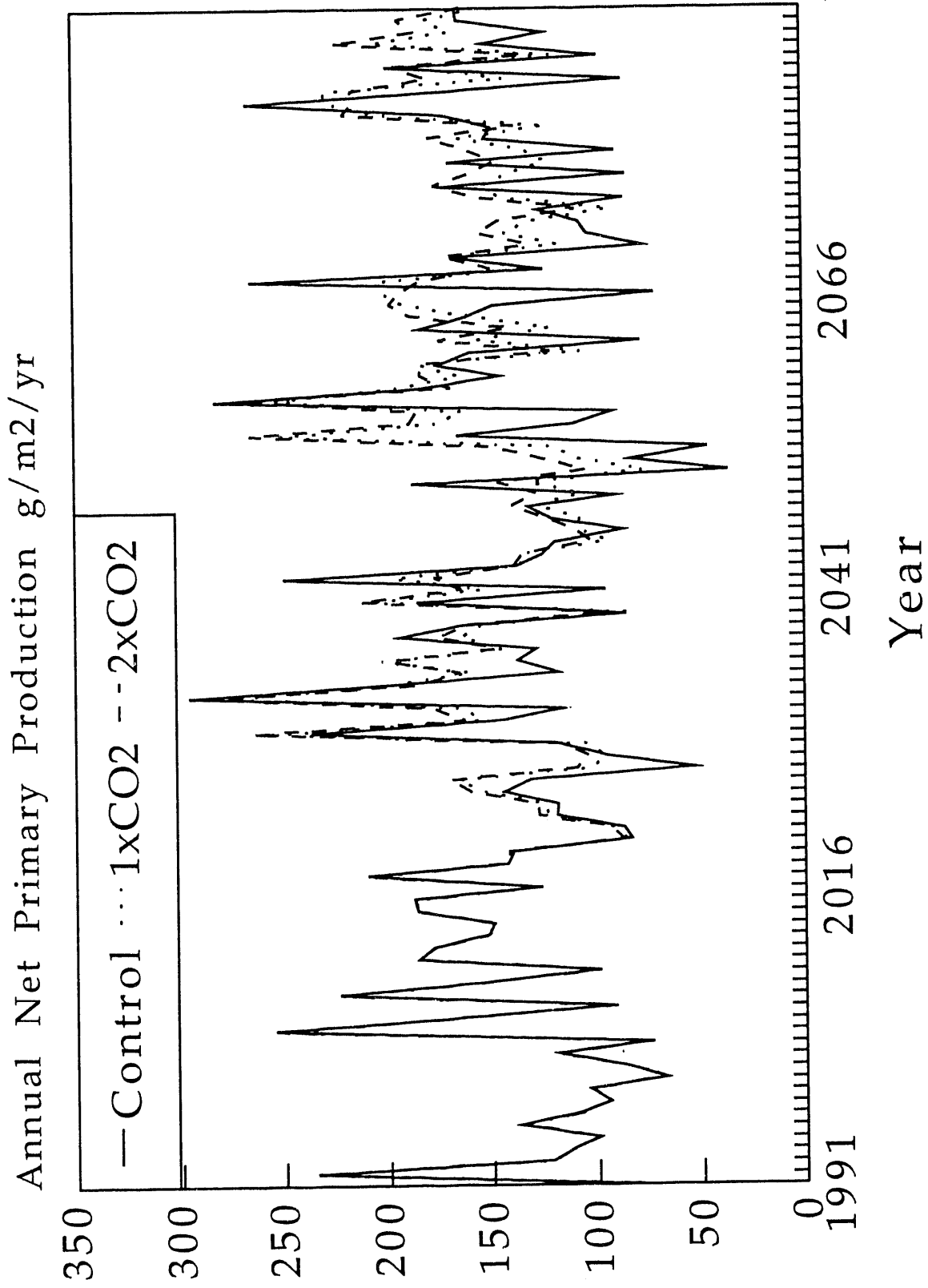
Fig. 6a

Colorado C3 - NPP
GFHI Model

Annual Net Primary Production g/m2/yr

— Control ··· 1xCO2 -- 2xCO2

300

250

200

150

100

50

0
1991   2016   2041   2066

Year
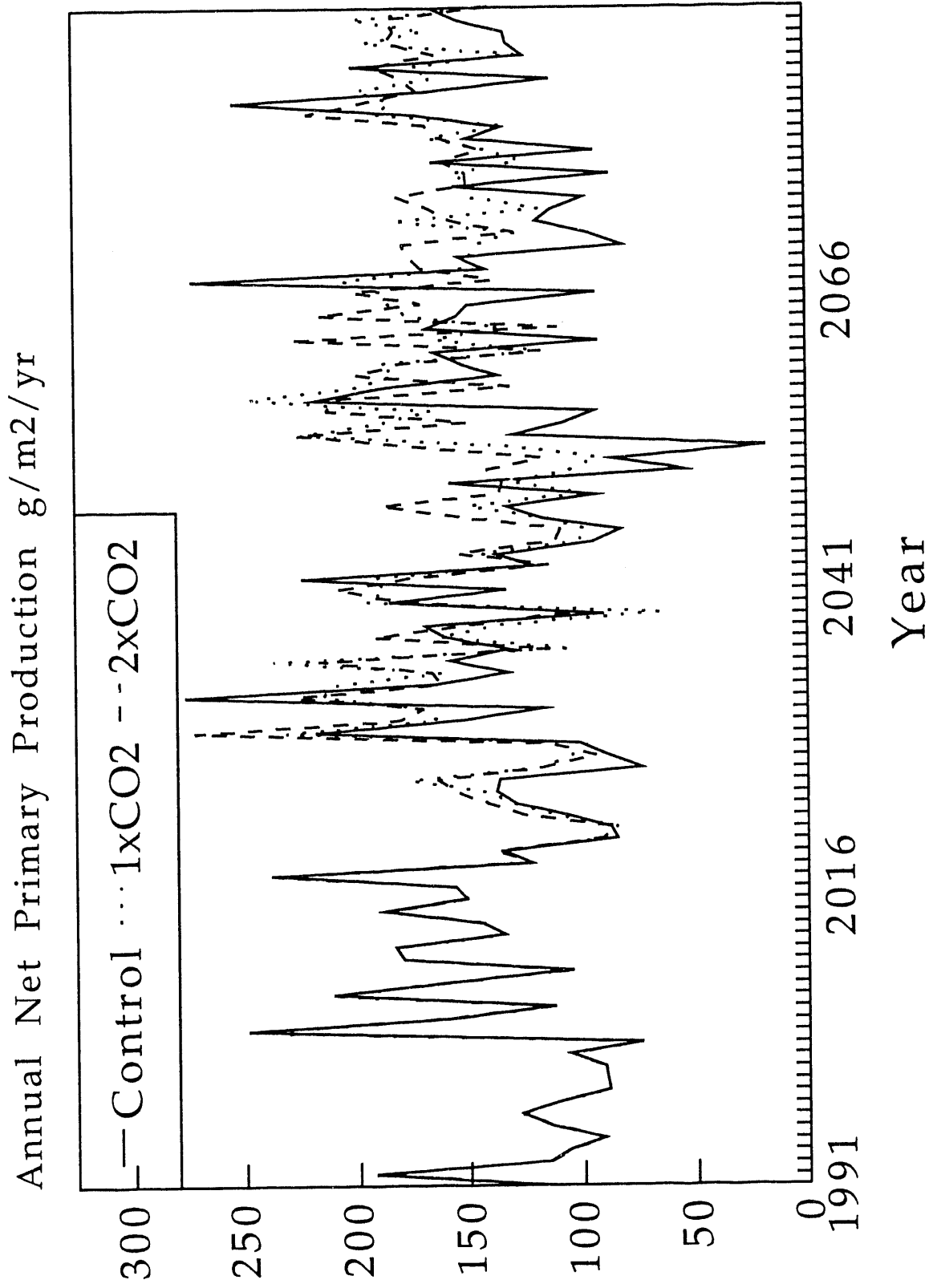
Fig. 6b

Kenya - NPP
GFHI Model

Annual Net Primary Production g/m2/yr

— No Change ···GSFDL --GSFDL 2xCO2

Year

2011   2036   2061   2086

0 200 400 600 800 1000
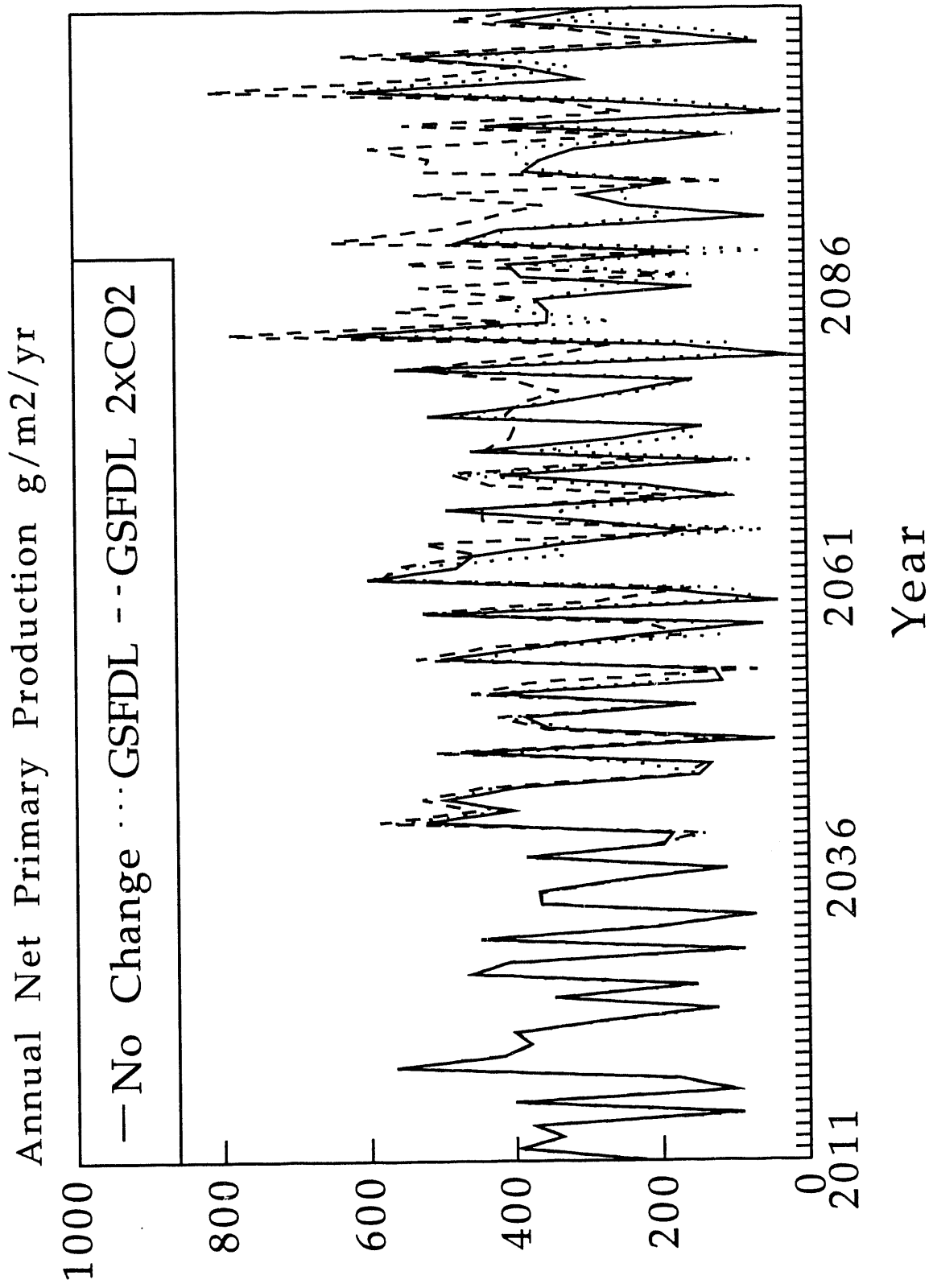
Fig. 6c

Colorado C4 - NPP
CCC Model

Annual Net Primary Production g/m2/yr

—Control ···1xCO2 --2xCO2

Year

350
300
250
200
150
100
50
0

1991   2016   2041   2066
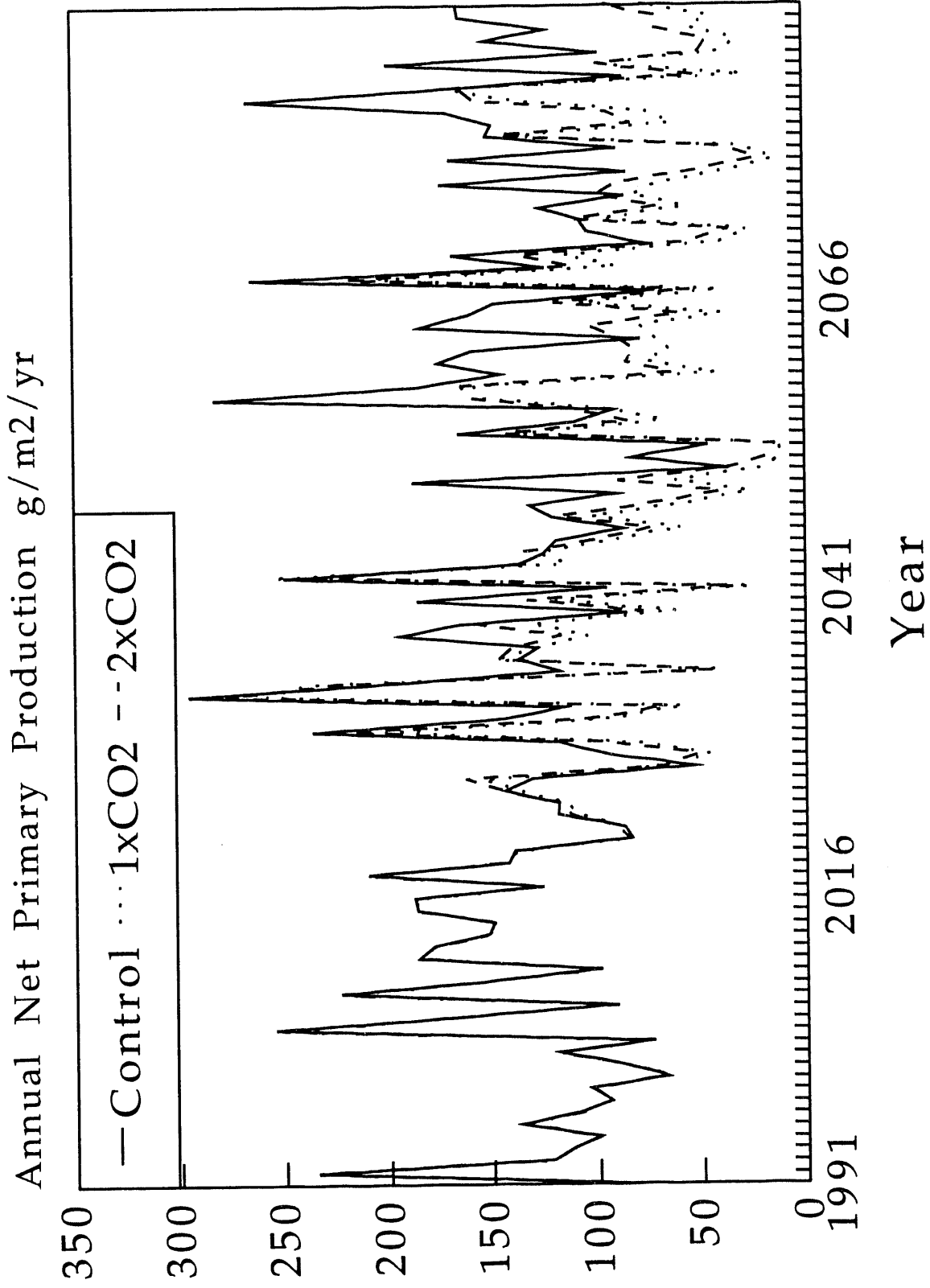
Fig. 7a

Colorado C3 - NPP
CCC Model

Annual Net Primary Production g/m2/yr

— Control   ···1xCO2   --2xCO2

300

250

200

150

100

50

0
1991   2016   2041   2066

Year
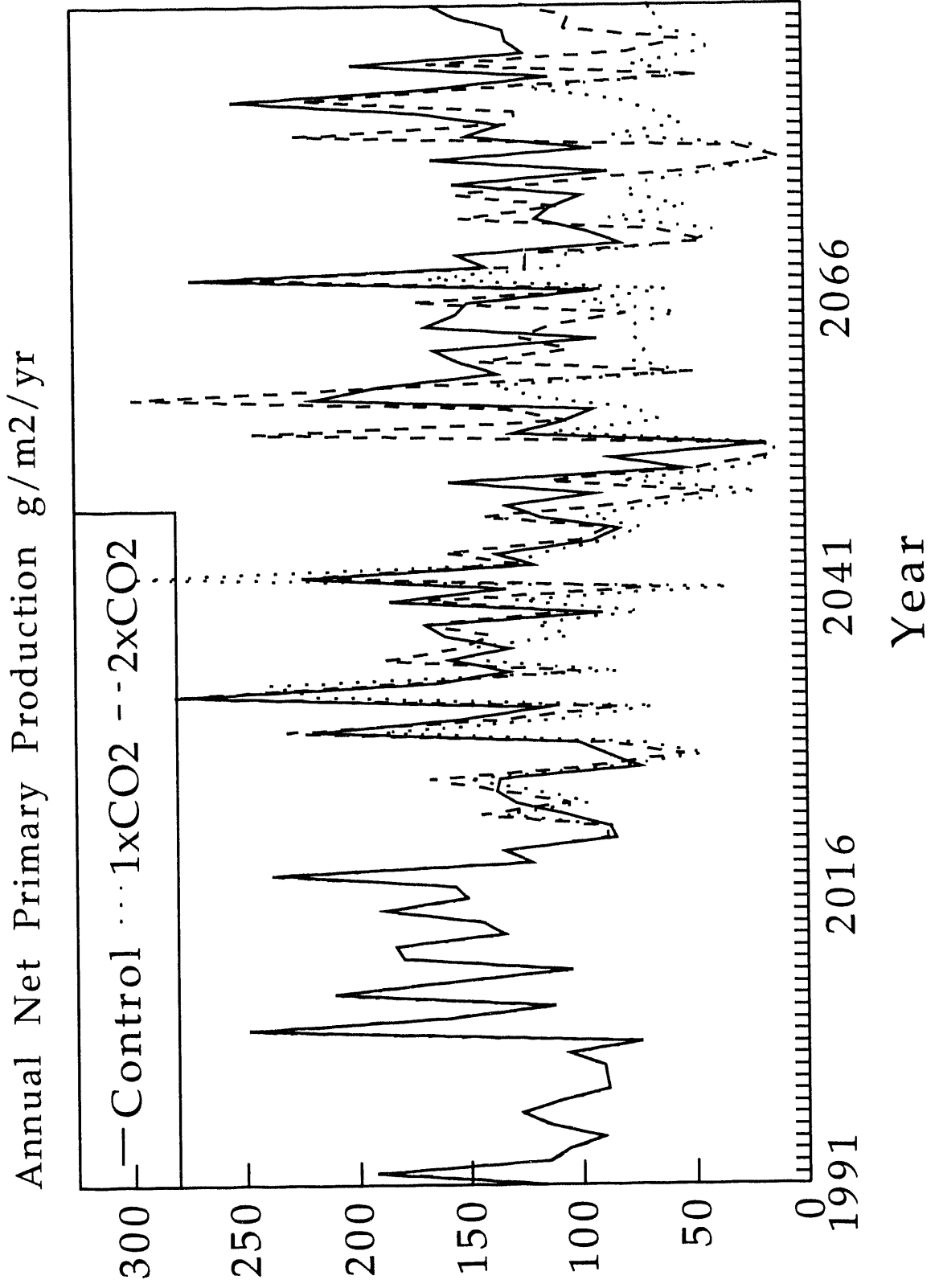
Fig. 7b

Kenya - NPP
CCC Model
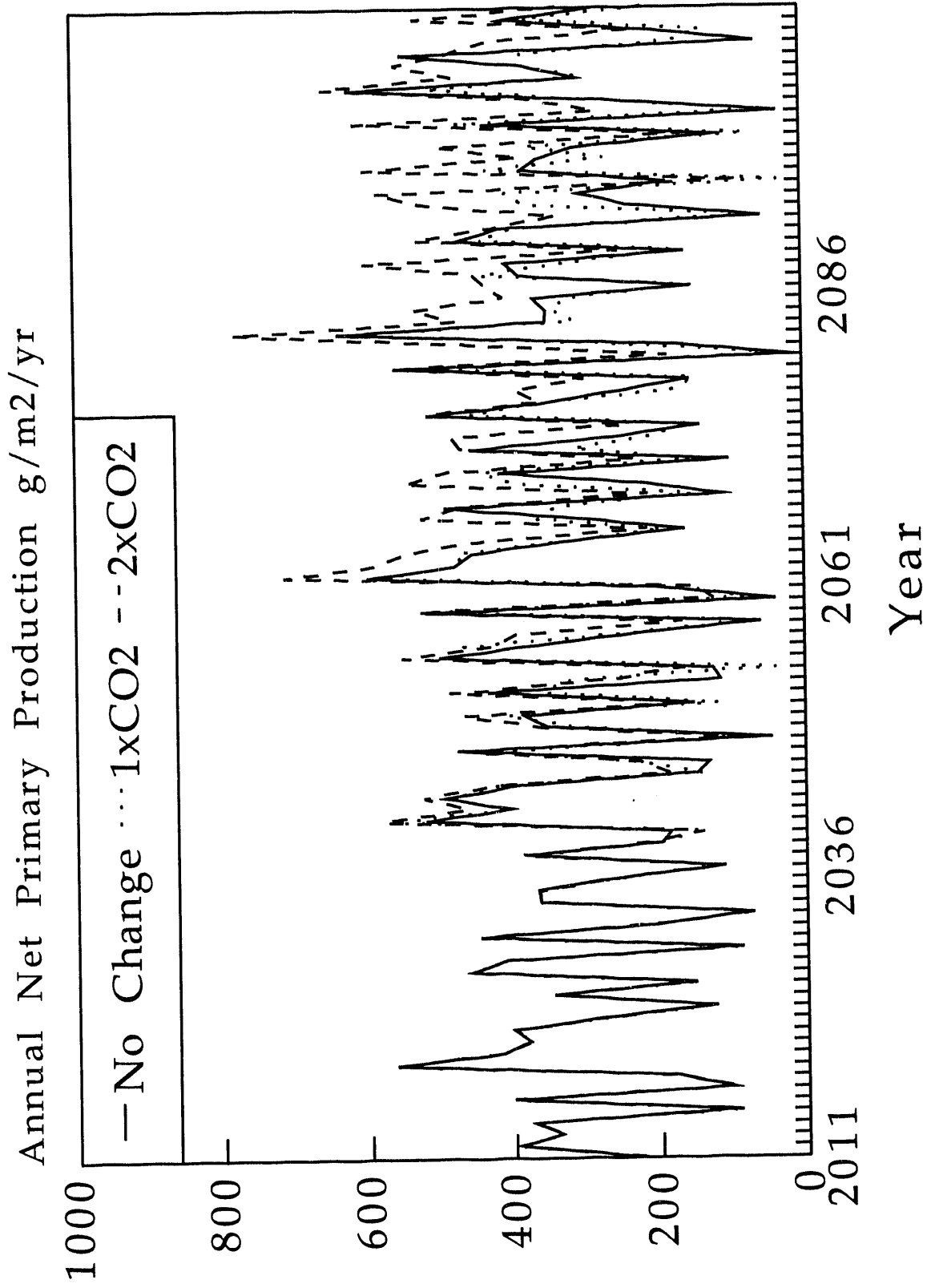
Fig. 7c

CHAPTER 4
Mod-X: A Modeling Environment for X-Windows, With Support for Multi-scaled Modeling

Introduction

Widely differing levels of resolution can be found among different ecosystem models. Models often have different levels of temporal resolution and different levels of mechanistic detail, depending upon the objectives of the model. Ecosystem models that run with daily time steps tend to be relatively detailed and strive toward mechanistic understanding. These models can be reasonably run for decades on personal computers and workstations. Ecosystem models that run on weekly or monthly time steps are used to examine longer-term ecosystem dynamics - over centuries or mellenia. These models tend to have less mechanistic detail than daily time step models. Less mechanistic models have also been developed to minimize information requirements for model parameterization.

The trade-offs between model complexity and simplicity suggest that there is an intermediate and optimal level of model complexity (Reynolds and Acock 1985). However, an intermediate resolution model may not be detailed enough for some, and at the same time it may be too detailed for scientists with broader objectives. Another solution is to use both simple and complex models, bringing the complementary strengths of both to bear upon a single problem. However, it is difficult for a single worker to manage two or more large models and make comparisons of their predictions and behaviors.

Additional insights can be gained by translating information from one model scale to another. Models operating on disparate time scales can interact, either by direct coupling, or through analytical procedures. The concepts of constraints and filters from hierarchy theory (O'Neill et al. 1986, Allen and Starr 1982) are useful in relating information at different temporal scales or levels of organization. In hierarchically organized systems, processes at higher levels of organization typically operate at slower rates and typically constrain faster processes at lower levels of organization. In contrast, detailed information is filtered out of fast processes as it flows from lower to higher levels in the hierarchy.

There is a less esoteric but important need to simply manage ecological models so that they can be more easily used, and so they can be used by a larger number of people. Past models have characteristically been quite "unfriendly". Software tools have been developed to make models more friendly than in the past. These range from simple questions and menus that are hard-coded into models, to menu-driven shells with tools to run models and analyze their behaviors (e.g., Kirchner 1989).

The Mod-X software described here was developed to provide an environment and set of linked tools for conducting modeling activities within the X-Windows environment on Unix-based workstations. It was specifically developed to interrelate models on different temporal scales. The user interacts with a series of menus and sub-menus, each comprised of "buttons". Button choices correspond to bits of information that are passed to underlying software applications.

Two model applications have been incorporated into the software. The GRASS-CSOM model is a detailed model of plant growth (GRASS) linked to a daily time step version of the CENTURY soil organic matter submodel (CSOM). The CENTURY model, on the other hand, simulates plant growth with a simplified model at monthly time steps.

34

Soil organic matter processes are simulated with a weekly time step. Other models can readily be incorporated into the system by adding additional menu items. However, the translation of information between different models depends on input-output routines that are written into the model.

System Menus

<u>Models Interface</u> - is the main menu (Fig. 1). It contains two buttons and two submenus. <u>Done</u> exits the system. <u>Help</u> is not yet functional. <u>Models</u> is a menu for model set-up and execution. <u>Data Analysis</u> is a menu for curve-fitting and data conversion.

I. <u>Models</u> - Pick from a list of models. Models are also referred to as applications. All applications have a generic interface with the following options. Currently you may pick between CENTURY and GRASS-CSOM.

<u>Model Name</u> - You have chosen a certain model (application), e.g., the GRASS-CSOM or the CENTURY model.

    A. <u>Setup Environment</u> - This menu allows you to specify the working directory for the current application. All files used in the application (parameter and data files) will be accessed from this directory. Setup environment must always be done first, as it puts you into the directory containing the appropriate parameter files, from which the model must be run.

    B. <u>View/Edit File</u> - This menu allows the user to edit and view any file from the directory specified in the Setup Environment. For example, you may want to edit parameter files for the models. In View/Edit, you select the file to view/edit with <u>Load File</u>. The <u>Save</u> button lets you save your changes. <u>Done</u> allows you to exit the menu. The <u>Edit</u> button puts you into an editor.
Within <u>Edit</u> are options to <u>Show</u>, <u>Paste</u>, <u>Cut</u>, <u>Search</u> and <u>Copy</u>. The <u>Show</u> button allows you to view the file in the window.

    C. <u>Century Parameter Input Files</u> - (for GRASS-CSOM only). This menu lets the user move parameters used in the CENTURY soil organic matter (CSOM) sub-model ("100 files") into parameter files for GRASS-CSOM. The CSOM model that is linked to GRASS is virtually identical to that used in CENTURY, except that it operates on a daily time step. An option box pops up and you must enter:
        1. The directory where the Century .100 parameter files reside.
        2. The "site".100 prefix name, i.e., "cper" for cper.100 (see Century Users Manual).
        3. The prefix name for the GRASS-CSOM .fix and .par files.
        4. The filename where the list of variables needed by the GRASS-CSOM resides. "Default" is probably acceptable. The conversion program then runs in a new window. All errors will be displayed in that window.

    D. <u>Century Output File</u> - (for GRASS-CSOM only). This menu allows the user to use the output of a CENTURY run as the starting place for a GRASS-CSOM run. Thus, after CENTURY is run for a long period of time, its results may be used as initial conditions for a shorter but

more detailed run with GRASS-CSOM. In this procedure, we are essentially using CENTURY to generate *constraints* for the GRASS model. You must enter the name of the <u>binary output file</u> that is created from a CENTURY run, i.e., cper.bin, etc. You must enter the full path name for this file. You must also enter the <u>starting time</u> for GRASS-CSOM in years. This must be within the range of years that was simulated in the CENTURY run.

E. <u>Run Options</u> - This allows you to set the options for a run.

For the GRASS-CSOM model, there are data fields and sub-menus for sensitivity analysis, weather files, irrigation and fertilization, burning schedules, and whether or not to use CENTURY output as a starting point for the run (Fig. 2). When all selections have been made, press <u>Done</u> and this invokes a data field for the <u>runtime file</u> name. The runtime file is an file containing your menu selections. This file will be created in the directory specified in the Setup Environment menu.

For CENTURY, this menu leads to a choice between entering the <u>file100</u> editor or the <u>event100</u> editor (see CENTURY manual).

F. <u>Run</u> - In this menu you enter the name of the runtime file created in Run Options. Run always brings up a <u>Terminal</u> window, where the application is actually running. All error messages and screen output will be found in this window. Pressing the <u>Done</u> button will exit you out of this window.

G. <u>Graph Output</u> - This menu lets the user view plots of model (Fig. 3).

<u>Load File</u> - brings up the contents of the directory specified in Setup Environment. Highlighting a file and pressing <u>Done</u> will make it the current file to be used for plotting (the plot file).

<u>Select X Var</u> - Allows you to select which variable on the plot file is X (not available in all applications).

<u>Select Y Var</u> - Allows you to select which variable on the plot file is Y (not available in all applications).

<u>Select Time</u> - Allows you to specify a sub-time (available only in GRASS-CSOM). It allows you to pick a single day for which variables will be plotted on an hourly basis. For example photosynthetic rate may be plotted each 2-hours on a given day.

<u>Graph Options</u> - Allows a user to specify axis labels, axis types (e.g., linear, log-linear), lines or points, whether or not to mark each point, an whether or not to display a grid.

<u>Plot</u> - This will bring up a new window with the plot. An option exists in this new window to produce a hard-copy print-out of the plot.

II. <u>Data Analysis</u> - This menu is where a user can perform functions such a curve fitting to real or modeled data, and plotting of data in a file. Each function is referred to as an application, just as are model in the <u>Models</u> menu.

Spline - This application fits a smooth curve through a fluctuating series of point data. It can be used, for example, to generate visually appealing plots of model output over time.

      A. Setup Environment - Set the working directory for the spline application.

      B. View/Edit Data File - Allows the user to look at filesin the Setup Environment working directory.

      C. Run Options - Here the user enters Input Data file name for the spline, and the Output file name. The user must also enter Slope for left and right endpoints. This option determines if you do not want the curve to flatten out. The default is 0, i.e., the curve will not flatten out. The Time Interval selects between Evenly Spaced subintervals, or an option to input time Subintervals From a File, with one time value per line.

      D. Run - This will run the spline routine. No window will come up.

      E. Graph Output - This contains options as described above under the Model menu to view the results, except that the fitted spline is plotted as well as the data.

Curve Fitting - This application fits predefined functions (equations) to real or simulated data. I is used to either estimate parameters for a function that is hard-coded into a model, or to derive a new function for a model that can be coded in. This is where *filtering* may take place, i.e., analysis of the simulation outputs of a fine-scaled model to provide parameter values for a function in a coarser-scaled model. When GRASS-CSOM is run, there are options to perform sensitivity analyses or filtering experiments. Output files are created which can be used as input to this curve-fitting application.

      A. Setup Environment - as above.

      B. Create/View Data File - As in View/Edit above, except the user may create a new data file as well.

      C. Run Options - Here the user enters Input Data file name for to fit the function to, and the Output file name. The Input Data file contains initial estimates of equation parameters for the equation which are displayed here. The Curvefit Function (equation) is selected (e.g., allometric, natural growth, cosine), as is the Number of Iterations to maximally use to attempt to fit the data.

      D. Run - This runs the curve-fitting routine.

      E. Graph Output - This contains options as described above under the Models menu to plot results from the curve fitting exercise. The fitted function is plotted along with the data.

Graph Data File - This application is the same as the Graph Output menu described above in the Model menu. It allows a user to plot model outputs or other data on a file.

37

Passing Information Between GRASS and CENTURY

The GRASS model can be started using output from the CENTURY model. This is useful, for example, to use CENTURY to project ahead to some distant point in the future, and then invoke the GRASS model to examine consequences of changed conditions in greater detail (Fig. 4). In essence, this would be using the CENTURY model to generate constraints for the GRASS model. The slow and intermediate turnover rate soil organic matter pools vary little over the span of a GRASS run, but they are nevertheless important for GRASS behavior. CENTURY can be used to simulate a 500 year period of elevated temperature, for example, which might reduce soil organic matter. The CENTURY output variables that will be read in as initial conditions for GRASS-CSOM include all of the belowground soil organic matter pools, live and dead shoot and root biomass, and soil water.

The process of translating fine-scale model output into a more aggregated model is much more involved. This process can be used to help parameterize an aggregated model by analyzing the responses of a detailed model. For example, CENTURY simulates plant growth as a function of the ratio of monthly available water to potential evapotranspiration. The GRASS model can be exercised in a variety of ways to find out how such a function might be parameterized. Thus, fine-scaled daily variations in GRASS are filtered out to develop a function of a monthly variable.

GRASS has an internal procedure which filters model variables over different time intervals. The filtering interval is a model parameter. If the filtering interval is set to 1 month, for example, then month-long means of variables are written to the filtering output file each month. The filtering output file is then analyzed in Mod-X. For example, to develop a function for CENTURY plant growth responses to monthly available water:PET ratio: (1) set the filtering interval to 30 days, (2) run the GRASS model using desired weather conditions, irrigation treatments etc., (3) enter the Curve Fitting procedure, load the filtering output file (filt.out), (4) enter the Graph Output procedure and select the total net primary production as the Y variable and available water:PET ratio as the X variable and, (5) plot the output. In this case, a curve should not be fit to the data, but visual examination of the plotted data should suggest how the CENTURY function should look.

The other technique is to perform sensitivity analyses with the model. GRASS has a sensitivity analysis routine that performs multiple model runs over a specified set of conditions. For example, a factorial experimental design involving five levels of ambient CO_2, three rainfall regimes, and five temperatures will be simulated with 5x5x3 simulation runs. Results can then be used to help formulate a function representing plant growth responses to CO_2 and temperature.

Literature Cited

Allen, T.F.H. and T.B. Starr. 1982. Hierarchy: Perspectives for Ecological Complexity. Univ. of Chicago Press, Chicago.

Kirchner, T.B. Time-Zero: The integrated modeling environment. Ecol. Model. 47:33-52.

O'Neill, R.V., D.L. DeAngelis, J.B. Waide and T.F.H. Allen. 1986. A hierarchical concept of ecosystems. Princeton University Press, Princeton.

Reynolds, J.F. and B. Acock. 1985. Predicting the response of plants to increasing carbon dioxide: a critique of plant growth models. Ecol. Model. 29:107-129.

Figure Legends

Figure 1. Example menus from Mod-X. The Models button on the main menu has been
selected, and the GRASS-CSOM (Grassom) model was chosen. The View/Edit
button was selected, in order to change a parameter value on a parameter file.

Figure 2. The Run Options menu for the GRASS-CSOM model.

Figure 3. Example Graph Output display, showing model output.

Figure 4. Using the CENTURY model to constrain the GRASS model and zooming in to a
finer level of resolution with the GRASS model.

Fig. 1

Models Interface

Done Help Models ▽ Data Analysis ▽

Grassom

Done Setup Environment View/Edit Data Files Century parameter input files Century output files Run Options Run Graph Output

Grassom Run Options

Done

Sensitivity Analysis ▽ No sensitivity analysis

Filtering experiment ▽ No

Fertilization ▽ No

Grassom to calculate transpiration removal ▽ Yes

Printing intervals: Multiple of timestep for 2 hour output 30 ▲▼

Multiple of timestep for daily output 8 ▲▼

Burn schedule ▽ Do not burn

Enter site id for fix and par input files cper

Files to use: Monthly cloud cover data filename: cloud.dat

Initial soil conditions data filename: soil.dat

Site soil parameter filename: site.dat

Output Validation data to a file ▽ No   Filename: _____

Weather ▽ Daily   Filename: daily.wth

Monthly Irrigation ▽ No   Filename: _____

Century Input data ▽ No   Filename: _____

Energy balance ▽ Complex energy balance

Abiotic model ▽ Daily

Fig. 2

Fig. 3

Fig. 4

CHAPTER 5
Application of a Synoptic Classification Scheme
for Analysis of GCM Climate Sensitivity Experiments

Introduction

Our long-term goal is to generate regional climate change scenarios by downscaling atmospheric general circulation model (GCM) results. Regional scenarios can be developed by using GCM upper air fields for initial and boundary conditions for a mesoscale atmospheric model, such as the Colorado State University Regional Atmospheric Modeling System (RAMS). The advantage of such nested regional simulations is that they use a finer grid spacing (e.g., 10 to 60 km) than in GCMs (400-800 km) and so can better account for effects of topography, large lakes, and land-ocean and vegetation contrasts on local and regional climates. However, such numerical simulations are computationally expensive.

An objective of this project was to develop a technique to categorize daily GCM output by synoptic class and to record the frequency of occurrence of these classes. RAMS simulations on days that typify each of these classes can then be used to evaluate how global forcing alters regional climates.

We developed a synoptic classification processor (SCP) for evaluating results of GCM climate sensitivity experiments. It is presumed that a change in climate, such as that potentially induced by elevated atmospheric CO_2, should be observable in prevailing synoptic conditions. By classifying air mass types over an extended period of time, a climatology of synoptic states can be constructed for comparing modeled climates. The SCP was tuned and evaluated using observed data sets.

In addition to classifying GCM output as a filter for RAMS regional simulations, the SCP can be used for rapid diagnosis of GCM experiment results in terms of three dimensional changes in atmospheric dynamics. This application of the synoptic classification processor was explored in this project and is discussed below.

Methodology

Approach. There have been numerous methods applied to synoptic classification. A summary of methodologies is presented in Yarnal (1993). The classes used in this study were developed by Lindsey (1980), who distinguished air mass types and their relation to one another to formulate a method of synoptic classification. The air mass types are maritime tropical, maritime polar, continental polar, and continental Arctic. In North America, maritime polar air originates in the cold waters of the north Pacific and Atlantic Oceans. Maritime tropical air has its roots in the Gulf of Mexico and in the warm Gulf Stream waters off of the east coast of the United States. Continental polar air develops in the central part of Canada, while the continental Arctic air originates further to the north.

These air mass types and their spatial orientation to one another are then used to classify synoptic conditions into five categories (Fig. 1, Table 1). Three of the categories — I, II, and III — are used to categorize the main areas of a developing extratropical cyclone. Category I is in the warm sector of developing cyclogenesis, while categories II and III are ahead of an approaching warm front and behind the cold front, respectively.

Class V is considered to be maritime tropical in origin and is in the region of a subtropical ridge. Finally, class IV is under a polar high.

The methods developed by Lindsey (1980) were further refined by Forbes and Pielke (1985) and Pielke et al. (1987). They generalized the atmospheric dynamics and thermodynamics of each category. For example, surface winds, temperature and vorticity advection, and precipitation patterns associated with differing categories were defined. It is selected parts of these definitions that form the basis of the Synoptic Classification Processor (SCP) developed by this project to automate the classification previously accomplished manually.

The Synoptic Classification Processor (SCP). The SCP ingests gridded data, such as the European Centre for Medium-range Weather Forecasting (ECMWF) analyzed fields, numerical climate model output, or any other data that can be objectively analyzed onto a grid.

The SCP employs four criteria stepwise to piece together the classification at a given point in space (Table 2). First, the location of the jet stream is evaluated using the wind speed at 200 mb. Classes I and V are south of the jet while the rest of the classes are north of the jet. Second, the Laplacian of mean sea level pressure is calculated at the grid points and is used to discern areas of high and low pressure, thus separating categories I, II, and III from high pressure categories IV and V. Temperature advection (at 700 mb) and vorticity advection (at 500 mb) are then used to distinguish classes I, II, and III.

For discriminating classes based on these diagnostic circulation parameters, thresholds were set for the Laplacian of pressure, temperature advection, and vorticity advection. These thresholds change from month to month according to a sinusoidal function. The maximums for these values are at the third and ninth months, when seasonal change is greatest and baroclinicity is at a maximum.

The points are classified according to the following algorithm: (Step 1) The Laplacian of the mean sea level pressure field is calculated. If the Laplacian of pressure is greater than the monthly threshold and temperature and vorticity advection are both positive, then class II (the region ahead of a warm front, Fig. 1) is inferred (Table 2). (Step 2) If the absolute value of the temperature and vorticity advection are below respective monthly thresholds, then that point belongs to class I (the warm air mass associated with a cyclonic storm, Fig. 1). If neither of these conditions apply a class III is assumed. (Step 3) If the Laplacian of pressure is less than the monthly threshold, then the SCP looks at temperature and vorticity advection magnitudes to see if they are less then the month's thresholds. If they are, then the point is set to class I. (Step 4) Finally, the location of the subtropical jet is used to differentiate between class IV and V. The jet is located by calculating the gradient of the 200 mb wind speed: the jet is taken to be approximately where the gradient is largest. Thus, if the point is south of the jet, it is class V and, if north, then class IV.

Verification of the SCP

The SCP was evaluated using ECMWF 2.5° latitude/longitude gridded analyzed upper air fields as input and, for comparison with SCP results, 2 years of manually classified daily data for the Shenandoah National Park, which was based on a subjective analysis of surface maps. This comparison was performed for fine tuning the adjustable

thresholds in the SCP. A complete description of the data for Shenandoah is reviewed in Stocker et al. (1991).

The full resolution of the ECMWF data was used. Daily classes were computed at the grid point closest to the Shenandoah National Park location. The SCP showed roughly 80 percent agreement with the subjective analysis. A 100 percent agreement was not expected since the ECMWF data has a 2.5° grid spacing, which represents a cell of roughly 300x300 km in the vicinity of the park. The data obtained from surface analysis has a finer spatial resolution, which would enable a better definition of fronts and other features with scales on the order of a few hundred kilometers.

Next, a degraded set of ECMWF data, half the original number of grid points, was analyzed and compared to the Shenandoah classes. The degraded computations were performed to obtain the impact of coarser resolutions on the results, since the GFDL GCM 1X and 2XCO$_2$ model runs had a 4.5° latitude x 7.5° longitude grid spacing. The results indicate that there is only slightly better agreement (and probably not a statistically significant difference) when the data set was degraded in resolution. The SCP has little difficulty in determining air mass of large spatial extent, like a subtropical ridge or polar high, while a developing extratropical cyclone is harder to discern. The good agreement that is achieved with both ECMWF data sets is due to dominance at this site by either a subtropical ridge or a polar high.

Comparison of 1x and 2xCO$_2$ GFDL Simulations

The next series of SCP runs were performed in order to compare output from GCM climate sensitivity simulations. For this exercise, we used three years of daily output from the GFDL 1x and 2xCO$_2$ climate experiments reported in Manabe and Wetherald (1987). If there is an overall climate effect of elevated atmospheric CO$_2$ in the simulations then we expect that this effect is observable in the seasonal and geographic distribution of air masses, and hence synoptic classes. Application of the SCP should aid in discerning such climatic sensitivity in a qualitative sense. Generally, an increase in tropospheric temperatures should be observable in the latitudinal location of the midlatitude jet. If there is significant warming then it should move northward. At a given latitude (mid-latitudes should have the strongest signal), this should manifest itself as more occurrences of class V.

For a north-south transect along longitude 97.5°W (through the middle part of North America), SCP was used to determine the percent frequency occurrence of each class by month (Fig. 2, refer to the key in Table 3). The plots in Figure 2 represent a 3-year average. First, notice that either class IV or V dominates at essentially all latitudes. As the latitude increases the percentage of class V drops off dramatically, and class IV becomes more prevalent. Because classes II and III would be attributable to regions of favored cyclogenesis their percentage increases at mid-latitudes. For example, at 54°N, class III occurrence is between 50 to 80% during winter months for both 1x and 2x simulations, while at lower latitudes it makes a only 10 to 25% contribution.

As mentioned earlier it was hypothesized that class V should be more observable at higher latitudes in the 2xCO$_2$ simulations. This is clearly not demonstrated in Figure 2. Generally, class V percentages for the 1x and 2xCO$_2$ simulations run within 10 percent of each other. As one moves northward the shapes of the curves maintain a general resemblance to each other, yet the month to month variability is greater in the 2xCO$_2$ simulation. In fact, at 54°N, the 2xCO$_2$ simulations shows a 25-30% increase in class V

values over the $1xCO_2$ run for the late summer months, possibly indicating a larger degree of warming. It is possible that more years are needed to be encompassed in the study to discern a clearer difference between the simulations. (Only three years of daily output were available for the GFDL runs).

There is a lack of large differences between the two GFDL simulations over the most of North America (Fig. 3). The upper panels of Figure 3 show the overall percentages of class V for the 1x and $2xCO_2$ simulations, averaged over 3 years (Fig. 3i,ii). The similarities are striking; it is not until close examination that the differences can be seen (Fig. 3iv). The lower left panel shows the percentage of class IV for the $1xCO_2$ simulation, minus the percentage of class IV for the $2xCO_2$ simulation for a three year average (dashed contours are for negative values, solid for positive). The lower right is the same, except class V is used for the difference field. One obvious pattern shows up in the class V difference field. Off the eastern coast of the United States there is a climatologically favored area of the location for a subtropical high (the Bermuda High). The high (class V) appears to be more prevalent in the $2xCO_2$ simulation (dashed contours in Fig. 3iv), possibly suggesting a slight warming trend. However, notice the small range of values; there is never more than a plus or minus 7% difference between the simulations. This is a fairly insignificant number and suggests little variability between the simulations.

Zonally averaged fields were also performed for a longitudinal band across North America, from 135°W to 62.5°W (Fig. 4). The differences between 1x (the A curve) and $2xCO_2$ (the B curve) simulations are minimal for the 3 year period analyzed. Statistically any observed differences in the curves are insignificant.

Summary and Conclusions

The first goal of the study, the development of an objective synoptic climatology processor has been met. The processor was developed to work with either model or observational data. The next step, verification of the applied algorithms, was also achieved by the comparison of manual classifications to the SCP classifications. Roughly 80% agreement is achieved between these 2 data sets, implying skill in the SCP algorithms. Finally, the comparison of 1x and $2xCO_2$ simulations revealed relatively small differences.

We are continuing to improve the processor and to apply it to other model data sets. There are several additional steps that are needed:

(1)   Application of the SCP to a greater number of years of ECMWF data in order to adjust the temperature and vorticity thresholds.

(2)   Application of the SCP to points other than Shenandoah to reduce any bias introduced by verification at one observation point. (It should pointed out that this was done to some degree by qualitative comparison to plots presented in Pielke et al., 1987).

(3)   The need for a longer data set for the 1x and $2xCO_2$ GCM simulations (i.e., more years of data) in order to assess the degree of difference in the climatology achieved by each simulation.

44

(4)   Explore the possibility that the GCM model grid spacing is too coarse to observe a difference in climatic between simulations.

As of the writing of this report these steps are being addressed to differing degrees. The validation of the SCP is now being done for 20 years worth of ECMWF data. In addition, the inclusion of other data points for verification is proceeding as mentioned. Under consideration is the employment of a finer scale model, with more than 10 years worth of data. This would address concerns pointed out by the last two items in the list.

Literature Cited

Forbes, G.S. and R.A. Pielke, 1985: Use of observational and model-derived fields and regime model output statistics in mesoscale forecasting. Presented at the Nowcasting Symposium at the IAMAP/IAPSO Joint Assembly, August 7, 1985, Honolulu, Hawaii. ESA J., 207-225.

Lindsey, C.G. 1980. Analysis of coastal wind energy regimes. M.S. Thesis: University of Virginia.

Manabe, S., and R.T. Wetherald. 1987. Large scale changes in soil wetness induced by an increase in carbon dioxide. J. Atmos. Sci. 44:1211-1235.

Pielke, R.A., M. Garstang, C. Lindsey, and J. Gusdorf, 1987: Use of a synoptic classification scheme to define seasons. Theor. Appl. Climatol 38, 57-68.

Stocker, R.A., M. Uliasz, and R.A. Pielke, 1991: Impact of local sources on Shenandoah National Park during an extended stagnation period. Prepared for the National Park Service, Denver, Colorado.

Yarnal B., 1993: Synoptic Climatology in Environmental Analysis, 195 pp., Belhaven Press, London and Florida

Table 1. Synoptic classification scheme (from Pielke *et al.* 1982; modified from Lindsey, 1980).

Category	Air mass	Reason for categorization [*]
1	*mT*	*In the warm sector of an extratropical cyclone.* In this region the thickness and vorticity advection is weak with little curvature to the surface isobars. There is limited low level convergence with an upper level ridge tending to produce subsidence. Southerly low-level winds are typical
2	mT/cP, mT/cA, mP/cA	*Ahead of the warm front in the region of cyclonic curvature to the surface isobars.* Warm air advecting upslope over the cold air stabilizes the thermal stratification, while positive vorticity advection and low-level frictional convergence can add to the vertical lifting. Because of the warm advection, the geostrophic winds veer with height. Low-level winds are generally north-easterly through south-easterly
3	*cP; cA*	*Behind the cold front in the region of cyclonic curvature to the surface isobars.* Positive vorticity advection and negative thermal advection dominate, with the resultant cooling causing strong boundary layer mixing. The resulting thermal stratification in the lower troposphere is neutral, or even slightly, superadiabatic. Gusty winds are usually associated with this sector of an extratropical cyclone. Because of the cold advection, the geostrophic winds back with height. Low-level winds are generally from the north-east through south-west
4	*cP; cA*	*Under a polar high in a region of anticyclonic curvature to the surface isobars.* Negative vorticity advection, weak negative thermal advection and low-level frictional divergence usually occur, producing boundary layer subsidence. Because of relatively cool air aloft, the thermal stratification is only slightly stabilized during the day, despite the subsidence. At night, however, the relatively weak surface pressure gradient associated with this category causes very stable layers near the ground on clear nights due to long-wave radiational cooling. The low-level geostrophic winds are usually light to moderate varying slowly from north-westerly to south-easterly as the ridge progresses eastward past a fixed location
5	*mT*	*In the vicinity of a subtropical ridge* where the vorticity and thickness advection, and the horizontal pressure gradient at all levels are weak. The large upper-level ridge, along with the anticyclonically curved low level pressure field, produces weak but persistent subsidence. This sinking causes a stabilization of the atmosphere throughout the troposphere. Low-level winds over the eastern United States associated with these systems tend to blow from the south-east through south-west

[*] This discussion applies to northern hemisphere.

Table 2. Criteria used in the Synoptic Classification Processor and the relative values used to discriminate classes. N stands for North and S means South.

Variable	Class I	Class II	Class III	Class IV	Class V
Location relative to Jet	S	N	N	N	S
Vorticity Advection	~ 0	$+$	$+$	~ 0	~ 0
Temperature Advection	~ 0	$+$	$-$	~ 0	~ 0
Laplacian of SurfacePressure	$\pm$	$+$	$+$	$-$	$-$

Table 3. Key to line labels in Figure 2. Classes 1 through 5 are identified by lines labeled A through E for $1xCO_2$ runs, respectively, and F though J for $2xCO_2$, respectively.

1x	2x	Class
A	F	1
B	G	2
C	H	3
D	I	4
E	J	5

Figure Legends

Figure 1. Example of a surface analysis chart (for January 9, 1964) showing the application of the synoptic climatological model for the five synoptic classes (reproduced from Pielke, 1982).

Figure 2. Three year average of SCP class percentages for 1x and $2xCO_2$ GFDL runs. Classes 1 through 5 are identified by lines labeled A through E for $1xCO_2$ runs, respectively, and F though J for $2xCO_2$ (see Table 3). Plots are for a south-north transect along 97.5°W longitude, at latitudes: (i) 31.5° N, (ii) 36° N, (iii) 40.5°N, (iv) 45°N, (v) 49.5°N, and (vi) 54°N.
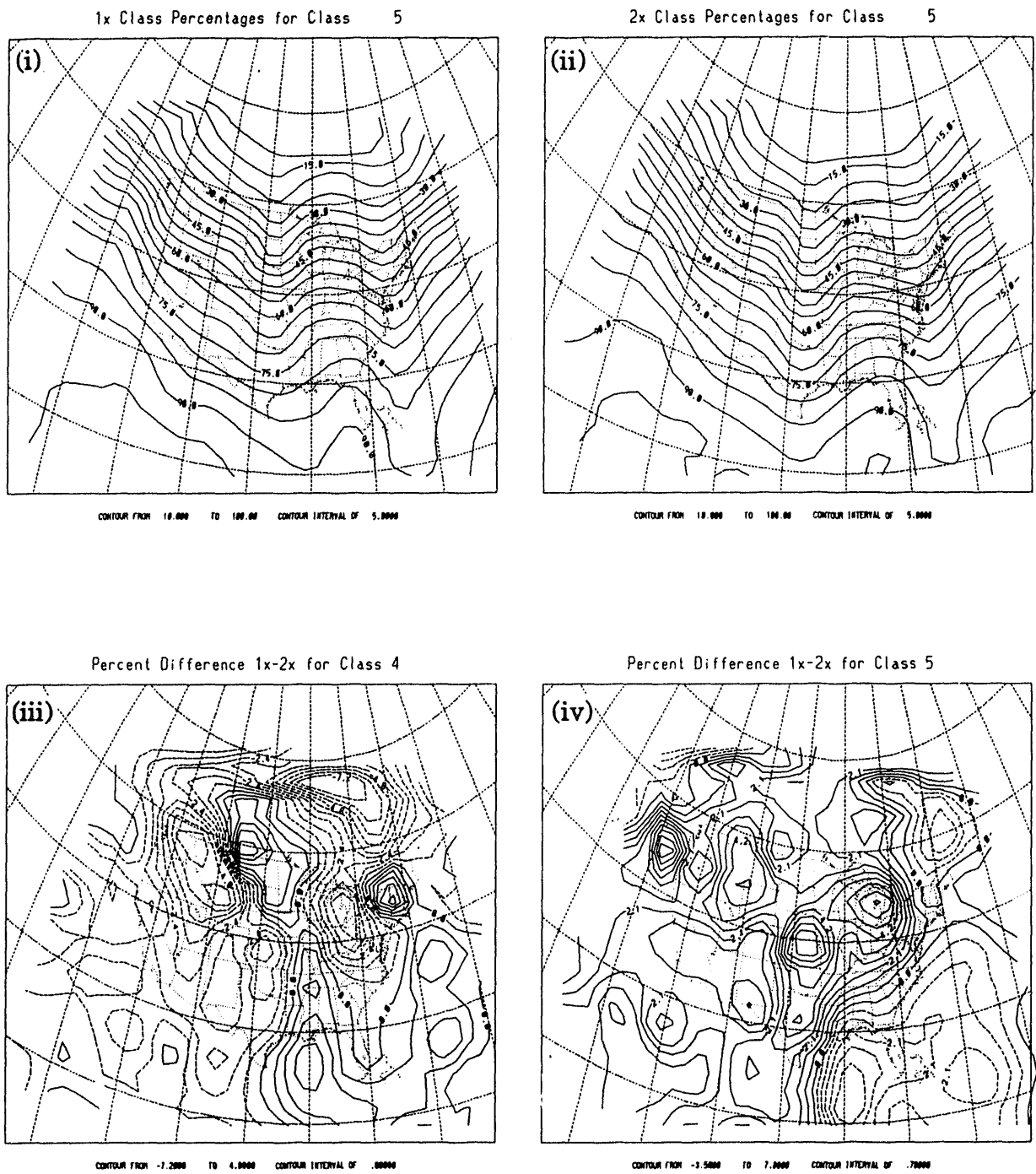
Figure 3. Upper panels: Three-year average of percentage of class V for (i) 1x and (ii) 2x CO_2 simulations across the U.S. (contour interval = 5%). Lower panels: Difference between 1x and $2xCO_2$ class percentages for (iii) class IV and (iv) class V (contour interval = 0.8 and 0.7%, respectively).

Figure 4: Zonally averaged class percent for classes (i) I, (ii) II, (iii) III, (iv) IV, and (v) V for $1xCO_2$ run (curve A) and $2xCO_2$ run (curve B).

Figure 1. Synoptic classification scheme illustrating typical (a) summer and (b) winter patterns.

1x Class Percentages for Class   5

2x Class Percentages for Class   5

Percent Difference 1x-2x for Class 4

Percent Difference 1x-2x for Class 5

Figure 3: Upper panels: Three-year average of percentage of class V for (i) 1x and (ii) 2x CO_2 simulations across the U.S. (contour interval = 5%).

Lower panels: Difference between 1x and 2xCO_2 class percentages for (iii) class IV and (iv) class V (contour interval = 0.8 and 0.7%, respectively).

Figure 4: Zonally averaged class percent for classes (i) I, (ii) II, (iii) III, (iv) IV, and (v) V for 1xCO$_2$ run (curve A) and 2xCO$_2$ run (curve B).
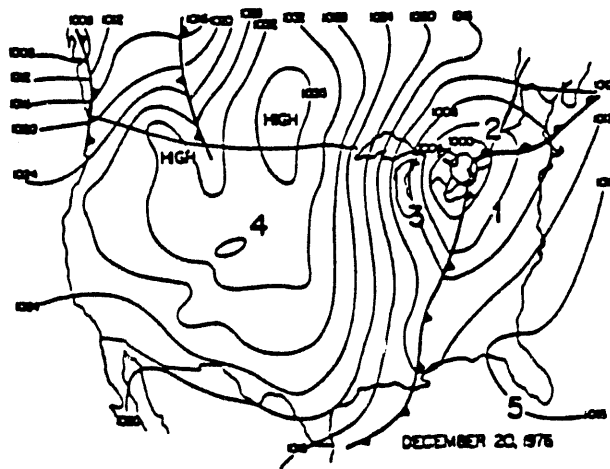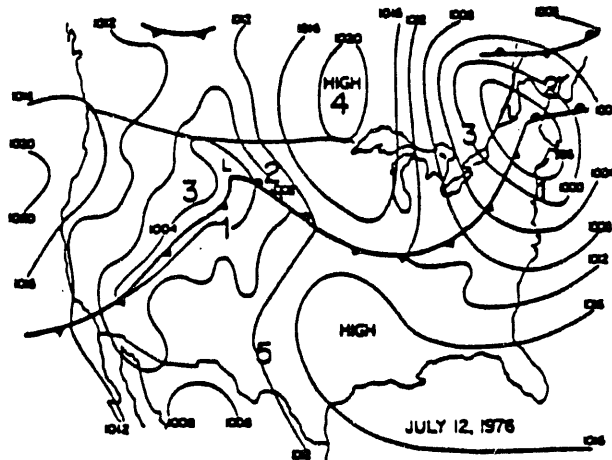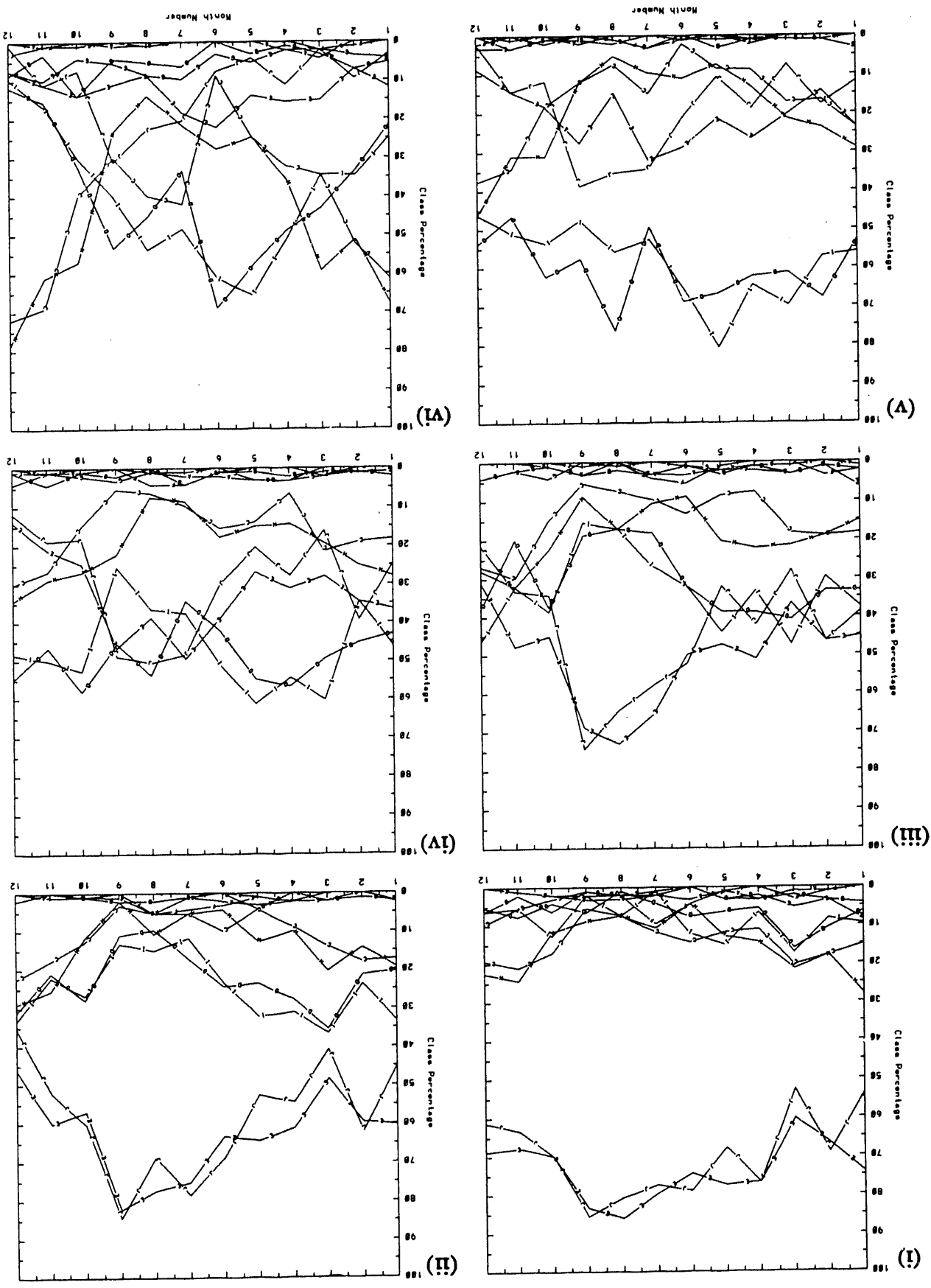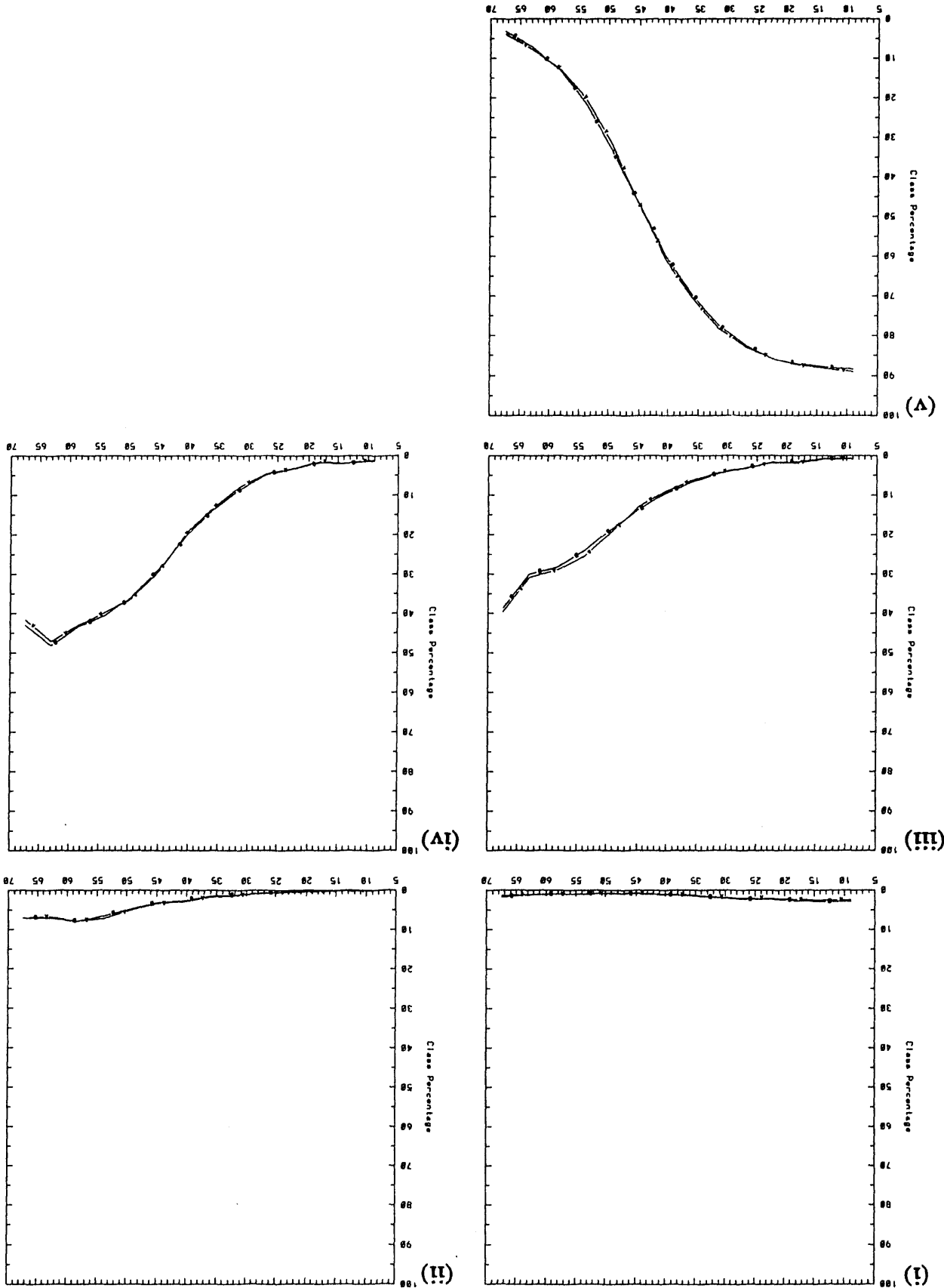
CHAPTER 6
Limitations of Current Models and Future Directions in Predicting Ecosystem Responses to Climatic and Atmospheric Change

Introduction

Models must represent many interacting processes to predict ecosystem responses to atmospheric change (e.g., Dahlman 1985, Reynolds and Acock 1985, Walker et al. 1990, Turner et al. 1990). Models must define the plant-level processes that are affected by CO_2, and the ecosystem-level processes that are related to CO_2 enrichment, such as water use and effects of nutrient limitation on CO_2 responses (Dahlman 1985). None of many models available in 1985 met all of the minimal requirements for modeling ecosystem responses to CO_2 (Reynolds and Acock 1985). A few current models can now meet those requirements, however new modeling requirements must be added to the list. For example, participants in a recent IGBP workshop agreed that models must respond to numerous climate variables including CO_2, and to disturbance, and that they should be able to predict temporal and spatial fluxes of carbon, nutrients, and water through plants and soils, as well as vegetation composition and structure (Walker et al. 1990).

An important task for modelers is to relate their findings to experimentalist. There is a need for far more interaction between modelers and experimentalist (Gifford 1991). Field studies need to be closely linked with mechanistic modeling to test predictions and identify research needs (Lawlor and Mitchell 1991). The lack of interaction between experimentalist and modelers has often limited the usefulness of the data for building predictive models. Often, critical pieces of information needed to parameterize a model for an experiment are not gathered simply because experimentalist are not aware of model requirements.

Limitations in Plant Physiological Ecology

The information needed to parameterize and implement state-of-the-art photosynthesis models remains very limited. To adequately parameterize photosynthesis models, data sets are needed that describe responses to light, temperature and CO_2. Responses to soil moisture and plant nitrogen levels are seldom considered in leaf-level experiments, yet these response curves are critical for ecosystem level modeling. Similarly, changes in water-use-efficiency resulting from stomatal responses to CO_2 are highly significant at the ecosystem level, particularly in water-limited ecosystems. However, studies of stomatal response in native species are relatively rare.

To successfully model biome-wide responses to increased CO_2 we need to understand much more about the CO_2 acclimation responses of plants (Drake 1992). Photosynthetic acclimation responses to elevated CO_2 have proven to be highly variable (Gifford, 1991). Many acclimation responses have been attributed to low rooting volumes, and subsequent feedback inhibition of photosynthesis (Arp 1991, Drake 1992). Yet, most photosynthesis models do not represent feedback inhibition of photosynthesis (Ascon-Bieto 1983, Foyer 1988, Luxmore 1991). Reduced tissue nitrogen contents and decreases in respiration are routinely observed under elevated CO_2. The GRASS model simulates whole-plant labile carbon, negative feedback effects of high labile C, and variable plant N:C ratios. However, it does not simulate starch accumulation at the site of C fixation or

the rate of C translocation out of the leaf. Accurate estimations of altered plant C:N ratio due to elevated Ps rates also depend upon accurate simulations of N uptake rate by roots. Ecosystem models need to pay more attention to N uptake kinetics, particularly the relative roles of diffusion and mass flow to root surfaces.

Explanations for decreases in N:C are still lacking, however. While it has been hypothesized that increased carbon fixation dilutes nitrogen, reduced N concentrations have been observed even when there is excess nitrogen in the environment (Drake 1992). There is increasing evidence that CO_2 may regulate biochemical-level processes directly (Stitt 1991). While we know that physiological adjustments occur, we need to be able to predict when and how they occur in particular environments. If no pattern emerges, and if acclimation cannot be mechanistically modeled, then the responses must be described empirically.

Experimentalist have repeatedly noted that we still understand too little about interactions between responses to CO_2 and other environmental variable such as moisture and soil fertility (Gifford 1991, Drake 1992). There is a need to study response to CO_2, temperature and water, alone and in combination (Mooney et al. 1991). It is becoming increasingly clear that plants respond to CO_2 with higher water- and nitrogen-use-efficiencies, and that CO_2 shifts photosynthetic temperature optima higher in C_3 plants. This understanding is obviously basic for predictions of ecosystem level responses to climatic change. The GRASS model simulates these interactions, but the simulated responses require further experimental support.

While progress has been made to generalize models of plant respiratory losses (e.g., Ryan 1991), understanding is still incomplete. The utility of highly accurate photosynthesis measurements is eroded by limited knowledge of respiratory losses. Estimates of root respiratory efflux by mature plants *in situ* are lacking, as are studies of respiratory responses to moisture stress. There is evidence that root respiration rate may be variable, and related to photosynthetic rate (Bunce 1989), but this has rarely been incorporated into models. However, the decrease in plant N concentration in response to elevated CO_2 reduces respiration rates in GRASS since maintenance respiration is dependent on N concentration. It is unknown whether this is the sole mechanism in nature.

The Neglected Role of Animals and Fire
in Ecosystem Responses to Climatic Change

Despite the fact that grasslands and savannas are heavily utilized by domestic and wild herbivores, few climate change modeling exercises have considered the role of herbivory. This seems to be a serious omission as we know that herbivory may greatly modify rates of plant growth and ecosystem nutrient cycling and their responses to atmospheric change. Interactions between climate and herbivory probably have important feedback effects on the climate system, through grazing induced changes in surface albedo and latent heat flux, for instance. It has been shown that reduced forage quality may induce compensatory increases in foraging by invertebrate herbivores (Lincoln et al. 1986). Among ruminant herbivores, however, the effect of reduced forage quality may be to decrease forage intake rate, as rate of passage is limited by digestibility. Models should be used to examine the ecosystem level consequences of these effects on herbivory.

Models of tropical grasslands and savannas must pay increased attention to non-microbial agents of plant biomass degradation. Large quantities of plant biomass may be

recycled by termites or lost to abiotic weathering. The ecosystem level consequences of climatic temperature increases on termite metabolic rate and thus food intake rates have not been considered. The implications of these losses for ecosystem carbon budgets and soil organic matter balance need more serious consideration. They are not considered in the CENTURY model, for instance.

There is a need to predict relationships between ecosystem processes (e.g., nutrient cycling and primary production) and animal numbers and biodiversity. While earlier grassland ecosystem models did contain herbivore submodels (e.g., Innis 1978), some of the more recent ecosystem models have tended to avoid consideration of consumers: Coughenour (1985) and McNaughton et al. (1988) modeled ecosystem impacts of herbivory in the Serengeti; Hunt et al. (1990) considered belowground food webs; impacts of altered forage quantity and quality on livestock production were simulated using the SPUR model (Hansen et al. 1993); and Pastor and Naiman (1992) incorporated moose browsing. Vegetation models have been used to predict changes in animal habitats (Shugart 1984). Other models have considered interacting populations of plants and animals (Walker and Noy-Meir 1982, Hilborn and Sinclair 1979, Pellew 1983). However, the latter models have limited or no ability to represent the vegetation, soil processes, or feedbacks between plants and soils that are important for predicting ecosystem responses to climate change. The SAVANNA model (Coughenour 1993) is a recent model that simulates ecosystem processes and herbivores at landscape to regional scales.

The role of fire needs more attention in modeling studies. Most tropical and warm temperate grasslands and savannas are subject to, indeed adapted to, regular burning. Like herbivory, fire might significantly modify grassland climate change responses. Ecosystem models should be used to examine possible implications of climatically-induced changes in fire regimes. While higher temperatures may reduce fuel moisture, increasing rainfall may have the opposite effect. Fuel loads could change in response to CO_2 fertilization. Models could be used to examine the extent to which potential carbon gains due to CO_2 fertilization in grasslands may be negated by increased burning.

Problems of Resolution and Scale

It has been argued that the trade-off between errors arising from aggregation and model complexity makes intermediate resolution models most optimal (Reynolds and Acock 1985). However, an intermediate level of resolution is probably less than optimal for making accurate or general predictions of climate change responses. While simplified models may minimize data requirements, model parameterization efforts and uncertainty; scientists who work at finer scales will be quick to point out errors of omission and aggregation.

The problems of relating processes at different temporal and spatial scales have not been solved (Rosswall et al. 1988). It has been suggested that since there is a hierarchy of time and space scales in nature, there should also be a corresponding hierarchy in our models (Reynolds and Acock 1985, Dahlman 1985). Similarly, a multi-scaled modeling approach was proposed to translate information among physiological, community and ecosystem level models using concepts from hierarchy theory (Kittel and Coughenour 1988).

Much attention has been focused recently on interfacing or linking fine and coarse resolution process models or physiological and population based models either directly or statistically (e.g., King et al. 1990, Luxmore et al. 1991, Smith et al. 1992, Friend et al. in

press). These ambitious efforts still remain in formative stages. However, fine and coarse time-step processes, and linkages between physiological and population processes have long been employed in sward-level models (e.g., Coughenour et al. 1984). Leaf-level photosynthetic models (e.g., Farquhar et al. 1980) are incorporated into ecosystem level models (e.g., GRASS-CSOM). Leaf-level models of photosynthesis, with time steps of minutes, are being incorporated into GCMs of the global climate (J. Berry pers. comm.).

A different set of problems occurs in the spatial modeling domain. Modeling relationships among processes at different spatial scales is problematic (Senft et al. 1987, Shugart et al. 1988). Models must translate the results of patch-scale processes to landscape and regional scales. Multiple non-spatial model runs driven with geo-referenced site data can be integrated over space using digital maps, geographic information systems or simple areal statistics (e.g., Shugart and Emmanuel 1985, Solomon 1986, Burke et al. 1990). A related schemes is to distribute sparsely sampled detailed model runs over space, in a statistical sense.

These methods are sufficient, as long as there are no significant flows of material or information among sites. Movement of organisms through dispersal and migration, and movement of and water and nutrients into and through large watersheds modify landscape- and regional-level ecosystem behavior, particularly over long time scales.

Modeling Data Bases

Model implementation over large spatial scales requires a "minimum data set" of model parameters and driving variables (Turner et al. 1990). Data set size is minimized to maximize the likelihood that the entire set is available at a large number of sites. A standardized set of measures, made at a wide range of sites would include, for example; weather, above and belowground live and dead biomass dynamics, nitrogen concentrations, litter decay rates, soil organic matter contents, and photosynthetic/stomatal responses to light, temperature, humidity and CO_2. This was accomplished during IBP biome studies (e.g., Sims and Singh 1978). The recent cross-site UNEP tropical grassland study (Long et al. 1992) is a more recent example of a standardized approach, as are the cross-site or network studies in the NSF Long-Term Ecological Research (LTER) program (Callahan 1984, Franklin et al 1990).

Models should be applied to as many extant data sets as possible. There is a considerable body of existing information that can be used to improve the models. In the SCOPE grasslands modeling group (Scopegram) effort, (Scopegram 1993a,b) data sets were assembled from many world grassland studies, many of which were from the UNEP study (Long et al. 1993). The CENTURY model was parameterized and tested against each. GRASS model testing was completed for two sites, with three other sites in progress. In attempting to assemble this data set, this project revealed that there is much past and ongoing experimental research that needs to be assimilated and explained by our models.

The data sets that have been most useful have described biomass dynamics and element flows through ecosystems over several or more years. Multiple years of data are needed to test models over a wide range of weather years and initial conditions. Data that show plant, soil and ecosystem level responses to a wide range of nutrient and moisture availabilities are most valuable. For example, data from irrigation/fertilization treatments on a shortgrass steppe during the IBP (Dodd and Lauenroth 1979) proved

51

invaluable, as models could be tested for their abilities to predict responses to nitrogen, water, and nitrogen-water interactions.

In the long-term, methods of computing model parameters from minimal data sets should be developed. For example, a suggestion was made to relate model parameters such as maximum photosynthetic rate to leaf longevity, which is a trait that can be empirically related to broad-scale climate and soil properties (J. Aber, pers. comm.). Trade-offs among parameter values due to biological constraints (Orians and Solbrig 1977, Grime 1977, Mooney and Gulman 1979, Chapin 1980, Tilman 1988) may prove useful for developing generalized model parameterizations. At the least, libraries of parameter values classified by vegetation or soils types must be assembled.
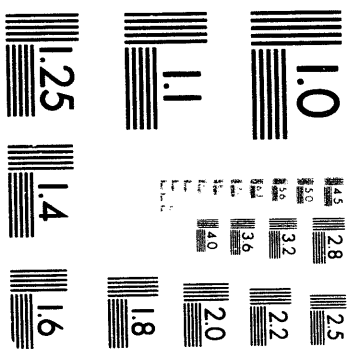
Literature Cited

Arp, W.J. 1991. Effects of source-sink relations on photosynthetic acclimation to elevated CO_2. Plan Cell Environ. 14:869-875.

Azcon-Bieto, J. 1983. Inhibition of photosynthesis by carbohydrates in wheat leaves. Pl. Physiol. 73:681-686.

Bunce, J.A. 1989. Growth rate, photosynthesis and respiration in relation to leaf area index. Ann. Bot. 63:459-463.

Burke, I.G., T.G.F. Kittel, W.K. Lauenroth, P. Snook , C.M. Yonker and W.J. Parton. 1991. Regional analysis of the central Great Plains: Sensitivity to climate variation. Bioscience 41:685-692.

Callahan, J.T. 1984. Long-term ecological research. Bioscience 34:363-367.

Chapin, F.S. III. 1980. The mineral nutrition of wild plants. Ann. Rev. Ecol. System. 11:233-260.

Coughenour, M.B. 1993. The SAVANNA Landscape Model. User Manual and Documentation.

Coughenour, M. B., S. J. McNaughton, and L. L. Wallace. 1984. Modeling primary production of perennial graminoids: Uniting physiological processes and morphometric traits. Ecological Modelling 23:101-134.

Dahlman, R.C. 1985. Modeling needs for predicting responses to CO_2 enrichment: plant, communities and ecosystems. Ecol. Model. 29:77-106.

Drake, B.G. 1992. The impact of rising CO_2 on ecosystem production. Water, Air and Soil Pollut. 64:25-44.

Farquhar, G.D., S. Von Caemmerer and J.A. Berry. 1980. A biochemical model of photosynthetic CO_2 assimilation in leaves in C_3 species. Planta 149:78-90.

Foyer, C.H. 1988. Feedback inhibition of photosynthesis through source-sink regulation in leaves. Pl. Physiol. Biochem. 26:483-492.

Franklin, J.F., C.S. Bledsoe and J.T. Callahan. 1990. Contributions of the long-term ecological research program. Biosc. 40:509-523.

Friend, A., H.H. Shugart, and S.W. Running. unpubl. ms. A physiologically based gap model of forest dynamics.

Gifford, R.M. 1991. The effects of CO_2 and climate change on photosynthesis, net primary production and ecosystem production. paper presented at SCOPE Workshop I on Modeling Coniferous Forest and Grassland Responses to Climatic Change, Woods Hole Mass.

Grime, J.P. 1977. Evidence for the existence of three primary strategies in plants and its relevance to ecological and evolutionary theory. Am. Nat. 111:1169-1194.

Hansen, J.D., B.B. Baker and R.M. Bourdon. 1993. Comparison of the effects of different climate change scenarios on rangeland livestock production. Agric. Syst. 41:in press.

Hilborne, R. and A.R.E. Sinclair. 1978. A simulation of the wildebeest population, other ungulates and their predators. pp. 287-309 in: Serengeti: Dynamics of an ecosystem. A.R.E. Sinclair and M. Norton-Griffiths (eds.). University of Chicago Press, Chicago. 389 pp.

Hunt, H.W., M.J. Trlica, E.F. Redente, J.C. Moore, J.K. Detling, T.G.F. Kittel, D.E. Walter, M.C. Fowler, D.A. Klein and E.T. Elliott. 1991. Simulation model for the effects of climate change on temperate grassland ecosystems. Ecol Model. 53:205-246.

Innis, G.S. (ed.). 1978. Grassland Simulation Model. Springer-Verlag, New York. 298 pp.

King, A.W., W.R. Emmanuel and R. O'Neill. 1990. Linking mechanistic models of tree physiology with models of forest dynamics: problems of temporal scale. pp. 242-248 in: Process modeling of forest growth responses to environmental stress. R.K. Dixon, R.S. Meldahl, G.A. Ruark and W.G. Warren (eds.). Timber Press, Portland.

Kittel, T.G.F. and M. B. Coughenour. 1988. Prediction of regional and local ecological change from global climate model results: A hierarchical modeling approach. in: R.A. Pielke, T.G. Kittel (eds.). Monitoring Climate for the effects of increasing greenhouse gas concentrations. Coop. Inst. for Res. in the Atmos., Colorado State University, Ft. Collins.

Dodd, J.L. and W.K. Lauenroth. 1979. Analysis of the responses of a grassland ecosystem to stress. pp. 43-58 in: Perspectives in grassland ecology, N.R. French (ed.). Springer-Verlag, New York.

Lawlor, D.W. and R.A.C. Mitchell. 1991. The effects of increasing CO_2 on crop photosynthesis and productivity: a review of field studies. Pl. Cell Environ. 14:807-818.

Lincoln, D.E., D. Couvet, and N. Sionit. 1986. Responses of an insect herbivore to host plants growth in carbon dioxide enriched atmospheres. Oecologia 69:556-560.

Long, S.P., M.B. Hones and M.J. Roberts. 1992. Primary Productivity of Grass Ecosystems of the Tropics and Sub-tropics. Chapham and Hall, London. 267 pp.

Luxmore, R.J. 1991. A source-sink framework for coupling water, carbon and nutrient dynamics of vegetation. Tree Physiol. 9:267-280.

Luxmore, R.J., A.W. King and M.L. Tharp. 1991. Approaches to scaling up physiologically based soil-plant modules in space and time. Tree Physiol. 9:281-292.

Mooney, H.A. and S.L. Gulman. 1979. Environmental and evolutionary constraints in the photosynthetic characteristics of higher plants. pp. 211-233 in Topics in Plant Population Biology, O.T. Solbrig, S. Jain, G.B. Johnson, and P.H. Raven (eds.). Columbia Univ. Press, New York.

Mooney, H.A., B.G. Drake, R.J. Luxmore, W.C. Oechel and L.F. Pitelka. 1991. Predicting ecosystem responses to elevated CO_2 concentration. BioScience 41:96-104.

Orians, G.H. and O.T. Solbrig. 1977. A cost-income model of leaves and roots with special reference to arid and semiarid areas. Am. Nat. 111:677-690.

Pastor, J. and R.J. Naiman. 1992. Selective foraging and ecosystem processes in boreal forests. Am. Nat. in press.

Pellew, R.A.P. 1983. The impacts of elephants, giraffe and fire upon the *Acacia tortilis* woodlands of the Serengeti. Afr. J. Ecol. 21:41-74.

Reynolds, J.F. and B. Acock. 1985. Predicting the response of plants to increasing carbon dioxide: a critique of plant growth models. Ecol. Model. 29:107-129.

Rosswall, T., R.G. Woodmansee and P.G. Risser (eds.). 1988. Scales and Global Change. John Wiley and Sons, London.

Ryan, M. 1991. The effects of climate change on plant respiration. Ecol. Appl. 1:157-167. '

Scopegram (Parton, W.J., M.B. Coughenour, J.M.O. Scurlock, D.S. Ojima, T.G. Gilmanov, R.J. Scholes, D.S. Schimel, T.Kirchner, J.C. Menaut, T. Seasteadt, E. Garcia-Moya, A. Kamnalrut, J.I. Kinyamario and D.O. Hall). 1994a. Grassland ecosystem modelling- Temperate and tropical. Chap. X. in: Global Biogeochemical Cycles. SCOPE, Paris.

Scopegram (Parton, W.J., M.B. Coughenour, J.M.O. Scurlock, D.S. Ojima, T.G. Gilmanov, R.J. Scholes, D.S. Schimel, T.Kirchner, J.C. Menaut, T. Seasteadt, E. Garcia-Moya, A. Kamnalrut, J.I. Kinyamario and D.O. Hall). 1994b. Modeling of global grassland production in relation to climatic change. Chap. X. in: Global Biogeochemical Cycles. SCOPE, Paris.

1.0

1.1

1.25

1.4

1.6

1.8

2.0

2.2

2.5

2.8

3.2

3.6

4.0

4.5

5.0

Senft, R. L., M. B. Coughenour, D. W. Bailey, L. R. Rittenhouse, O. E. Sala, and D. M. Swift. 1987. Large herbivore foraging and ecological hierarchies. Bioscience 37:789-799.

Shugart, H.H. 1984. A theory of forest dynamics.: the ecological implications of forest succession models. Springer-Verlag, New York. 278pp.

Shugart, H.H. and W.R. Emmanuel. 1985. Carbon dioxide increase: the implications at the ecosystem level. Plant Cell Environ. 8:381-386.

Shugart, H.H., P.J. Michaels, T.M. Smith, D.A. Weinstein and E.A. Rastetter. 1988. Simulation models of forest succession. pp. 125-151 in: Scales and Global Change. T. Rosswall, R.G. Woodmansee and P.G. Risser (eds.). John Wiley and Sons, London.

Sims, P.L. and J.S. Singh. 1978. The structure and function of ten western North American grasslands II. Intra-seasonal dynamics in primary producer compartments. J. Ecol. 66:547-572.

Smith, T.M., J.F. Weishampel and H.H. Shugart. 1992. The response of terrestrial C storage to climate change: Modeling C dynamics at varying temporal and spatial scales. Water Air Soil Pollut. 64:307-326.

Tilman, D. 1988. Plant strategies and the dynamics and structure of plant communities. Princeton University Press, Princeton.

Turner, S.J., R.T. Prinsley, D.M Stafford-Smith, H.A. Nix and B.H. Walker (eds.). et al. 1990. The impact of global change on agriculture and forestry. pp. 53-94. in: Proceedings of the Workshops of the Coordinating Panel on Effects of Global Change on Terrestrial Ecosystems. Rep. No. 11, International Geosphere Biosphere Programme. Stockholm.

Walker, B.H. and I. Noy-Meir. 1982. Aspects of the stability and resilience of savanna ecosystems. pp. 556-590 in: Ecology of Tropical Savanna, B.J. Huntley and B.H. Walker, eds.). Springer Verlag, Berlin.

Walker, B.H. (ed.). 1990. A framework for modelling the effects of climate and atmospheric change in terrestrial ecosystems. pp. 1-22 in: Proceedings of the Workshops of the Coordinating Panel on Effects of Global Change on Terrestrial Ecosystems. Rep. No. 11, International Geosphere Biosphere Programme. Stockholm.

Woodmansee, R.G. 1988. Ecosystem processes and global change. pp. 11-27 in: Scales and Global Change. T. Rosswall, R.G. Woodmansee and P.G. Risser (eds.). John Wiley and Sons, London.

CHAPTER 7

Conclusions

The main objectives of this project were fulfilled. The ecological modeling activities of the principle investigator were mainly concerned with bringing a high resolution plant model up to date and linking it with a nutrient cycling model to address ecosystem responses to climate and elevated CO_2. This state-of-the-art model (GRASS) is a major product of this research. Another long-lived product developed on this project was an integrated, ecological modeling environment for use on X-Windows workstations. The project's atmospheric research was concerned primarily with methods to down-scale coarse resolution GCM model output to ecologically useful spatial scales. The development of a synoptic classification processor (SCP) was a major accomplishment of that research.

Early in the project, before GRASS was completed, we use a multi-scaled modeling approach to predict North American grassland responses to climate change. We examined the impact of modifying parameterizations within CENTURY to provide a simplified representation of direct CO_2 effects currently not included in CENTURY. These modifications were based on simulations with a more detailed plant-soil ecosystem model (GEM; Hunt et al. 1991). The resolution of GEM is intermediate between that of CENTURY and GRASS. GEM simulations for southeastern Wyoming shortgrass and mid-grass grassland stands showed that doubling CO_2 enhanced plant-level water use efficiency (WUE; net primary production/water uptake) by 45% and nitrogen use efficiency (NUE; plant N:C) by 25%. To represent physiological effects of elevated CO_2 in CENTURY, we increased the model's plant-level WUE and NUE by 30%. The effects of increasing WUE or NUE by 30% did not individually or jointly increase NPP by a commensurate amount (i.e., by 30%), but rather by only 0.3-8% over the response to climate change alone.

The GRASS model, when linked with a nutrient cycling model, provided some of the first predictions of ecosystem responses to elevated CO_2 using a mechanistic photosynthesis submodel. In short-term (10 yr) experiments, the model predicted a Colorado C_4 grass production increased 9% between 350 ppm and 750 ppm NPP at current temperatures. The increase in NPP of a C_3 grass between 350 and 750 ppm CO_2 was 15% under current climate conditions. Between 350 ppm and 750 ppm CO_2, Kenyan C_4 grass NPP increased 47%. In longer-term (125 yr) experiments, doubling CO_2 without climatic change increased NPP 6%, 5% and 40% in Colorado C_4 and C_3, and the Kenya C_4 grasslands, respectively. However, one GCM scenario with $2xCO_2$ decreased NPP by 25% and 37% in C_3 and C_4 grasses respectively while another GCM scenario with $2xCO_2$ increased NPP 13% in the C_3 and 21% in the C_4 grass. NPP increased 46% in Kenya under both scenarios of CO_2 doubling and climatic change.

Significantly, the responses of plants to elevated CO_2 were strongly modified by ecosystem-level feedbacks. While nutrient limitation reduced positive CO_2 responses, increased water use efficiency led to greater nutrient availability and positive plant growth responses. Thus, predicted increase of NPP in a tropical C_4 grassland was much higher than expected.

By supporting GRASS modeling, this project provided a substantial contribution to the SCOPE project "Ecosystem response to climate change: The effects of climate change on production and decomposition in coniferous forests and grasslands" which involved several workshops over a four year period. This project adopted the GRASS and

CENTURY models to evaluate world-wide grassland responses to climate change (Scopegram 1993a,b). While GRASS model parameterization was only completed for three sites, it provided critical justification for the CENTURY model, which was applied to 37 sites worldwide. GRASS model parameterizations for grasslands in New Mexico and Kansas were mostly completed, and a parameterization for Russia in progress. It is likely that GRASS will be applied to many more sites in the future, providing increased support for global and regional scale predictions.

Efforts to provide more accurate local-scale climate predictions involved use of a mesoscale model (RAMS) and construction of a synoptic classification processor (SCP) for GCM output. RAMS was used to test the sensitivity of a mid-latitude squall line to broad-scale climate change predicted from a GCM. Control RAMS runs were based on a case study of the development of a mid-latitude squall line. Results suggested that under global climate change mid-latitude convective storms will be more severe, with greater runoff (contributing to flooding events) and stronger winds (increasing the likelihood of forest blowdown events). This demonstrated the importance of complementing GCM climate change studies with mesoscale simulations.

The SCP was developed to evaluate results of GCM climate sensitivity experiments. It is presumed that a change in climate, such as that potentially induced by elevated atmospheric CO_2, should be observable in prevailing synoptic conditions. By classifying air mass types over an extended period of time, a climatology of synoptic states was constructed for comparing modeled climates. The In addition to classifying GCM output as a filter for RAMS regional simulations, the SCP can be used for rapid diagnosis of GCM experiment results in terms of three dimensional changes in atmospheric dynamics.

Some of our original goals (Kittel and Coughenour 1988) were not completed within the scope of the present project. We originally proposed to construct a hierarchical GIS to interrelate spatial scales. That portion of the project could not be funded, however we are pleased that other research groups are working on this problem (e.g., I. Burke and S. Walker at the CPER and Niwot LTER sites). We originally proposed to link plant community simulators with ecological process models to predict vegetation change. We are happy to see that this approach has also been adopted by others (e.g., Luxmore et al. 1990, Smith et al. 1992) as well as the global change modeling community, including the IGBP (Walker 1991) and the recent "Terrestrial Ecosystem Modeling Activity" initiative (Hall and Melillo 1993). We were unable to complete the linkage from fine-scaled atmospheric to ecological models, however, this work is still in progress.

As a result of these accomplishments, we are now in a much better position to coordinate modeling efforts at fine and coarse levels of resolution, at short and long temporal scales, and over small and large spatial domains. The results of the fine scaled ecological modeling work has proven highly useful for substantiating simplifying assumptions of coarse scaled models which, at the current time, are being used to estimate regional and global scale interactions of grassland ecosystems and the atmosphere.

Literature Cited

Hall, D. and J. Melillo. 1993. Terrestrial ecosystem modeling activity: A general prospectus. Proceedings of an international community modeling workshop held in London, April 1993.

Hunt, H.W., M.J. Trlica, E.F. Redente, J.C. Moore, J.K. Detling, T.G.F. Kittel, D.E. Walter, M.C. Fowler, D.A. Klein, and E.T. Elliott. 1991. Simulation model for the ecosystem level effects of climate change in temperate grasslands. Ecological Modelling, 53:205-246.

Kittel, T.G.F. and M. B. Coughenour. 1988. Prediction of regional and local ecological change from global climate model results: A hierarchical modeling approach. in: R.A. Pielke, T.G. Kittel (eds.). Monitoring Climate for the effects of increasing greenhouse gas concentrations. Coop. Inst. for Res. in the Atmos., Colorado State University, Ft. Collins.

Luxmore, R.J., A.W. King and M.L. Tharp. 1991. Approaches to scaling up physiologically based soil-plant modules in space and time. Tree Physiol. 9:281-292.

Scopegram (Parton, W.J., M.B. Coughenour, J.M.O. Scurlock, D.S. Ojima, T.G. Gilmanov, R.J. Scholes, D.S. Schimel, T.Kirchner, J.C. Menaut, T. Seasteadt, E. Garcia-Moya, A. Kamnalrut, J.I. Kinyamario and D.O. Hall). 1994a. Grassland ecosystem modelling- Temperate and tropical. Chap. X. in: Global Biogeochemical Cycles. SCOPE, Paris.

Scopegram (Parton, W.J., M.B. Coughenour, J.M.O. Scurlock, D.S. Ojima, T.G. Gilmanov, R.J. Scholes, D.S. Schimel, T.Kirchner, J.C. Menaut, T. Seasteadt, E. Garcia-Moya, A. Kamnalrut, J.I. Kinyamario and D.O. Hall). 1994b. Modeling of global grassland production in relation to climatic change. Chap. X. in: Global Biogeochemical Cycles. SCOPE, Paris.

Smith, T.M., J.F. Weishampel and H.H. Shugart. 1992. The response of terrestrial C storage to climate change: Modeling C dynamics at varying temporal and spatial scales. Water Air Soil Pollut. 64:307-326.

Walker, B.H. (ed.). 1990. A framework for modelling the effects of climate and atmospheric change in terrestrial ecosystems. pp. 1-22 in: Proceedings of the Workshops of the Coordinating Panel on Effects of Global Change on Terrestrial Ecosystems. Rep. No. 11, International Geosphere Biosphere Programme. Stockholm.

DATE
FILMED
1 / 10 / 94

END